RESEARCH REPORT

Simulation of Wind Driven Rain and Wetting Patterns on Buildings

Canada

CMHC SCHL
HOME TO CANADIANS

CMHC—HOME TO CANADIANS

Canada Mortgage and Housing Corporation (CMHC) has been Canada's national housing agency for more than 60 years.

Together with other housing stakeholders, we help ensure that Canada maintains one of the best housing systems in the world. We are committed to helping Canadians access a wide choice of quality, affordable homes, while making vibrant, healthy communities and cities a reality across the country.

For more information, visit our website at **www.cmhc.ca**

You can also reach us by phone at 1-800-668-2642 or by fax at 1-800-245-9274.

Outside Canada call 613-748-2003 or fax to 613-748-2016.

Canada Mortgage and Housing Corporation supports the Government of Canada policy on access to information for people with disabilities. If you wish to obtain this publication in alternative formats, call 1-800-668-2642.

SIMULATION OF WIND-DRIVEN RAIN AND WETTING PATTERNS ON BUILDINGS

By

D. Inculet and D. Surry

BLWT-SS30-1994

November 1994
Revised February 1995
Final Report

This report forms part of a larger study into Wind Rain and the Building Envelope, sponsored by Canada Mortgage and Housing Corporation.
Prepared for Jacques Rousseau and Pierre-Michel Busque, Housing Innovation Division.

NOTE: **DISPONIBLE AUSSI EN FRANÇAIS SOUS LE TITRE:**

SIMULTATION DE LA PLUIE BATTANTE ET DE LA DISTRIBUTION DU MOUILLAGE SUR LES BÂTIMENTS

DISCLAIMER

This study was conducted for Canada Mortgage and Housing Corporation under Part IX of the National Housing Act. The analysis, interpretation and recommendations are those of the consultants and do not necessarily reflect the views of Canada Mortgage and Housing Corporation or those divisions of the Corporation that assisted in the study and its publication.

CMHC MANDATE

Canada Mortgage and Housing Corporation, the Federal Government's housing agency, is responsible for administering the National Housing Act.

This legislation is designed to aid in the improvement of housing and living conditions in Canada. As a result, the Corporation has interests in all aspects of housing and urban growth and development.

Under Part IX of this Act, the Government of Canada provides funds to CMHC to conduct research into the social, economic and technical aspects of housing and related fields, and to undertake the publishing and distribution of the results of this research. CMHC therefore has a statutory responsibility to make available, information which may be useful in the improvement of housing and living conditions.

This publication is one of the many items of information published by CMHC with the assistance of federal funds.

CONTENTS

EXECUTIVE SUMMARY

Seeking to find methods of reducing rain penetration problems in high rise residential buildings and to increase the durability of building designs, Canada Mortgage and Housing Corporation has sponsored this research initiative into the modelling of wind-driven rain. The project included the following components:

1) Demonstration of the capability of physically modelling wind-driven rain in a wind tunnel and its interaction with buildings;

2) A study of the effects of wind direction and wind speed on wetting patterns using a model which will allow comparisons with field experience;

3) An exploratory investigation of the effects of building height and architectural features on wetting patterns.

Rain was simulated in the low speed test section of Boundary Layer Wind Tunnel II at the University of Western Ontario using an array of nine nozzles. This tunnel has a cross section 4m high and 5m wide. A target model droplet size distribution was arrived at by using published data on full-scale rain and Froude number scaling. The length scale used was 1:64, giving wind speed and time scales of 1:8. The scaling used was a good workable compromise between modelling of the wind and modelling of the rain.

Each wind speed required a calibration of droplet sizes at the test site to enable a layout of the array. Three wind speeds were used, all with a suburban exposure. The droplet size distributions achieved at the test site were slightly biased towards the larger drop sizes, but the effect of this was not believed significant.

A visual picture of the wetting patterns on the building faces was accomplished using a water sensitive paper which turned from yellow to blue immediately on contact with water. A permanent record of these patterns is recorded in photographic form in this report. The method also allowed a quantitative analysis to be performed by sizing the droplet stains on the paper. Local intensity factors which relate the wetting rate to the rainfall rate were calculated for selected locations.

The "classic" wetting pattern was obtained on the windward face of a building whereby the top corner is the wettest followed by the top and side edges. Local intensity factors in the top corners ranged from about 0.15 to 2.5 in the cases examined, with the corners being subjected to 2 to 50 times the rain impact as the central region of the face. The side wall remains relatively dry. For glancing wind angles, there can still be significant wetting along the top edge, upstream edge, and occasionally even the downstream edge for angles of 30, 45 and 60 degrees between the building face and the wind direction. Local intensity factors can increase fairly significantly with increasing wind speed. The general wetting pattern on a windward wall remains the same regardless of building height, although the intensity of wetting along the top edge likely increases with increasing height. Cornices and peaked roofs may reduce rain impact on the front face, while providing a good opportunity for drainage and therefore protection of the building face from surface migration.

The research has made a significant step forward in the understanding of wetting patterns on building faces - needed to understand the requirements of a rainscreen. Further, it has laid the foundation for studying ways of mitigating wetting rates. Both are invaluable to building design.

ACKNOWLEDGEMENTS

This study of rain simulation and wetting patterns on buildings was initiated by Canada Mortgage and Housing Corporation. The financial contributions of both Canada Mortgage and Housing Corporation and the Natural Sciences and Engineering Research Council of Canada are acknowledged. The authors acknowledge Canada Mortgage and Housing Corporation for their part in the test program development.

Acknowledgement is made of the contributions by various members of the Laboratory staff: Mr. D. Garnham constructed the model and Mr. G. Dafoe both constructed the nozzle spray rack and carried out the experimental phases of the study. Mr. M. Mikitiuk helped with the photography work and Ms. L. Hadden did a part of the droplet stain size analysis. The substantial contributions to the project by Mr. C. Harris, in particular during Phase II, are gratefully acknowledged.

Finally, the authors would like to acknowledge the general direction, advice and encouragement received from Dr. A. G. Davenport, Director of the Boundary Layer Wind Tunnel Laboratory.

1 Modelling of Wind-Driven Rain in the Wind Tunnel

The modelling of wind-driven rain requires that simultaneous scaling of the wind and of the rain be achieved. The modelling of the wind is a standard procedure at the Boundary Layer Wind Tunnel Laboratory and will be discussed only briefly here. However, the modelling of rain at a scale congruent with the wind presents several new challenges and the details are presented.

1.1 Modelling of the Wind

Scaling requirements of the rain (see Section 1.2.1 below) necessitated that the tests be conducted in the low-speed test section of the Boundary Layer Wind Tunnel II at the University of Western Ontario. This tunnel has a cross section of 5m wide x 4m high and a length of 52m. A fortuitous advantage of this tunnel is the existence of a wave tank beneath the moveable floor, thus allowing water to be sprayed in the wind tunnel and subsequently drained from the floor.

The initial test building was modelled after a building in Ottawa with a suburban exposure; a suburban upstream exposure was used for all the tests. The resulting profiles (mean speed and local turbulence intensity) are shown in Figure 1. As seen, the power law exponent was approximately 0.28. The roughness length, z_o, was approximately 0.3m from the lower boundary layer. As discussed further in Section 1.2.2, the length scale used was 1:64.

The wind speeds were selected, in part, by considering the Driving Rain Wind Pressures given in [5]. Wind tunnel speeds of 0.6 , 1.5 and 2.3 m/s at Phase I building height corresponded to full-scale driving rain wind pressures at 10m in open country of 15, 75 and 200 Pa respectively.

1.2 Model Scaling of Rain Drop Sizes

1.2.1 Scaling Parameters

By looking at the equations of motion for a droplet in wind, neglecting turbulence, the following similarity requirements are found for the droplets:

1) $\left[\frac{V_t}{U}\right]_{MS} = \left[\frac{V_t}{U}\right]_{FS}$ where: V_t= terminal speed

U= wind speed

(this defines the driving rain angle)

2) $\left[\frac{U^2}{Hg}\right]_{MS} = \left[\frac{U^2}{Hg}\right]_{FS}$ where: H= building height

g= gravitational constant

(this is Froude number scaling)

Thus, for any length scale (here taken as 1:64), the wind speed scale is simply the square root of the length scale (1:8 here), and the time scale is the length scale divided by the speed scale (again, 1:8 here).

1.2.2 Target Model-Scale Drop Size Distribution

The determination of the desired drop size distribution in model-scale first requires determining the full-scale distribution. This is accomplished here through published works. Then, using the velocity scaling on the terminal velocity of the drops (published data on terminal velocities is also required), the model-scale distribution can be determined.

In full-scale, drop sizes may range from about 100μm to 6000μm. Several theoretical models for the distribution of full-scale rain drop sizes have been proposed. The following are perhaps the most widely used:

a) Best [1]:

$F = 1 - e^{-(d/a)^n}$ where: $a = AI^p$

F is the fraction of liquid water in air having drops of diameter less than d (mm), I is the intensity of rainfall (mm/hr), and the values of A, p and n are 1.3, 0.232 and 2.25 respectively. Also,

$G = CI^q$

G is the volume of liquid water per unit volume of air (mm^3/m^3) and the values of C and q are 67 and 0.846 respectively.

b) Marshall et al. [11]:

$n(d) = n_o e^{-\Lambda d}$ where: $\Lambda = 4.1\, I^{-0.21}$ mm^{-1}

$n(d)$ is the number of drops per cubic metre of air per unit diameter at diameter d (mm) and $n_o = 8 \times 10^3\ m^{-3}mm^{-1}$.

Experimental data and models for the terminal velocities of drops are also available. Gunn and Kinzer [7] report experimental data for drops in stagnant air having diameters 100μm to 5800μm (pressure 760mm, temperature 20C, relative humidity 50%). Markowitz [10] established the following expression for terminal velocity:

$$V_t = 9.58\left[1 - \exp\left\{-\left(\frac{d\,(\text{mm})}{1.77}\right)^{1.147}\right\}\right] \quad \text{(m/s)}$$

This expression matches the data of Gunn and Kinzer well for drop diameters greater than 300 μm.

The results of Marshall's model are shown in Figure 2 for full-scale rainfall intensities of 1, 10 and 100 mm/hr. Note that the results are presented as an accumulated volume percentage *on a horizontal surface*, although drop size distributions are normally given for a *volume of air*. A factor equivalent to the terminal speeds has been incorporated into Marshall's model. This presentation is due to the measurement technique used in this study which gives the distribution collected on a horizontal surface over time.

Using the model of Marshall et al. and a combination of Stokes law (for $d \le 80\mu m$), the Gunn and Kinzer data (for $100 \le d \le 300\mu m$) and the Markowitz expression (for $d > 300\mu m$) (see Appendix E for the graph of terminal velocity versus drop diameter), the desired model scale drop

size distribution was determined. It is shown in Figure 3 for the same full-scale rainfall intensities as given in Figure 2. It was not intended in this first study to model a specific rainfall intensity, rather the aim was to be within an acceptable range.

In arriving at the target distribution, it was necessary to keep the velocity scale as large as possible (very small drops lead to the problem of evaporation) while not compromising on an appropriate scaling for the boundary layer. An adequate scaling was achieved with a 1:8 velocity scaling and, consequently, a 1:64 geometric scaling.

It is interesting to note that above an equivalent drop diameter of 4000μm, there is very little further increase in terminal speed with drop size because the increase in drop weight is compensated by a corresponding increase in deformation - larger droplets tend to have flattened bottoms. At 500 μm diameter, the "drop distortion parameter" is 0.98, at 1000 μm it is 0.93, at 2500 μm it is 0.71 and at 4000 μm it is 0.52 [2]. It is, of course, impossible to model this distortion at a small scale using water but this is not believed to be a significant parameter. It is worthy of mention, however, that because of the flattening of the terminal velocity curve at large drop sizes, it becomes difficult to model drops having a full-scale drop diameter greater than, say, 6000 μm. The required one to one correspondence between full-scale and model-scale drop sizes through their terminal speeds would concentrate the large diameter part of the full-scale spectrum into a narrow band of the model scale spectrum.

Since the model scale drop sizes do not follow a constant geometric scaling, the model-scale rainfall rate must be related to the equivalent full-scale rate through the full-scale frequency distribution of rain drop sizes and the associated rainfall rate.

1.3 Simulation of Rain Using Nozzles

Two possibilities exist for simulating the rain drop size distribution. One is to use a set of nozzles which generate the correct spectra of drop sizes. The other is to "build" the rain drop size distribution from a series of independent tests each having uniform drop sizes. Each has its advantages and disadvantages but the equipment involved in the latter is more costly and the testing more labour intensive. Hence, for this first study, nozzles generating a spectra of drop sizes were used.

In either case, there is an implicit assumption that there is very little interaction between raindrops, even in heavy rain, hence implying that the *shape* of the chosen spectrum defines the equivalent full-scale rainfall rate, rather than the actual *intensity* of the rainfall modelled. For illustration, Marshall's relation predicts about 3000 drops per cubic metre in a 10 mm/hr rain. This gives, on average, about 6 cms between drops. The average spacing of the sizable drops containing the bulk of the water mass must be larger still.

Another implicit assumption is that the addition of the modelled rain to the boundary layer wind simulation does not improperly distort the wind characteristics, particularly the turbulence properties. A brief experiment described in Appendix F suggested that the effect of the modelled rain on the modelled wind was inconsequential.

1.3.1 Nozzle Selection

A nozzle was selected to approximately generate the distribution shown in Figure 3. The "TN8 Unijet Spray Nozzle Tip" available from Spraying Systems Company was chosen (hollow cone, fine spray, standard pressure). The drop diameter at 10% accumulated volume is 100 μm and at 90% it is 300 μm (in a volume of air). While several nozzles may have been suitable with respect to drop size, this one was chosen for its relatively low capacity - at 25 psi, the capacity is approximately 350 ml/min. This was important so that longer duration tests could be run (see Section 2.2). The spray angle was about 80 degrees at 25 psi.

1.3.2 Calibration of One Nozzle

If it were possible to have an arrangement of nozzles whereby the nozzles completely lined the wind tunnel ceiling with virtually no space between them then, without evaporation, the drop size spectra anywhere in the wind-driven rain would be the same as that generated by an individual nozzle. However, this is not feasible and instead, a discrete array of nozzles was planned. This led to the problem of the "filtering effect" on drop sizes in the wind tunnel and the need for a calibration of drop sizes as explained below.

For any one wind speed, smaller drops will be carried further from the nozzle than larger drops due to the difference in their terminal velocities. Hence, for each wind speed, drop sizes at the test site were calibrated as a function of the distance between the test site and the upstream nozzle location (with the nozzle height held constant). Such a calibration allows the upstream spacing of nozzles to be designed. It is important to note here that, due to the filtering effect, drop sizes from any one of the nozzles will always decrease with height along any vertical line within the simulated wind-driven rain. The shape of the distribution may also differ. Hence, vertical profiles of drop size distribution were also taken for selected upstream locations to ensure that all heights of the building would be subjected to a representative range of drop sizes.

Also involved in the calibration was a measure of the lateral spread of the droplets. With increasing distance from the nozzle, the spread pattern widens due to the turbulence. This was again necessarily calibrated for each speed and distance between the test site and upstream nozzle. It was only done so at ground level. Results showed that drop sizes did not vary laterally, the number of drops merely decreased with lateral distance from the nozzle as would be expected.

Measurements for the calibrations were based on two techniques:

1) a laser-based measuring instrument (MALVERN 2600 Particle Sizer)
2) a water-sensitive paper produced by Ciba-Geigy which permanently changes colour from yellow to blue on contact with water. Note that the blue stains show as red in some of the photographs due to the use of a filter on the camera.

The two techniques gave reasonably similar size distribution results although error difficulties are encountered in both for this application. The techniques are described in some detail in Appendix A.

It was attempted to conduct the calibrations under a high relative humidity (say > 65%) so drops remained approximately the same size during their fall through the boundary layer. In the tests, the nozzles were always at a 2m height to minimize the evaporation while also ensuring the

droplets had ample time to reach their terminal speed (the terminal speed is normally reached in less than .025m by droplets less than 100μm diameter and 0.7m for a 500μm droplet). It was also attempted to conduct the calibrations at the same relative humidity as the final wetting pattern tests. However, some error will have arisen as it proved difficult to control the humidity in the wind tunnel and it fluctuated between 60 and 80%.

It should also be noted that the nozzles were directed *upstream* such that the droplets were indeed carried horizontally by the wind and not forced by the nozzle pressure. This nozzle direction also allowed for more turbulent mixing of the spray upon exit from the nozzle.

1.3.3 Design of Nozzle Array and Resulting Drop Size Distributions

Based on the calibration of a single nozzle, the layout for an array of nine nozzles was designed. A photograph of the nozzle array in the wind tunnel is given in Figure 4. The upstream spacing was chosen to give at least the range of drop sizes shown in Figure 3. It was not possible to precisely model these distributions, especially for all heights, but it is believed that an adequate modelling was achieved for this first study. An example of the model-scale drop size distributions resulting from the array is given in Figure 5 for the middle wind speed. The corresponding full-scale distribution is given in Figure 6. Distributions for all three wind speeds are given in Appendix B. These results are for the distributions in the centre of the tunnel for heights at the base of the Phase I building, very near the top of the building, and four heights in between. All heights were tested simultaneously for a 2 second duration. In comparing Figures 2 and 6, or Figures 3 and 5, it is seen that the achieved drop size distributions were biased towards the larger drops, relative to their target distributions. However, referencing the work of Choi [4], this is not believed to be a significant problem. It is also the authors' comment that short duration rainfall rates may be higher than the published hourly rates, suggesting larger drop size distributions. The analysis technique works on only a very small sample of the water sensitive paper and hence the curves are not as smooth as a more comprehensive analysis would yield. A few droplets were analysed as having been larger than physically possible when converted to their full-scale equivalents and these droplets have been removed from the distributions. The analysis technique is outlined in Appendix A. The Malvern was not used in the analysis for the array.

The lateral spacing of the nozzles was arrived at by overlaying the spread patterns found on 1m long strips of water sensitive paper laid across the tunnel until an equal density of droplets was found across the strip. It should be noted here that the tests from which the spacings were derived were only a 5 second duration and hence, the spacing was not necessarily ideal for a longer duration test or any other 5 second test (5 seconds model-scale equals 40 seconds full-scale).

Also shown in Figures 5 and 6 and in Appendix B are the model-scale and full-scale rainfall rates at each of the heights, calculated from the droplet stains on the water sensitive paper (see Appendix A). Averaging the rainfall rates over the Phase I building height, they are 24.5 mm/hr, 11.7 mm/hr and 3.0 mm/hr for building height wind speeds of 0.6 m/s, 1.5 m/s and 2.3 m/s respectively, all in model-scale. These translate to full-scale values of 0.69 mm/hr, 0.24 mm/hr and 0.06 mm/hr for building height wind speeds of 4.8 m/s, 12.0 m/s and 18.4 m/s respectively[1]. While the presumption of the rain simulation is that the droplets behave independently of one another and hence the rainfall rate is not important (aside from its effect on drop size distribution), it is

[1]Again, note that the *distributions* of drop sizes were representative of much higher full-scale rainfall rates.

ultimately necessary to know the rate such that a factor relating wetting rate on the building to rainfall rate can be determined. A simple collection and weighing of the rainfall in a dish at ground level was performed and gave similar values - over a 2 minute period, this simple method gave rainfall rates in the wind tunnel of 24.0 mm/hr, 9.8 mm/hr and 4.0 mm/hr for the same wind speeds mentioned above. The agreement is almost remarkable given that the water sensitive paper tests were only 2 *seconds* long. This lends confidence to the water sensitive paper method of testing and analysis and the authors consider this a very encouraging result. It should be mentioned that the practice of removing droplets which were larger than physically possible from the full-scale analysis does not result in any easily recognizable conversion trend from model to full-scale rainfall rates (these droplets were retained in the model-scale analysis).

The rainfall rates at ground level both across the wind tunnel and along the centreline of the tunnel at the building location are given in Table 1, in model-scale and full-scale. The rainfall rates are relatively consistent across the wind tunnel to a distance of 1 m from the centreline (important, as the edge of the test building is placed at up to 0.65 m from the centreline). As expected, there is more variation along the length of the tunnel, particularly for the lowest wind speed. The tests were run separately from the vertical profiles of rainfall rate discussed above, and while both sets of tests should ideally have been for a 2 second duration, there is likely some unavoidable error in the timing causing a discrepancy in the calculation of the rainfall rates. It should be noted though that an important design feature of the nozzle system was the addition of a release valve which allowed the spray to be turned off almost instantaneously. This allowed more control on the duration of the tests and prevented problems with variation in drop sizes during shut-down.

2 Wetting Patterns on Buildings

Two phases of testing were conducted. The first was to study the effect of wind speed and wind angle on the wetting patterns for a "basic" building, with an exploratory look at the effect of surface features - in this case, balconies. The second phase was a study of the effect of building height and larger scale architectural features such as cornices and a peaked roof.

2.1 Test Buildings

2.1.1 Phase I

The basic test building chosen by CMHC was an 18 storey block type apartment building located in Ottawa. The full-scale height is approximately 60m with plan dimensions of 81m x 18m. Balconies protrude from the wide sides of the building. The exposure is suburban. The geometric scale of 1:64 resulted in a simple model having height, width and depth dimensions of 0.94m, 1.3m, and 0.29m respectively. The model was constructed with a wooden core and a foam exterior with provision for optional balconies. Each balcony is 1.2 m high, 2.4 m wide, and protrudes 0.75 m from the face of the building in full-scale.

2.1.2 Phase II

In this phase, three "basic" buildings were studied:

Building A: 60m high x 40m wide x 20m deep (full-scale)
Building B: 40m high x 40m wide x 20m deep
Building C: 20m high x 40m wide x 20m deep

These allowed a study of the effect of building height within the same boundary layer, with inherent changing aspect ratio. The width of these buildings was decreased from that of Phase I to reduce the blockage in the wind tunnel.

Along with the basic buildings, the effect of several large architectural features were studied:

- **Cornice** - the first was 2m deep x 4m high (full-scale), while the second was 1m deep x 4m high. Both cornices fit around all four sides of the building and did not increase the overall height of the building.

- **Peaked Roof** - gable ended with the two sloping sides at 45 degree angles. The gable ends were at the narrow sides of the building.

- **Inset Corners** - an extension was added to the narrow ends of the building which provided an inset corner of approximately 2.5m x 2.5m (full-scale) the full height of the building.

In addition, the wetting pattern on a circular building was briefly explored.

2.2 Test Method

While several options were examined, the water-sensitive paper was used in the study of wetting patterns. In each test, masonite boards the size of the building faces were covered with a grid pattern of the water-sensitive paper and were fastened to the model. In this way, the water-sensitive paper method provided an immediate and permanent visual picture of the wetting pattern on the building faces, while also allowing quantitative analysis. For most of the tests, one of each of the wide and narrow sides of the building was covered with the water sensitive paper (the sides tending to windward).

The test durations were timed according to the valve on/off. This avoided complications in timing when the rain starts/stops hitting the building, as there is a delay between the time the nozzles are turned on/off and the time the rain starts/stops hitting the building. The duration of the tests was dictated by the wettest area of the building - it was attempted to stop the tests before individual drops became indistinguishable on the water-sensitive paper, although this proved difficult. Before testing, the relative humidity in the wind tunnel was adjusted to the calibration humidity if necessary. Typically, it needed to be increased, and this was accomplished by running the nozzles for a period of time with the wind tunnel fan on.

A summary of the tests conducted for Phases I and II is given in Table C.1 in Appendix C and Table D.1 in Appendix D respectively. Note that a building angle of 0 degrees corresponds to the wide side of the building being oriented as a windward wall, as shown in Figure 7.

Also included as part of the test program was a video of the interaction of the water droplets with the wind flow around the building. In particular, smoke was injected into the airflow at the same time to illustrate the differences in flow patterns of the droplets and the air.

2.3 Analysis Method

As mentioned, the method of covering the building faces with a grid of water sensitive paper gave a permanent visual picture of the wetting patterns. These pictures themselves provided valuable information, allowing general observations to be made as well as quickly identifying the effects of specific architectural features. This visual and qualitative method was used in both Phases I and II. Note, however, that there is some distortion in the visual comparisons arising from the non-linear relationship bewteen full-scale and model-scale drop sizes. Although this is unlikely to alter qualitative assessments of the patterns, the quantitative assessments must account for this non-linear relationship.

The test method also allowed a quantitative analysis of *relative wetting rates* at select locations on the building by sizing the droplet stains on the water sensitive paper and calculating the volumes of water they represented (see Appendix A). Further, *wetting rates* were calculated by incorporating the test duration in the calculations, and "*local intensity factors*" were determined by further using the rainfall rate (the averages of the rainfall rates over the height of the building given in Section 1.3.3 were used). The local intensity factors are a ratio of the wetting rate on the building to the rainfall rate. As the quantitative analysis proved very labour intensive, it was not possible for all locations or all tests. Instead, this detailed analysis was conducted for only a select number of locations in the Phase I tests.

2.4 Results

2.4.1 Phase I - Visual

An example of the wetting patterns on the grid of water sensitive paper for the basic building are shown in the photographs in Figure 8 for a building angle of 0 degrees and a wind tunnel speed of 1.5 m/s at building height; photographs of the wetting patterns from all tests are given in Appendix C. The complete wetting patterns from one test, that is the wetting patterns on both faces obtained simultaneously, are shown in Figures a) of each. Figures b), c) and d) of each show the same wetting patterns in more detail - Figures b) show the upper corner of the wide face, Figures c) show even more detail in this upper corner, and Figures d) show the upper half of the narrow face. Note that Figures d) are turned sideways on the page. It is possible to see the effects of both angle and speed on the wetting *pattern* (*i.e.*. relative intensities of wetting on the same building face). Also, for each wind speed, the effect of angle on the intensity of wetting can be directly inferred since the test durations for each speed remained constant. The effect of speed on the intensity of wetting cannot be seen directly from the photographs since rainfall rates and test durations varied between speeds.

The following observations can be made:

Effect of Angle on Wetting Pattern

Windward Wall:

- A wetting pattern similar to that shown in [12] is found, where the top corner of the face is the wettest, followed by the top and side edges. See Figures C.1b, C.4b , C.9b, C.3d, C.8d, and C.11d.

Side Wall (i.e. parallel to the wind direction):

- The side face remains relatively dry. See Figures C.1d, C.4d , C.9d, C.3b, C.8b, and C.11b.

Other Angles (30, 45 and 60 degrees):

- The effect of angle on the wetting pattern is partially dependent on the aspect ratios of the building:

  For the *wide* face of the basic building tested, the upstream edge is the wettest with the downstream edge remaining relatively dry. The top edge also still sees relatively heavy wetting, particularly towards the upstream edge. The more heavily wetted region seems to get smaller, approaching the upstream edge, as the inclination between the building face and the wind direction decreases (see for example Figures C.4b, C.5b, C.6b, C.7b and C.8b).

  For the *narrow* face and inclinations of 45 and 60 degrees between the face and the wind direction, the wetting pattern is similar to that for a windward wall (see Figures C.2d, C.6d, C.7d and C.10d). However, for the inclination of 30 degrees, higher wetting occurs along the downstream edge of the face than the upstream (see Figure C.5d). This is presumably due to separation. Note that this last observation stems from only one test.

Effect of Angle on Intensity of Wetting

- In general, there is a trend towards less intense wetting of a face as it changes from a windward exposure to a side exposure.

Effect of Speed on Wetting Pattern

Windward Wall:

- It appears that increasing wind speed results in greater wetting in the centre region of the face relative to the edges, although this is not conclusive from these tests. It is particularly apparent in comparing tests from the lowest wind speed (4.8 m/s full-scale) with either of the other two speeds for the narrow face (compare Figures C.3d, C.8d and C.11d).

45° Angle:

- There seems to be a similar effect for the wide face where, with increasing wind speed, the wetted region "spreads" downstream further from the upstream corner (compare Figures C.2b, C.6b and C.10b). This effect is not so visible for the narrow face where the wetting pattern more closely resembles that for a windward face.

Effect of Balconies

- The effect of this surface feature seems minimal for wind perpendicular to the building face (see Figures C.12a,b). However, there is some *local* sheltering effect of the balconies for glancing wind angles (see Figure C.12c). As expected, very little wetting still occurs for winds parallel to the face (see Figure C.12d).

It should be noted that, again, these tests were only between 5 and 10 seconds long, representing approximately one minute in full-scale. Unfortunately, this may result in considerable variability from test to test. Nevertheless, the trends mentioned above are evident.

An interesting observation recorded on video was the "sheeting action" of the rain as it responds to the gustiness of the wind.

2.4.2 Phase I - Quantitative

Results of the quantitative analysis are shown in Figures 9 to 12. The numbers indicated on the building faces in these figures are the local intensity factors. They have been determined from a 0.4 m^2 area (full-scale) centred about the points shown. Very generally, the trends shown by the local intensity factors agree with the visual results given in Section 2.4.1.

The local intensity factors do, however, show some inconsistencies. In critiquing the method, a comparison was made between the local intensity factors actually obtained, and the expected trend of values from a simple visual inspection of the water sensitive paper samples. The two were often but not always in agreement. It should be emphasized here that the quantitative analysis was conducted only once for each location and that it is partially subjective. Some possibilities for errors are given in Appendix A.

Effect of Angle on Local Intensity Factors

Windward Wall:

- Aside from the inconsistencies mentioned, the local intensity factors shown in Figures 9 and 10 seem to relate the "classic" wetting pattern. Corner intensity factor values ranged from about 0.15 to 2.5 with ratios from about 2 to 50 between the rain impact at the corners and that at the central region of the faces.

Other Angles (30, 45 and 60 degrees):

- For the *wide* face, the effect of a glancing wind angle is shown in Figure 12 for an angle of 45 degrees between the wind direction and the face. The observation of Section 2.4.1 that wetting decreases significantly from the upstream edge of the face to the downstream edge is confirmed with an indication of the magnitude of this variation. Along the top edge for example, it varies from a value of approximately 0.7 at the upstream corner to a value of 0.05 at the downstream corner for a wind speed of 12.0 m/s. Of note is that the local intensity factor for this upstream corner is quite close in value to that for a windward wall at the same speed.
- For the *narrow* face, Figure 11 shows the effect for angles of 30 and 45 degrees between the wind direction and the face. It is seen that the observation that wetting of a face is less intense as it changes from a windward exposure to a side exposure is particularly true in the lower 80% of the face. Some zones along the top edge remain quite heavily wetted, even for the angle of 30 degrees where the local intensity factor at the downstream top corner is still 0.52.

Effect of Speed on Local Intensity Factors

Windward Wall:

- Local intensity factors can increase fairly significantly with increasing wind speed. Figure 9 shows the local intensity factors for the *narrow* face for three wind speeds. With increasing speeds of 4.8 m/s, 12.0 m/s and 18.4 m/s at building height (full-scale), top corner values were approximately 0.15, 0.7 and 2.5 respectively; corresponding values in

the central lower half of the face were approximately 0.003, 0.4 and 0.7 respectively. A similar effect of wind speed is seen in Figure 10 for the *wide* face where with wind speeds of 12.0 m/s and 18.4 m/s, corner values were approximately 0.9 and 1.5 respectively; corresponding values in the central lower half of the face were approximately 0.2 and 0.8 respectively.

- Of note is that for the highest wind speed (18.4 m/s full-scale), the local intensity factors seem lower overall for the wide face than for the narrow face. This effect is not so apparent for the lower wind speed of 12.0 m/s, and a comparison is not available for the lowest wind speed.

It would be of great interest to compare the local intensity factors herein with results obtained numerically, such as those by Choi [3]. While a direct comparison with Choi's work is impossible due to differences in building geometry and the fact that his local intensity factors are averaged over much larger areas, some encouraging comments can be made:

1. The local intensity factors obtained in the current study and those obtained by Choi are generally within range of each other. Choi's numerical results are for buildings of H:W:D of 4:1:1 and 4:8:2, wind speeds at building height (40m) of 6.3 m/s and 12.6 m/s, and a similar mean wind speed profile as the current study. Hence, the statement stems from a rough comparison between the "wide" face in the present tests with Choi's 4:8:2 building, and the "narrow" face in these tests with Choi's 4:1:1 building. Only results for the front faces perpendicular to the wind direction are available.
2. Choi also found the local intensity factors over the front face to increase significantly with increasing wind speed
3. Choi found that as a building gets wider, the local intensity factors decrease. This is in agreement with observations in the current study for the highest wind speed.

2.4.3 Phase II - Visual

The effect of building height and architectural features on the wetting pattern and its intensity can be directly inferred from the Phase II test photographs since the durations for each test remained constant. The photographs from all Phase II tests are shown in Appendix D. The following observations can be made:

Effect of Building Height

Photographs of the wetting patterns on the grid of paper for the three basic buildings of Phase II are shown in Figures D.1 to D.3. Figures a), b) and c) of each show the wetting patterns for Buildings B, A and C respectively.

Windward Wall:

- The general wetting pattern remains the same, regardless of building height. It does appear, however, that the intensity of wetting along the top edge increases with building height, likely due in part to the increase in wind speed at building height (see Figures D.1 and D.3).

Side Wall:

- It appears that there is little if any effect of building height on the wetting of a side wall. The side wall remains quite dry in all cases (see Figure D.3).

45° Angle:

- The results for this building angle (see Figure D.2) are inconclusive when related to the results of Phase I and would require further investigation for an explanation. The wetting patterns on both faces of the shortest building, Building C, resemble that for a windward face. As the building height progressively increases from Building C to Building A, the wetting on both faces becomes progressively more intense at the upstream edge relative to the downstream edge.

Effect of Cornice

- The cornice provides excellent protection to the face of the building in the area directly below the cornice. This applies to all heights and to all angles examined (0, 45 and 90 degrees). The dry area for the 2m cornice is approximately 1.5 m high and extends the entire width of the building; that for the 1m cornice is approximately 0.75 m high. However, the cornice itself sees extensive wetting. The wetting pattern on the cornice resembles that on a building face itself. See Figures D.4, D.5 and D.6.
- Aside from the top dry zone, the wetting pattern on the building face is the same as for that without a cornice. It does appear, however, that the intensity of wetting is less at the edges. The middle region of the faces seems to have received the same amount of rain impact as for the case without the cornice.

Effect of Peaked Roof

- It appears that, like the cornice, the peaked roof is also successful in reducing rain impact on the front face (although perhaps not as effectively as the cornice). Compare Figure D.7 with the base case in Figure D.1a. The general wetting pattern is the same as the base case.
- The windward side of the peaked roof receives significant rain impact; the leeward side is relatively dry near the peak with a little wetting towards the base of the roof. The end of the roof, like the side face, is dry.

Effect of Inset Corners

- This architectural modification does not seem to have any effect on the windward face. Of note though is that the windward face of the indentation receives very little rainfall. That which it does receive falls mostly in the top corner. (see Figure D.8)

Circular Cylinder

- The top windward edge to approximately 45° either side of the centreline receives the greatest rain impact, followed by the windward centreline. There is no wetting past approximately 60° either side of the windward centreline. (see Figure D.9)
- The roof is wettest towards the back (i.e. downstream), with wetting approximately constant in the back two-thirds.

Longer Duration Test with Cornice

- The wetting pattern for a 27 second duration test with the 2m cornice is shown in Figure D.10. The droplet stains are no longer distinguishable from one another, but the wetting pattern is quite distinct. It must be realized though that there may in fact be more contrast in wetting between the cornice and the central portion of the building face than it appears since the water sensitive paper can only indicate a *first* wetting. The test was continued until water started dripping from the cornice; the test is invalid for this situation of surface water migration.

3 Conclusions

This report has presented the development and findings of a new method which simulates both wind-driven rain and the wetting patterns on buildings. The results are, for the most part, encouraging. The following main conclusions can be made:

Simulation of Wind-Driven Rain

1. An array of 9 nozzles directed upstream at a 2m height in the Boundary Layer Wind Tunnel II can be used to simulate wind-driven rain; modelling can be achieved with a length scale of 1:64 and a velocity scaling of 1:8 (Froude scaling). A calibration for a single nozzle is required for each wind speed to determine the layout of the array.
2. The drop size distributions obtained at the test site were measured as being slightly biased towards the larger drops relative to the target distributions. This was not believed to be a significant problem.
3. Due to the "filtering effect" with discrete nozzles, it is impossible to obtain a *completely* uniform drop size distribution at a test site in the wind tunnel. However, the uniformity achieved over the building height and across its width was believed adequate.
4. Two methods were found for the drop size analysis - a water sensitive paper which turned from yellow to blue on contact with water, and a laser-based particle sizer. Some errors are encountered for both in this application, but reasonably similar results are obtained for each.
5. Rainfall rates in the wind tunnel are measured quite successfully with the water sensitive paper.

Simulation of Wetting Patterns on Buildings

1. The wetting patterns on building faces can be determined using a grid of water sensitive paper. The method allows an immediate visual picture of the impact wetting pattern (not surface migration).
2. Wetting rates can be calculated by sizing the droplet stains on the water sensitive paper and using the test durations. Local intensity factors can further be calculated using the rainfall rates.

3. Test durations are very limited with the water sensitive paper as it is necessary to keep the droplet stains distinct from one another. This may cause considerable variability in results.

Effect of Building Angle and Wind Speed on Wetting

1. The "classic" wetting pattern is found for the windward wall whereby the top corner of the face is the wettest, followed by the top and side edges. Local intensity factors at the corners ranged from about 0.15 to 2.5 in the cases analysed. The corners were subjected to 2 to 50 times the rain impact as the central region of the face.
2. The side wall remains relatively dry. The wetting pattern for glancing wind angles varies with aspect ratio and angle; there can be significant wetting along the top edge, upstream edge, and occasionally even the downstream edge for angles of 30, 45 and 60 degrees between the building face and the wind direction .
3. Local intensity factors can increase fairly significantly with increasing wind speed.

Effect of Building Geometry and Architectural Features on Wetting

1. The general wetting pattern on a windward wall remains the same regardless of building height, although the intensity of wetting along the top edge likely increases with increasing height.
2. A wide face may have lower local intensity factors than a narrow face in a windward situation, but this is not conclusive.
3. A cornice can be very successful in protecting the top of a building face just below the cornice. It may also decrease the wetting at the side edges. The cornice itself gets very wet, but provides a good opportunity for drainage and therefore protection of the building face from surface migration.
4. A peaked roof also seems to reduce rain impact on the front face.
5. Balconies only have a local sheltering effect for glancing wind angles.

Recommendations for Future Work

This first study known to these authors of wind-driven rain and wetting pattern simulation in a wind tunnel has shown it to be a viable method. Being a new area of research, there remain many opportunities for improvements and further study. Some suggestions are listed below.

- To reduce the problems of "filtering" of drop sizes encountered with a discrete nozzle system, provide additional mixing at the nozzle exits to create a large cloud of droplets.
- Explore the idea of uniform drop sizes and "building" the spectra.
- Examine tracer and electrostatic charging methods for measuring wetting rates which would allow longer test durations.
- Continue the work on architectural modifications to mitigate wetting rates.

REFERENCES

[1] Best, A. C. " The Size Distribution of Raindrops", Quarterly Journal of the Royal Meteorology Society", Vol. 76, pages 16-36, 1950.

[2] Brazier-Smith "On the Shape and Fall Velocities of Raindrops", Journal of the Royal Meteorological Society", Vol. 118, pages 756-, 1992.

[3] Choi, E.C.C. "Simulation of Wind-Driven Rain around a Building", Journal of Wind Engineering and Industrial Aerodynamics, Vol. 46-47, pages 721-729, 1993.

[4] Choi, E.C.C. "Parameters Affecting the Intensity of Wind-Driven Rain on the Front Face of a Building", Proceedings of the Invitational Seminar on Wind, Rain and the Building Envelope, The University of Western Ontario, London, Canada, May 16-18, 1994.

[5] CAN/CSA-A440-M90 (1990), Windows, A National Standard of Canada.

[6] Ciba-Geigy Limited "Water-Sensitive Paper for Monitoring Spray Distribution", Basel, Switzerland.

[7] Gunn, R. and Kinzer, G. D. "The Terminal Velocity of Fall for Water Droplets in Stagnant Air", Journal of Meteorology, Vol. 6, Pages 243-248, 1949.

[8] Inculet, D., Surry, D. and Skerlj, P.F. "The Experimental Simulation of Wind and Rain Effects on the Building Envelope", to be presented at the International Conference on Building Envelope Systems and Technology, Singapore, December 7-8, 1994.

[9] Malvern Instruments "2600 Particle Sizer User Manual", Malvern, Worcestershire, England.

[10] Markowitz, A. M. "Raindrop Size Distribution Expressions", Journal of Applied Meteorology, Vol. 15, Pages 1029-1031, 1976.

[11] Marshall, J. S., Langille, R. C. and Palmer, W. McK. "The Distribution of Raindrops with Size", Journal of Meteorology, Vol. 5, pages 165-166, 1948.

[12] Robinson, G. and Baker, M. C. "Wind-Driven Rain and Buildings", Division of Building Research, National Research Council of Canada, Technical Paper No. 445, 1975.

[13] Surry, D., Inculet, D.R., Skerlj, P.F., Lin, J-X., and Davenport, A.G. "Wind, Rain and the Building Envelope: A Status Report of Ongoing Research at the University of Western Ontario", Proceedings of the Invitational Seminar on Wind, Rain and the Building Envelope, The University of Western Ontario, London, Canada, May 16-18, 1994 (to be published in the Journal of Wind Engineering and Industrial Aerodynamics).

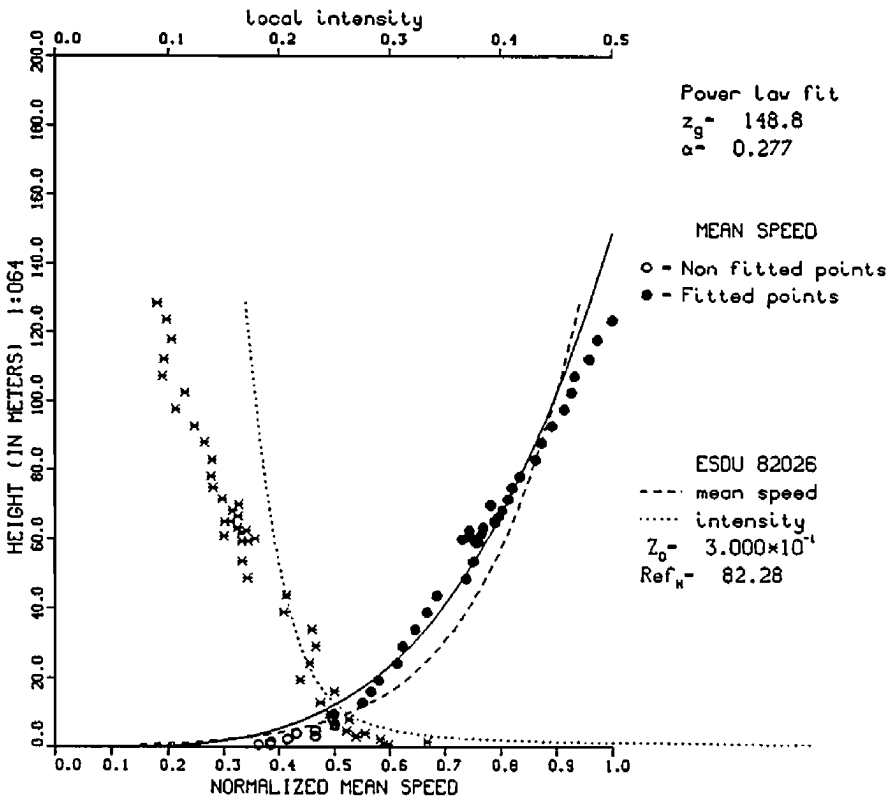

Figure 1. Mean Speed and Turbulence Intensity Profiles at the Test Site

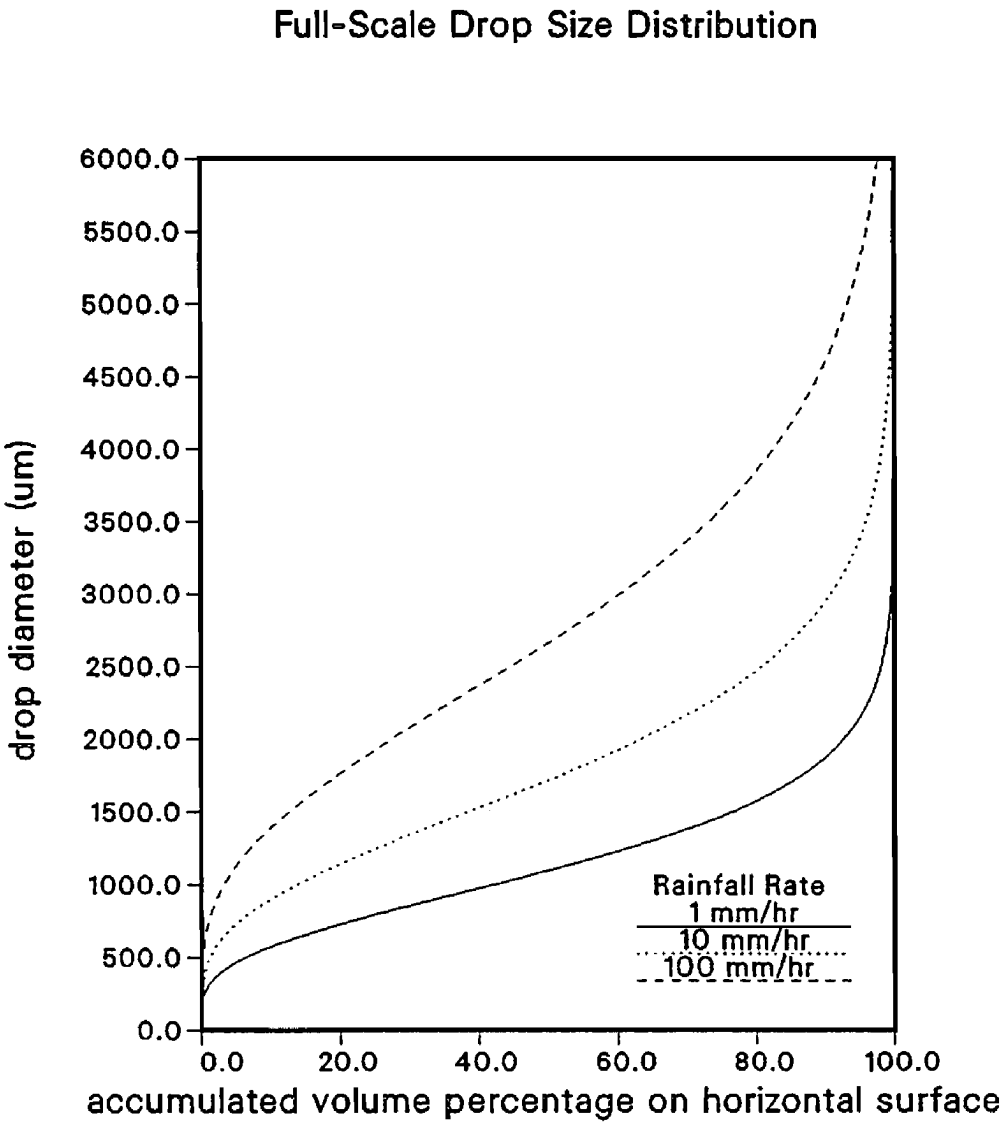

Figure 2. Target Full-Scale Drop Size Distribution

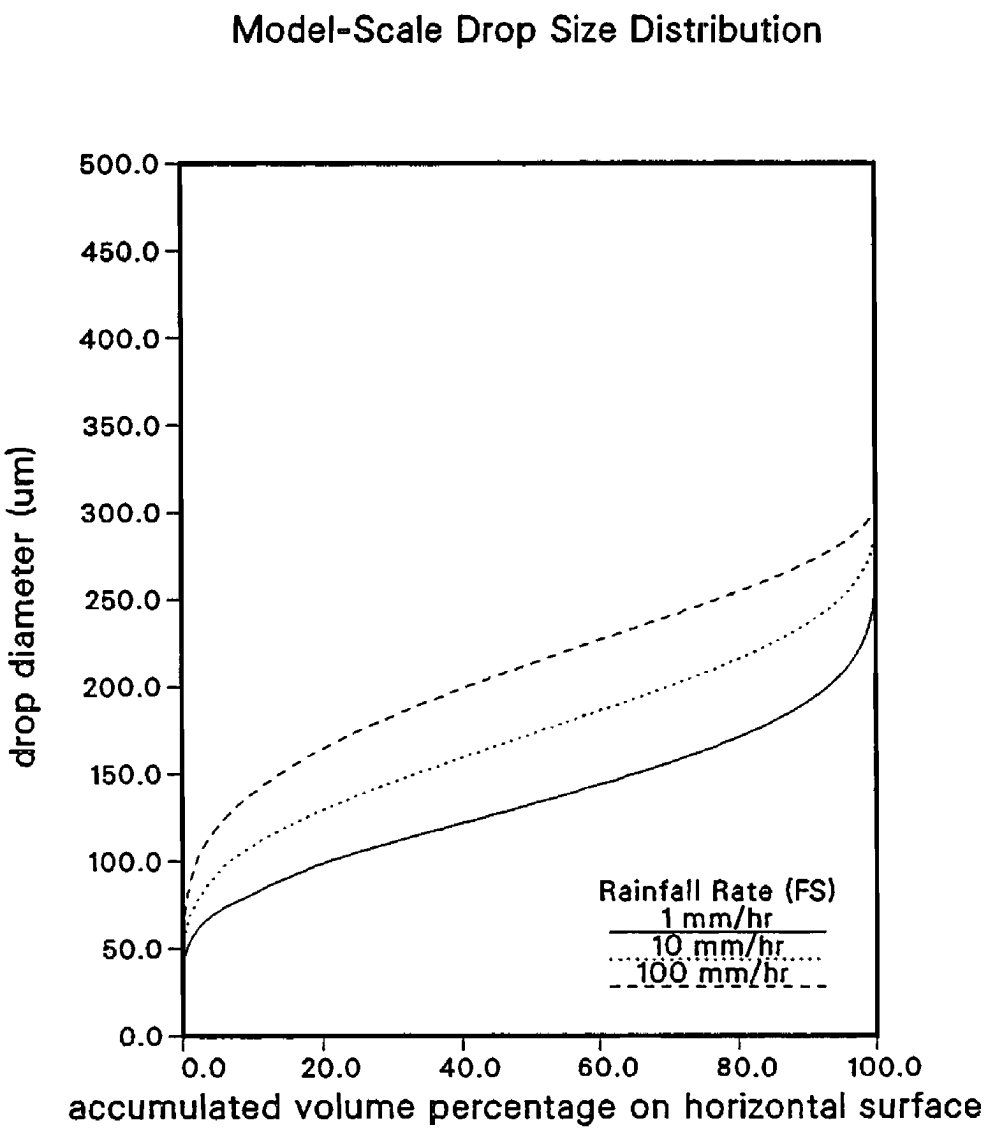

Figure 3. Target Model-Scale Drop Size Distribution

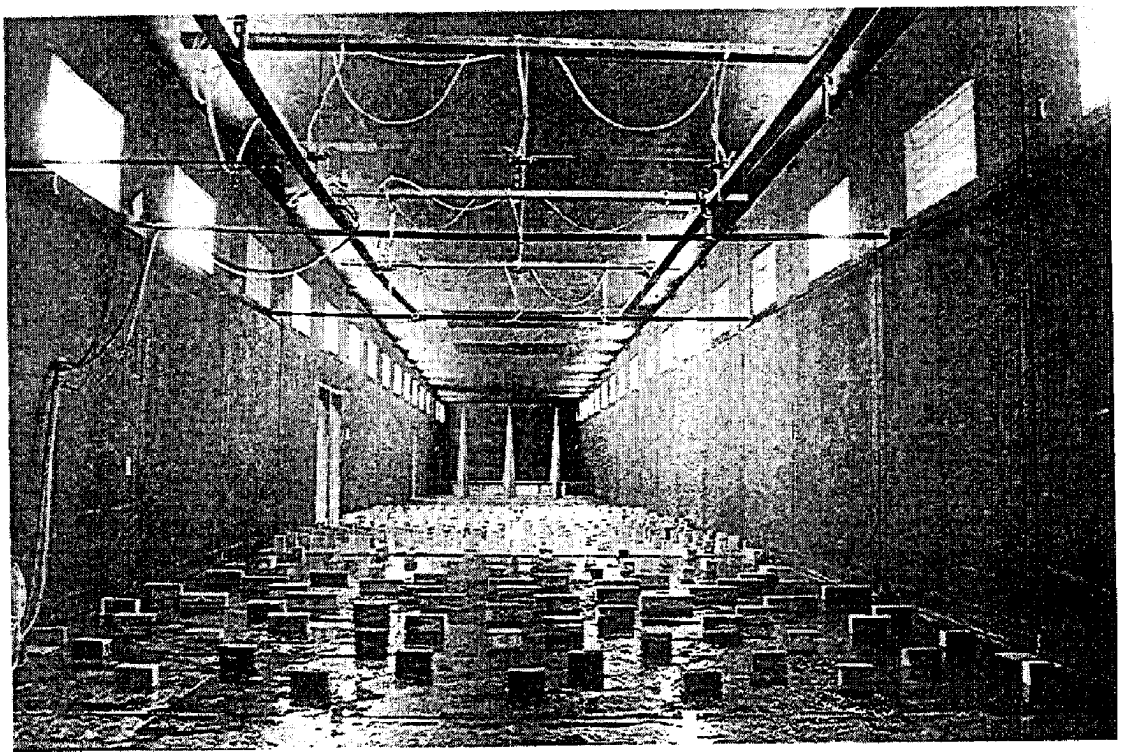

Figure 4. Nozzle Array in the Wind Tunnel

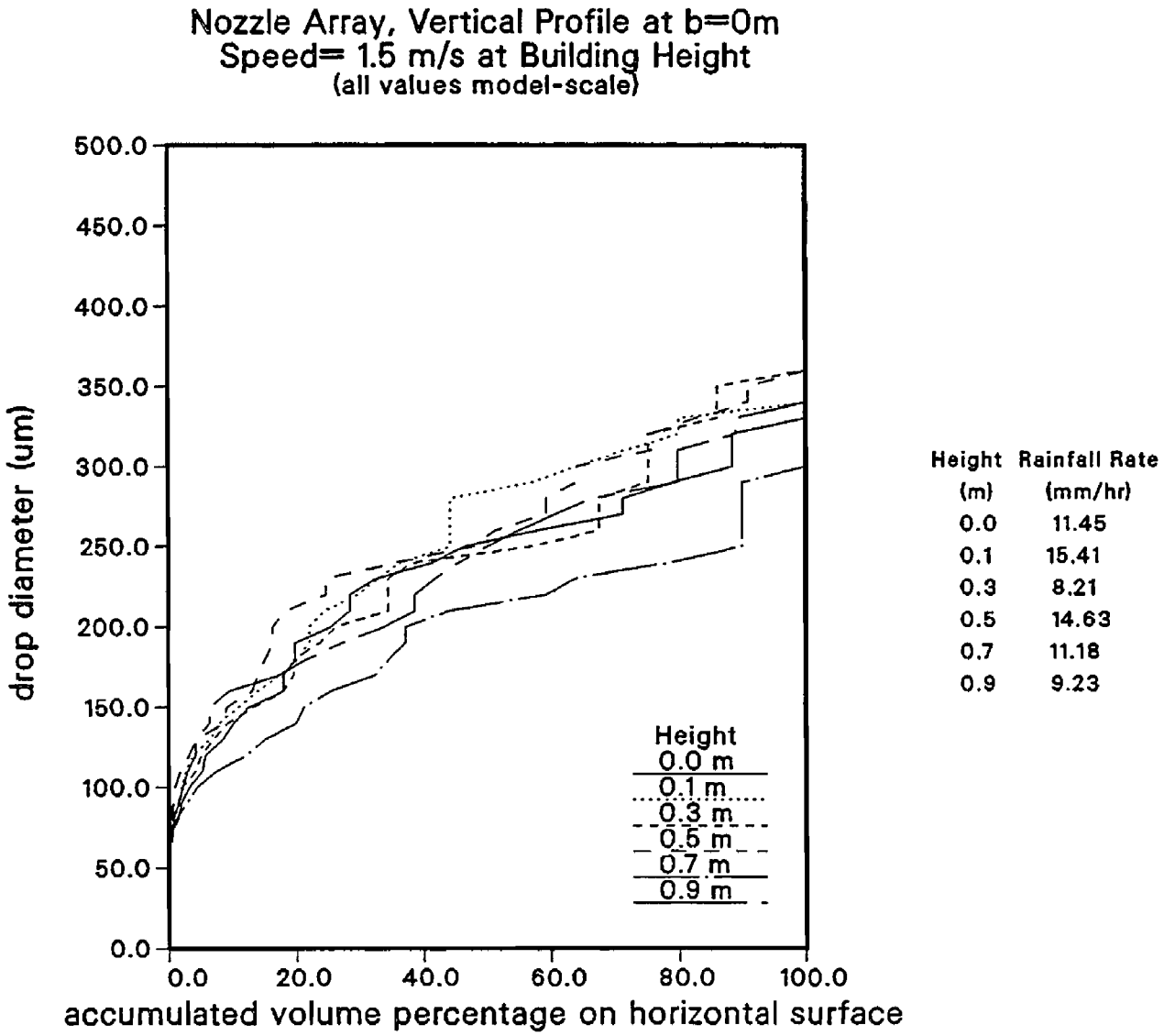

Figure 5. Model Scale Drop Size Distributions from Nozzle Array, Wind Tunnel Speed at Building Height= 1.5 m/s

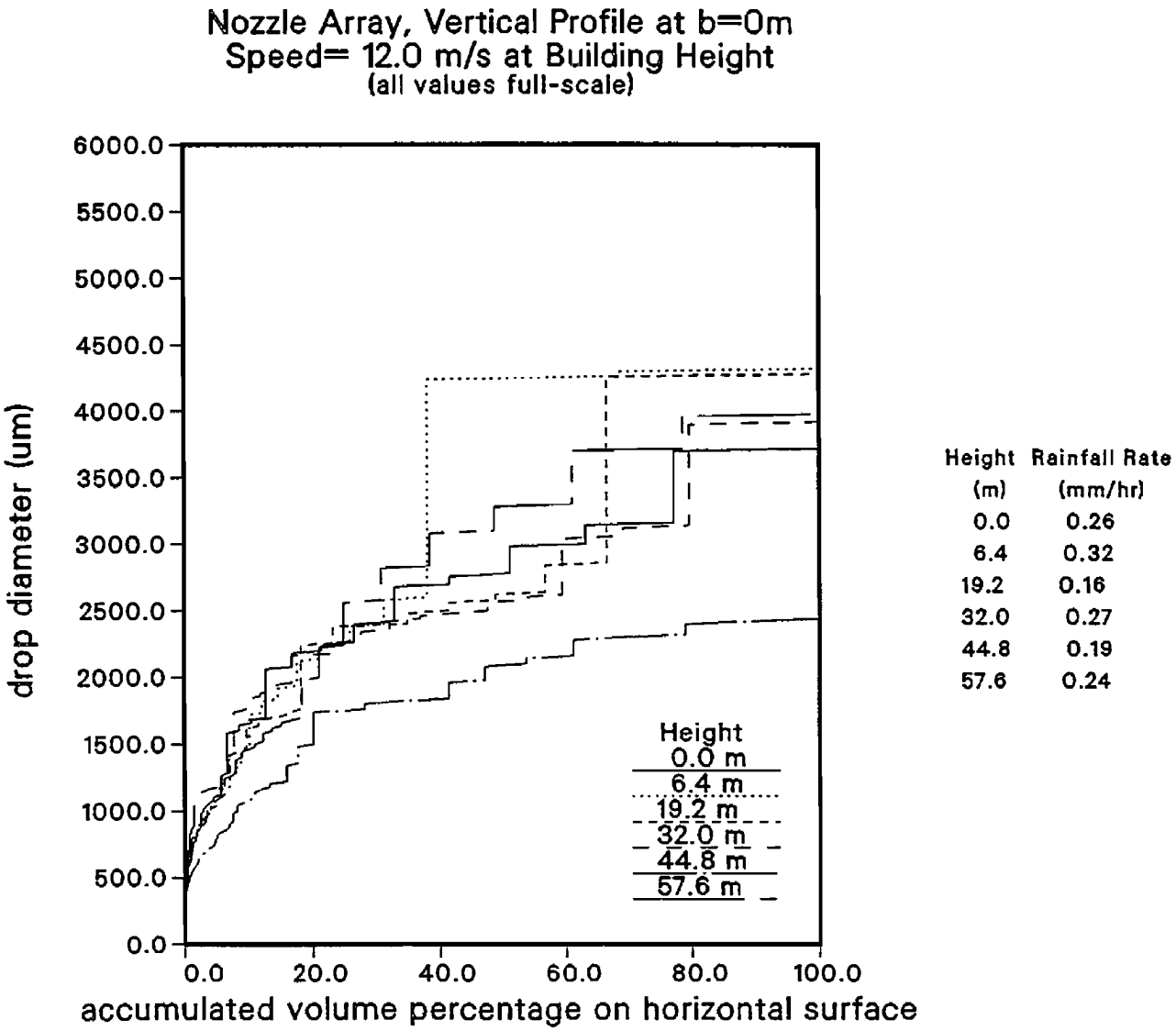

Figure 6. Full Scale Drop Size Distributions from Nozzle Array, Wind Speed at Building Height= 12.0 m/s

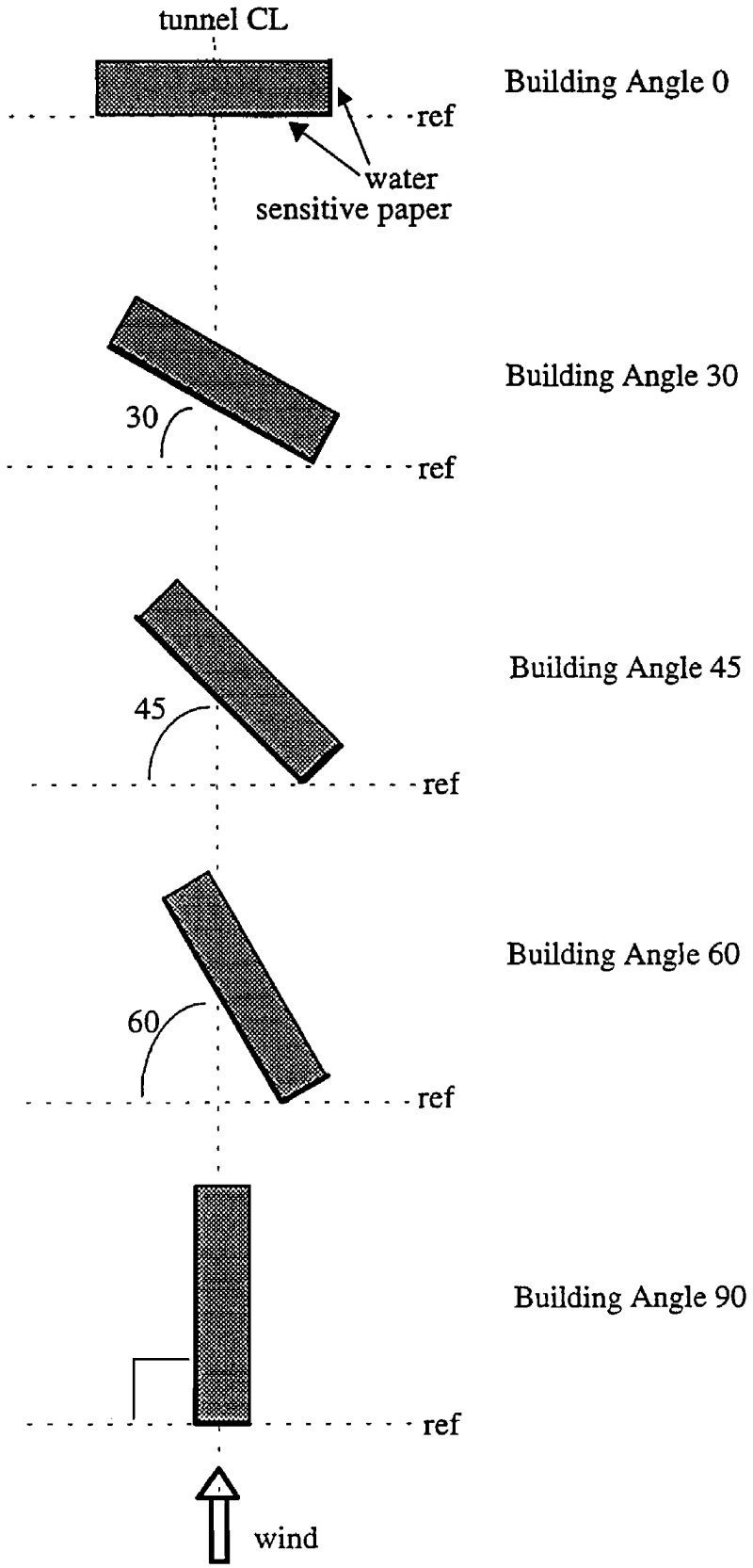

Figure 7. Schematic of Building Angles Tested , Phase I

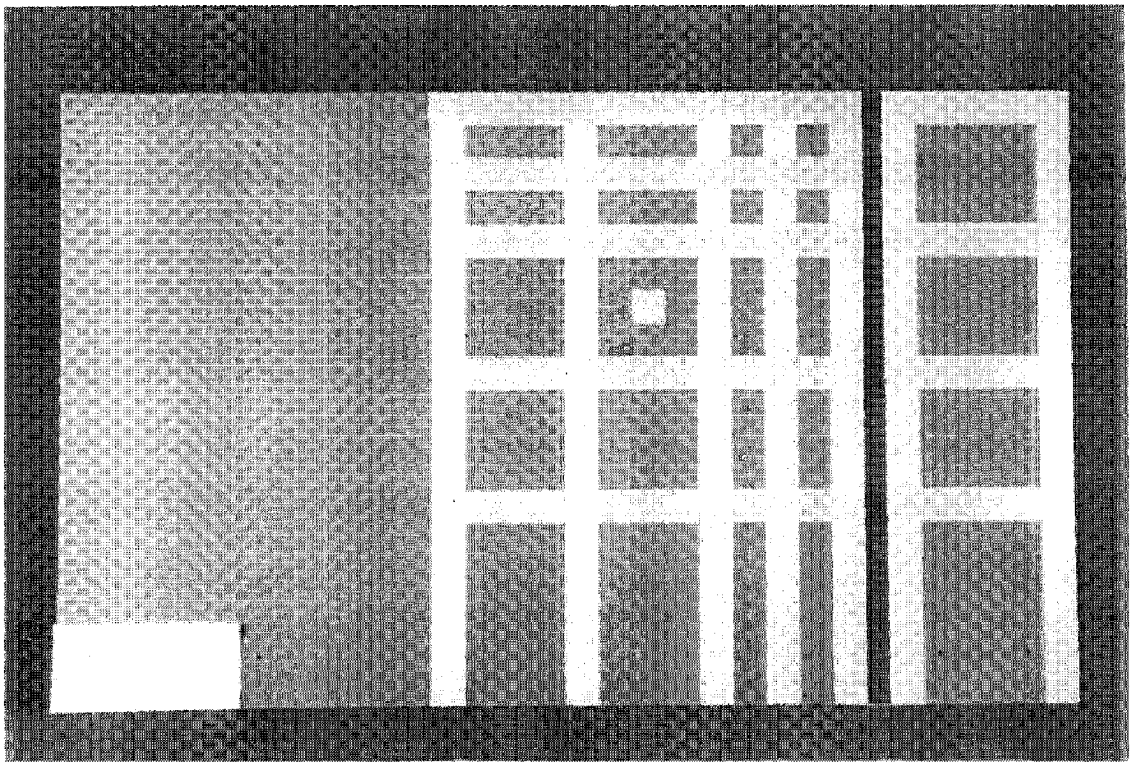

a) complete

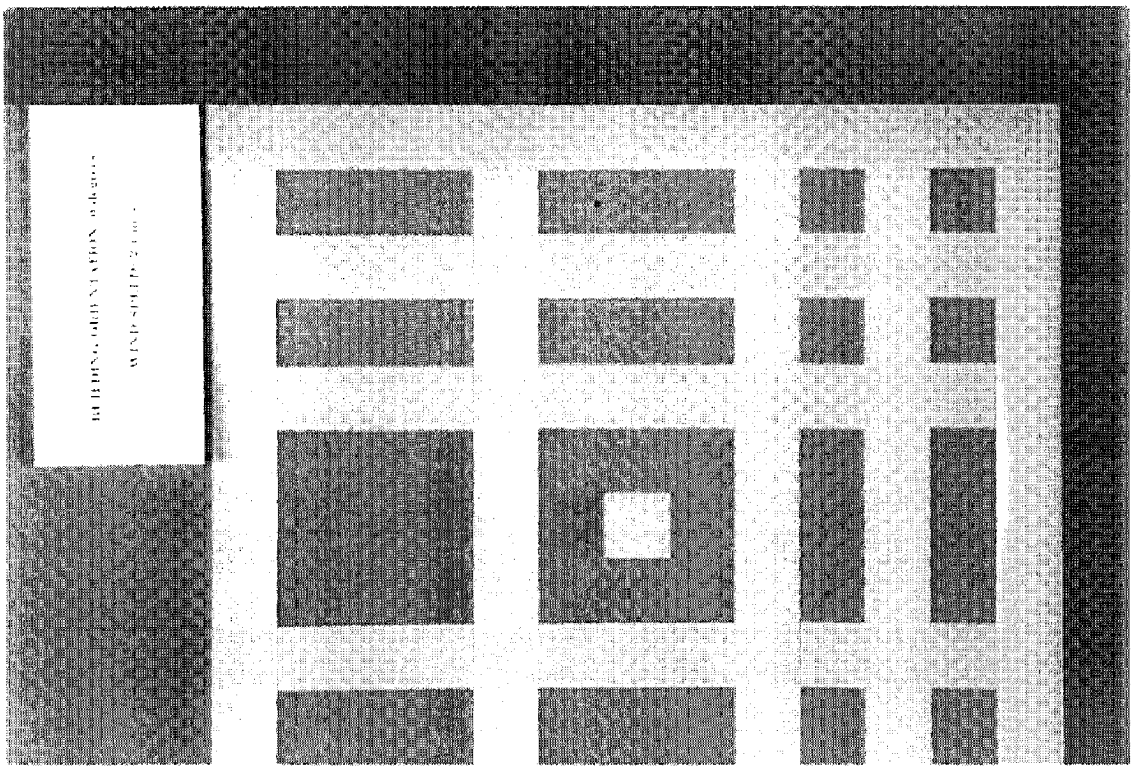

b) wide side, top quarter

Figure 8. Wetting Patterns for Phase I, Building Angle= 0 degrees, Wind Tunnel Speed= 1.5 m/s at building height

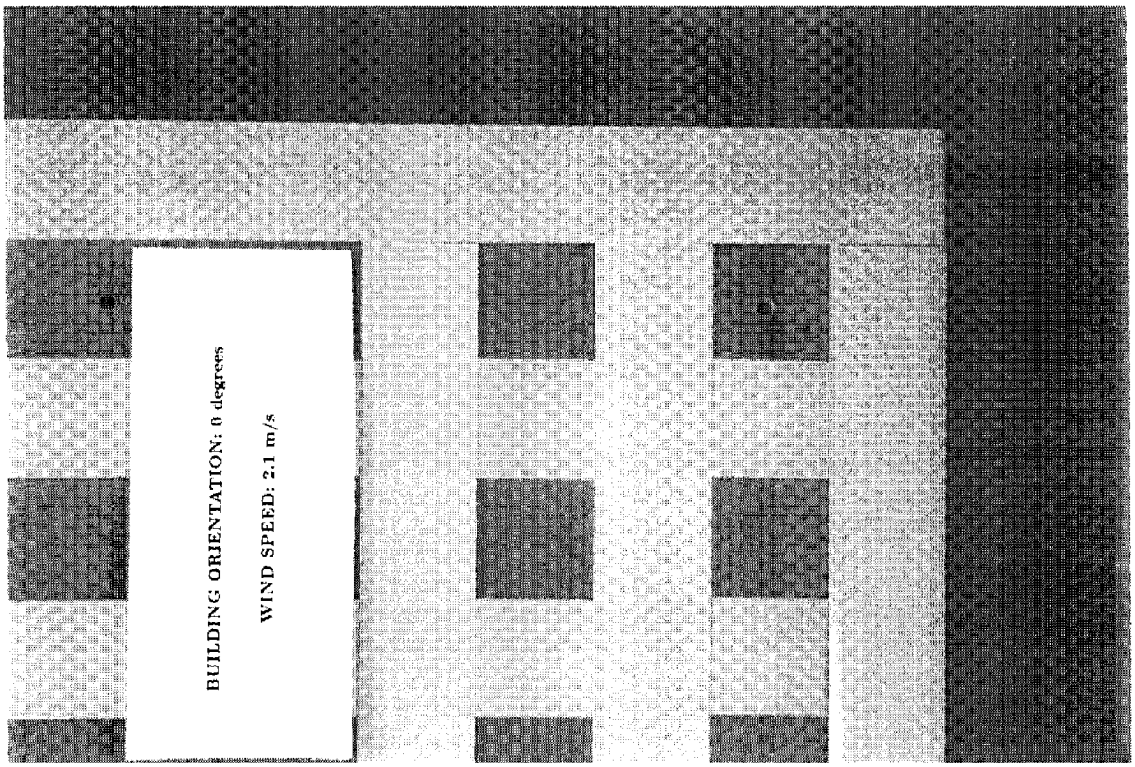

c) wide side, top corner

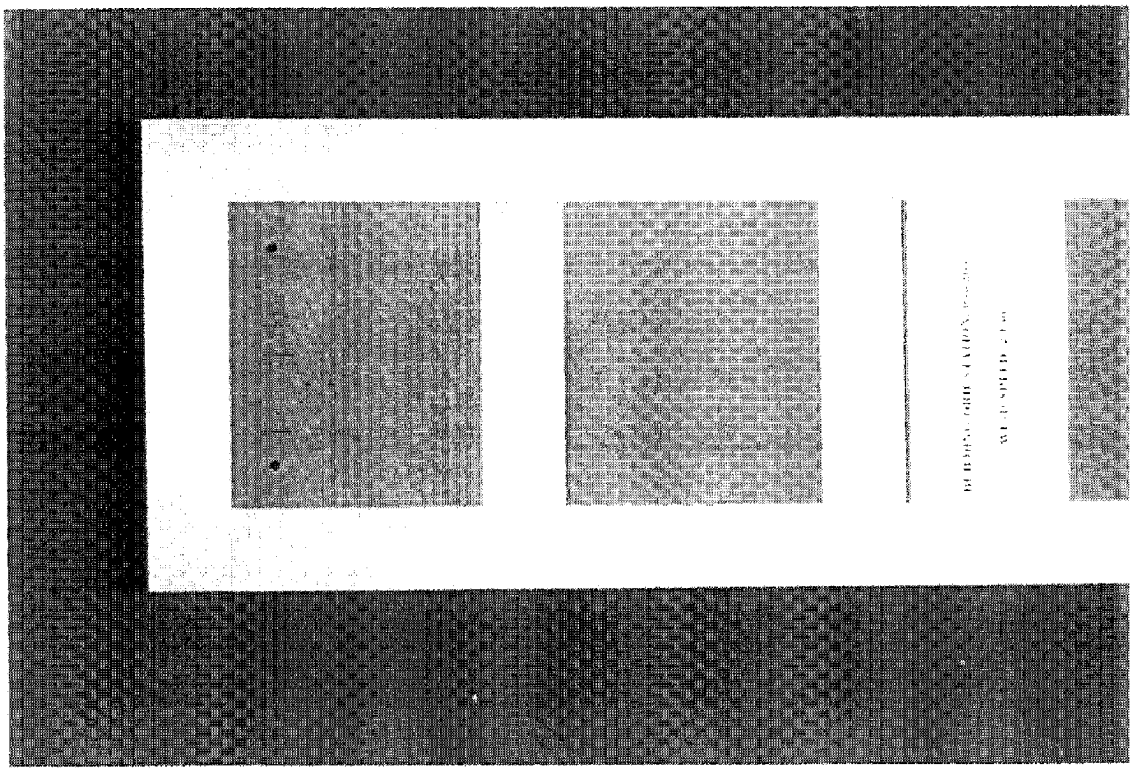

d) narrow side, top half

Figure 8. Cont'd

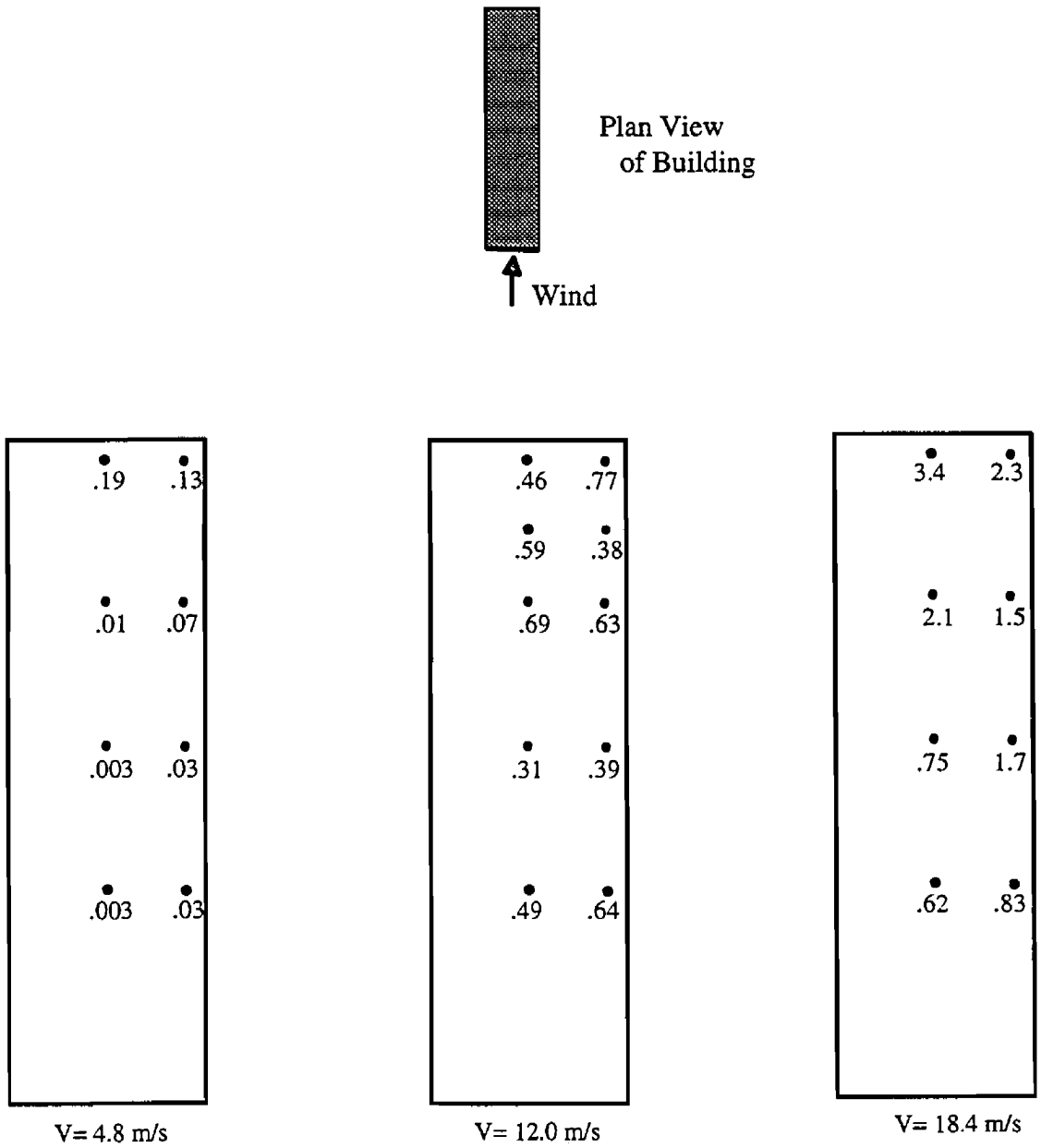

Figure 9. Full-Scale Local Intensity Factors for Narrow Face, Building Angle= 90 degrees

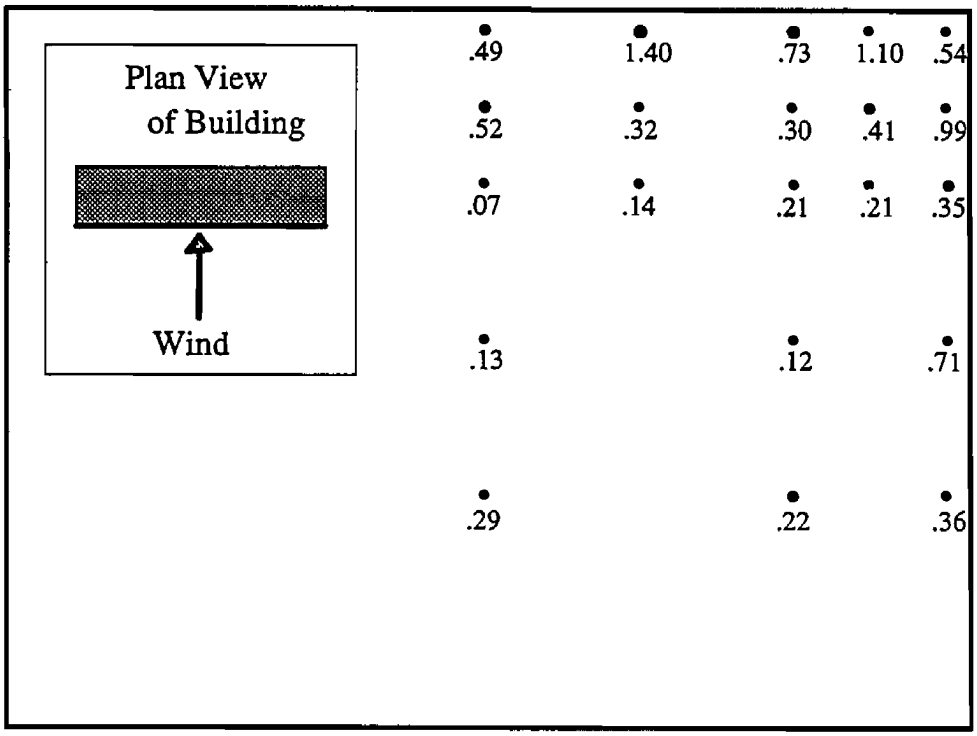

V= 12.0 m/s

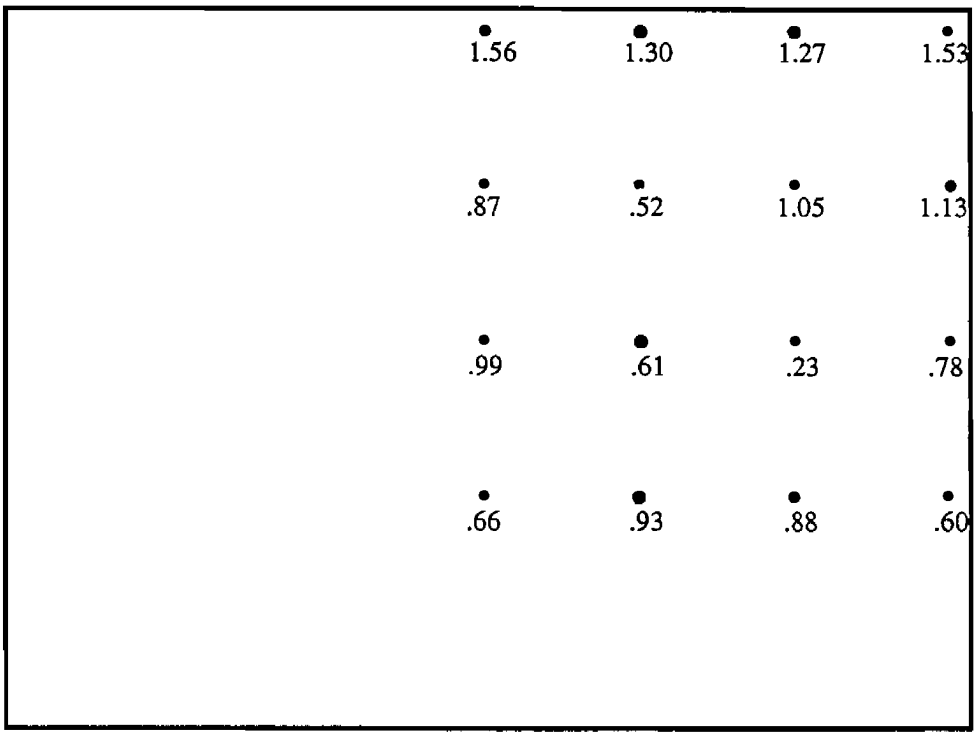

V= 18.4 m/s

Figure 10. Full-Scale Local Intensity Factors for Wide Face, Building Angle= 0 degrees

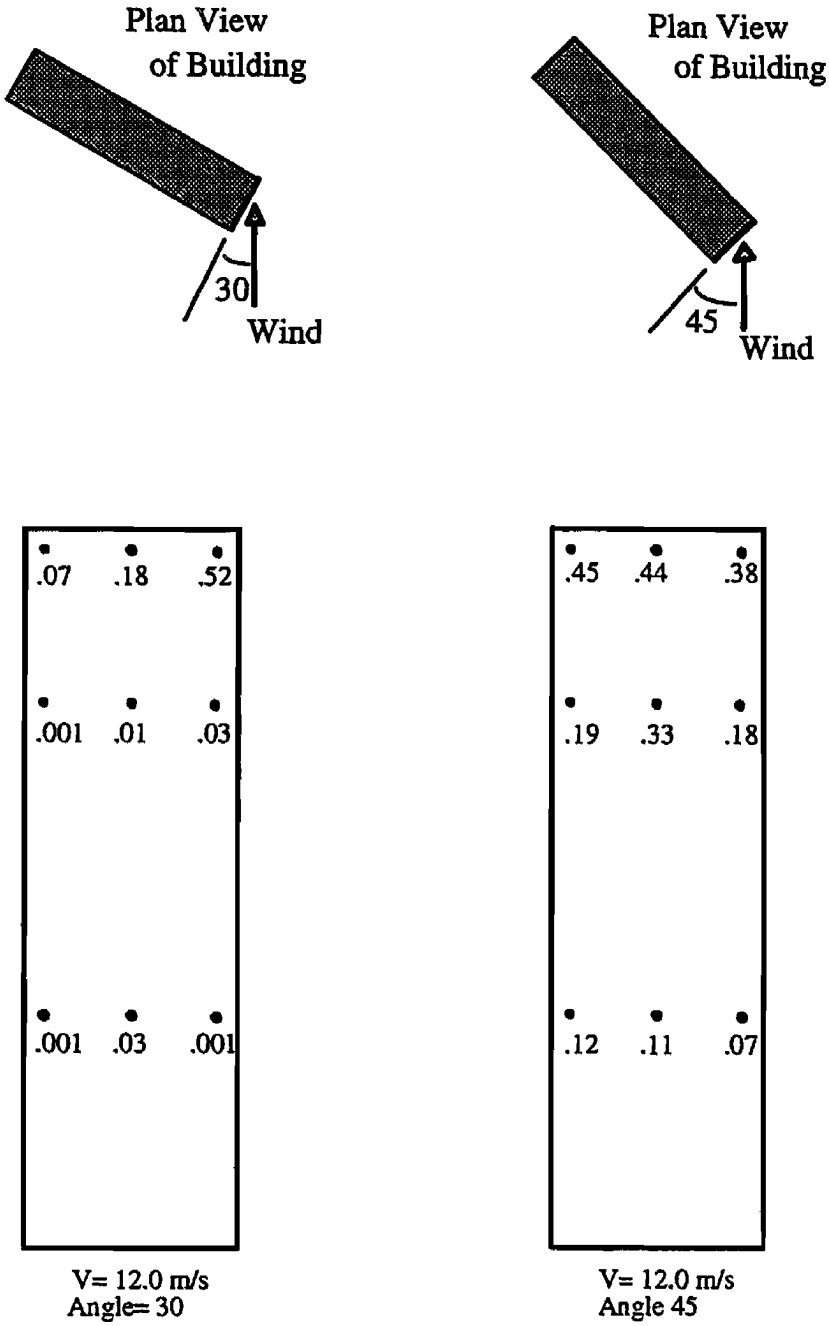

Figure 11. Full-Scale Local Intensity Factors for Narrow Face, Building Angle= 30 and 45 degrees

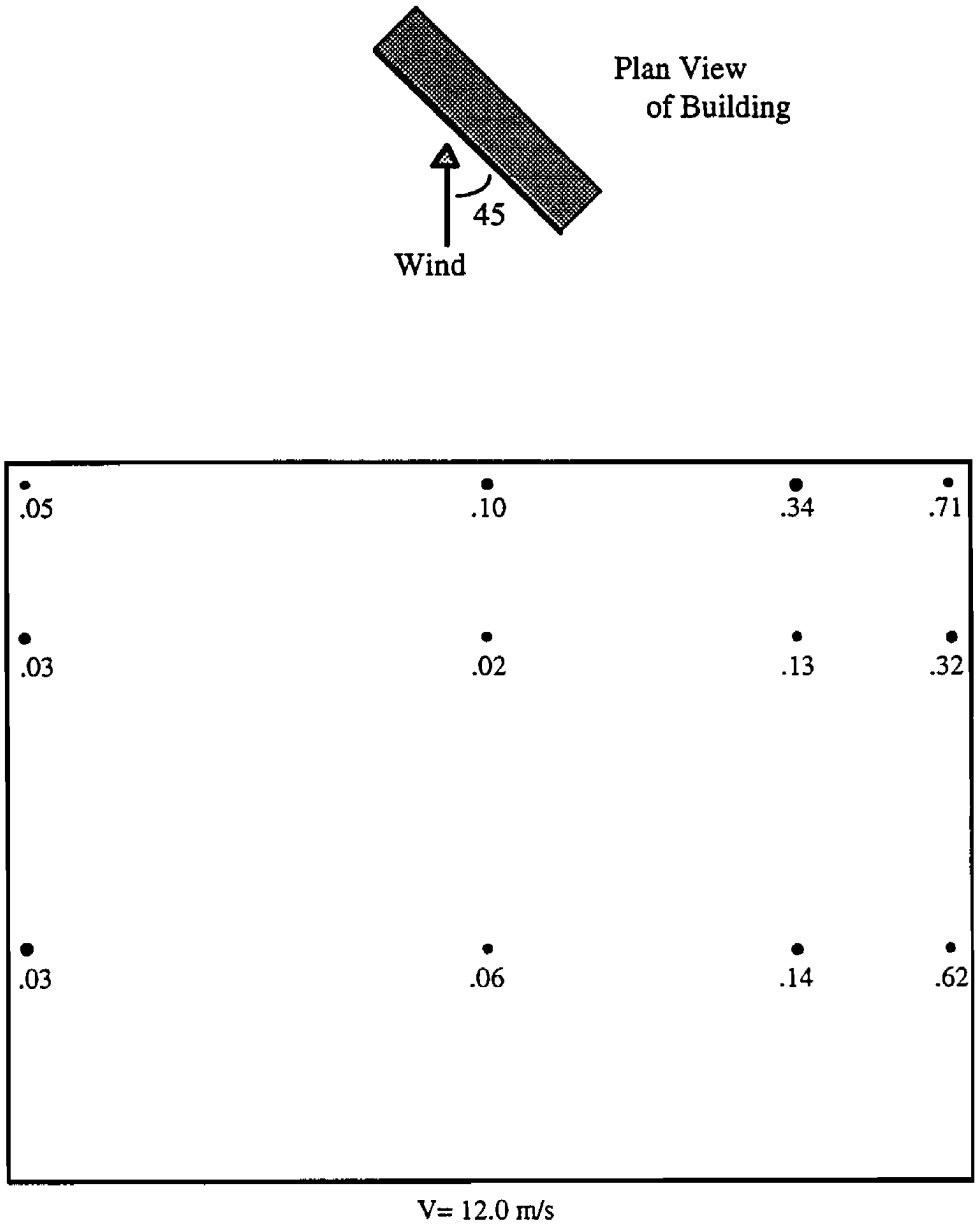

Figure 12. Full-Scale Local Intensity Factors for Wide Face, Building Angle= 45 degrees

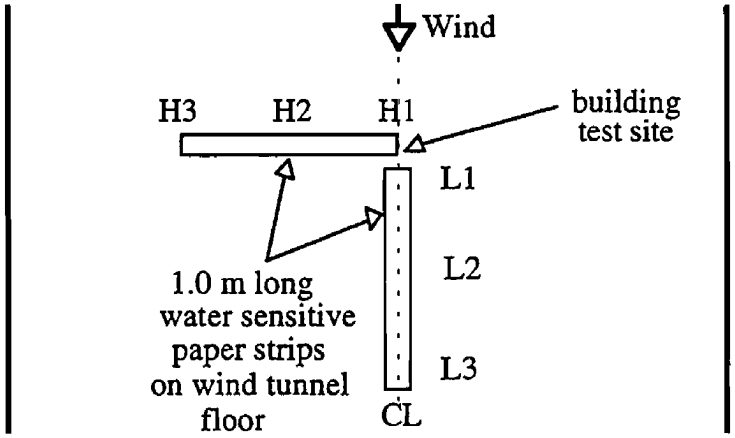

Location	Model-Scale Wind Speed (m/s)	Model-Scale Rainfall Rate (mm/hr)	Full-Scale Wind Speed (m/s)	Full-Scale Rainfall Rate (mm/hr)
H1	0.6	20.1	4.8	0.37
H2		8.2		0.37
H3		14.2		0.23
L1		21.2		0.19
L2		17.1		0.48
L3		4.7		0.05
H1	1.5	6.6	12.0	0.11
H2		6.2		0.16
H3		6.8		0.14
L1		8.1		0.25
L2		7.2		0.15
L3		6.4		0.12
H1	2.3	2.2	18.4	0.04
H2		1.4		0.04
H3		2.5		0.03
L1		2.0		0.03
L2		1.7		0.03
L3		2.4		0.06

Table 1. Rainfall Rates Across and Along Centreline of Wind Tunnel Floor

APPENDIX A

TECHNIQUES FOR MEASURING DROP SIZES

MALVERN 2600 Particle Sizer [9]

The Malvern 2600 Particle Sizer is a laser-based instrument which analyzes size distributions in the range 5 to 560μm with a 300 mm lens. In the present study, it was used to measure the size distribution by weight of water droplets in air.

It uses the principle of Fraunhofer Diffraction as the measurement means. The incident light diffracted by particles illuminated with a low power laser beam gives a stationary diffraction pattern regardless of particle movement. As particles pass through the illuminated area, the diffraction pattern "evolves", always reflecting the instantaneous size distribution. By integrating over a suitable time period and a continuous flux of particles, a representative sample of particles contributes to the final measured diffraction pattern. A Fourier transform lens focuses the diffraction pattern onto a multi-element photo-electric detector which produces an analogue signal proportional to received light intensity. A computer uses the method of non-linear least squares analysis to find the size distribution which gives the closest fitting diffraction pattern. By inputting the sample length (the length of spray illuminated by the laser), concentration of the spray can also be measured.

Used on the floor of the wind tunnel at the test site to analyze size distributions from one nozzle under the various wind speed and upstream distances, the MALVERN indicated that sample concentrations were too low for accurate analysis. Albeit, the results seemed reasonable in most cases. It should be noted here that the MALVERN is a fairly obtrusive instrument insofar as wind flow is concerned - it is approximately 2.5m long and 0.35m high. As such, it would yield the most accurate results if it were embedded in the wind tunnel floor. This was not done for the current study.

Water-Sensitive Paper [6]

Ciba-Geigy Limited has developed a "water-sensitive paper". This is a rigid paper with a specially coated, yellow surface which is stained dark blue by water droplets impinging on it. It was developed for agricultural spraying applications.

The droplet density and sizes on the cards can be estimated quickly with a visual comparison with standard cards of known droplet density and volume mean diameters. Alternatively, a more accurate evaluation can be made with an automatic image analyser provided the droplet density is sufficiently small for the individual drops not to overlap with each other. A "spread factor" applied to the stain diameter of the drops yields the actual drop diameter. The laboratory spread factor ranges from approximately 1/1.7 to 1/2.1 for water stain diameters of 100 to 600μm respectively. It is relatively insensitive to relative humidity.

Some possible errors involved with the use and analysis of the water sensitive paper in the current study are as follows:

- With the quantity of water being sprayed in the wind tunnel, the tests were necessarily short so that the stains from each drop remained distinct from one another. Thus, repeat tests show some variance.
- In the more heavily wetted areas, it is virtually impossible to ensure that there is no overlap of the droplet stains on the paper. Hence, on average, analysis of drop size will yield larger drop sizes than the true value. If the overlapped drops are removed from the analysis with the automatic image analyser, the distribution becomes skewed.
- Use of the automatic image analyser requires user judgement in matching the size of the displayed image to the actual image.
- The spread factor is published for water droplets reaching the paper at terminal velocity. In the wind tunnel, the velocity at impact will be higher due to the horizontal velocity component due to the wind.
- At higher wind tunnel speeds, the shape of the droplet stains deviates from a round shape, approaching a more oval shape. The equivalent diameter used for these droplets in calculating a spread factor may not yield the appropriate correction.

Analysis of Drop Size Distribution and Rainfall/Wetting Rates

Albeit the errors indicated above are numerous, the water sensitive paper and the automatic image analyser were used to estimate the drop size distribution and the volume of water impacting on *a square centimetre* of the water sensitive paper. A frame grabber/PC based analysis system was used for this study. The process required two stages since many of the water sensitive paper samples had some overlapping droplet stains:

- In the first stage, only *isolated* droplets were considered. This was accomplished through setting certain parameters ranges in the program IPPLUS such as a "roundness factor", and by manual editing. Both stain area and average diameter for each isolated droplet were output by the program. By applying the appropriate spread factors to the average diameters, the volume of water they represented could be determined. Then, a factor relating the total volume of water to the total stain area could be calculated for use in the second stage. The isolated droplets from this first stage were used in the estimation of drop size distribution.
- In the second stage, *all* droplet stains were considered in IPPLUS. Then, in a separate program, the isolated droplets were "screened" on the basis of their roundness and area. The volume of each isolated droplet thus obtained was determined and summed to arrive, again, at a total volume of isolated droplets. While this volume should ideally match that of the first stage, it may not as this second stage did not involve manual editing to choose the isolated droplets. All droplet stains not identified as "isolated" then had their areas summed and the factor from stage one was applied to estimate the volume of water they represented. The total volume of water was calculated as the sum of the volumes of the isolated and the overlapping stains.

The rainfall or wetting rates were calculated with the total volume of water and the test duration.

APPENDIX B

MODEL AND FULL-SCALE DROP SIZE DISTRIBUTIONS FROM NOZZLE ARRAY

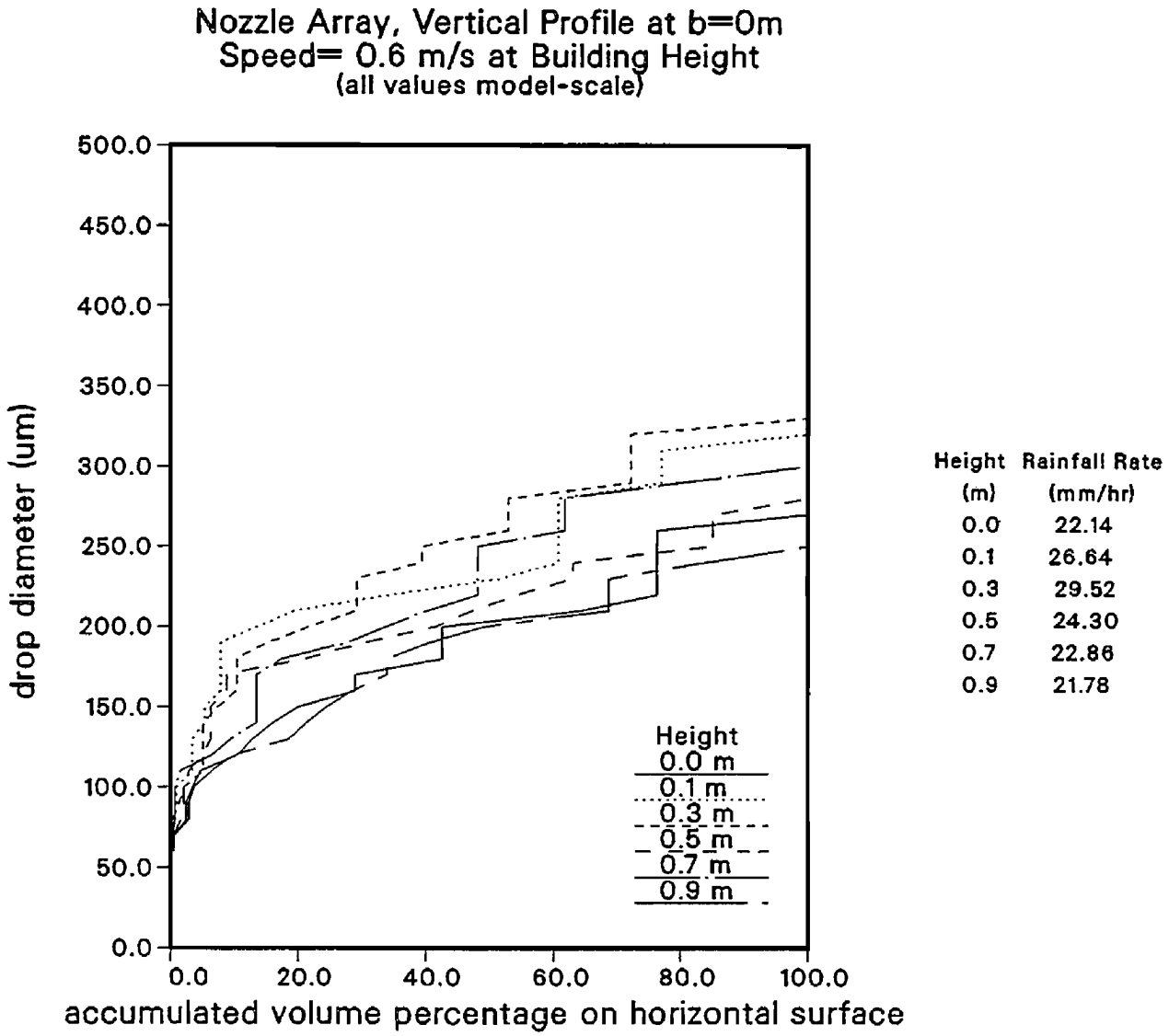

Figure B.1a. Model Scale Drop Size Distributions from Nozzle Array, Wind Tunnel Speed at Building Height= 0.6 m/s

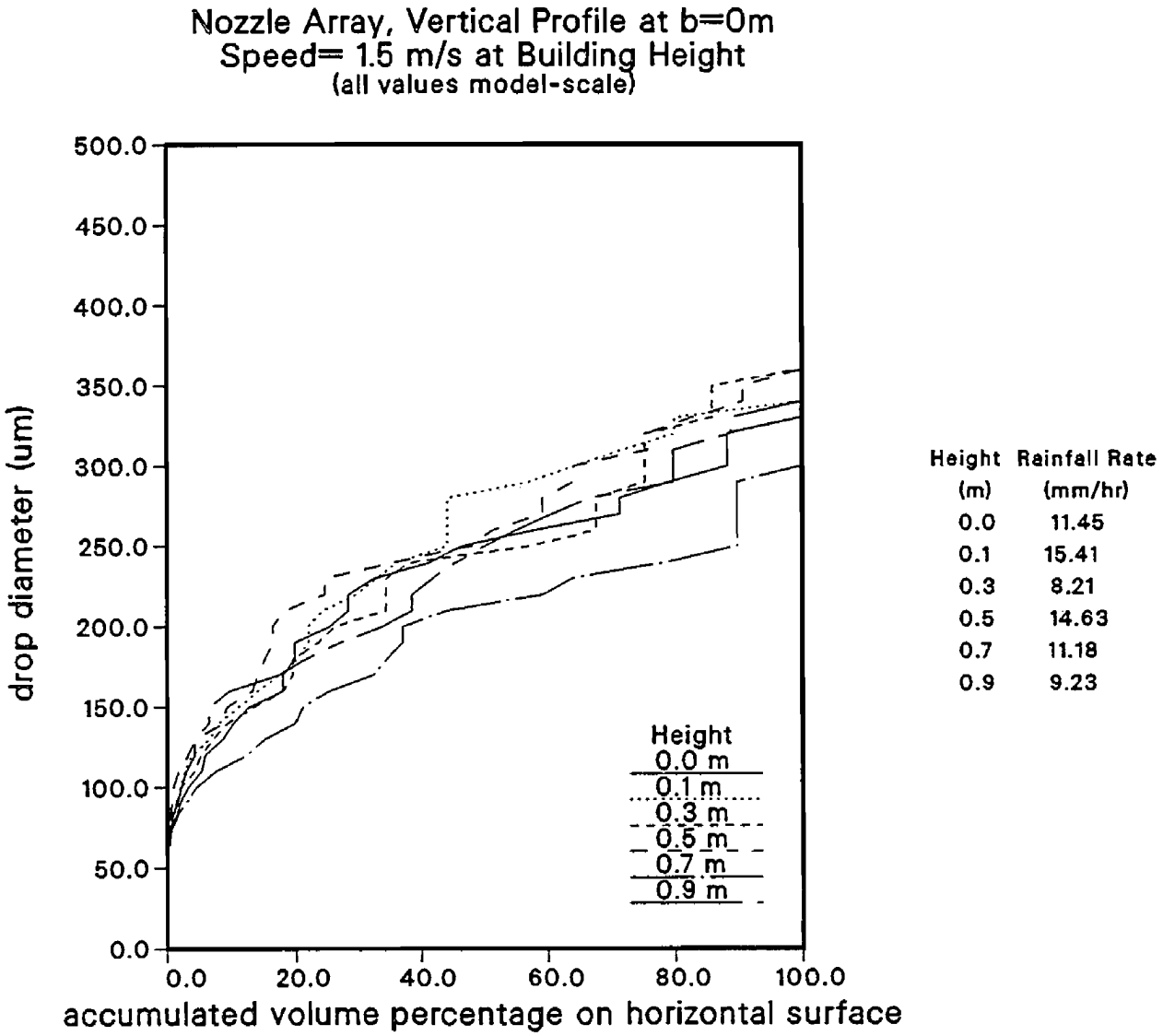

Figure B.1b. Model Scale Drop Size Distributions from Nozzle Array, Wind Tunnel Speed at Building Height= 1.5 m/s

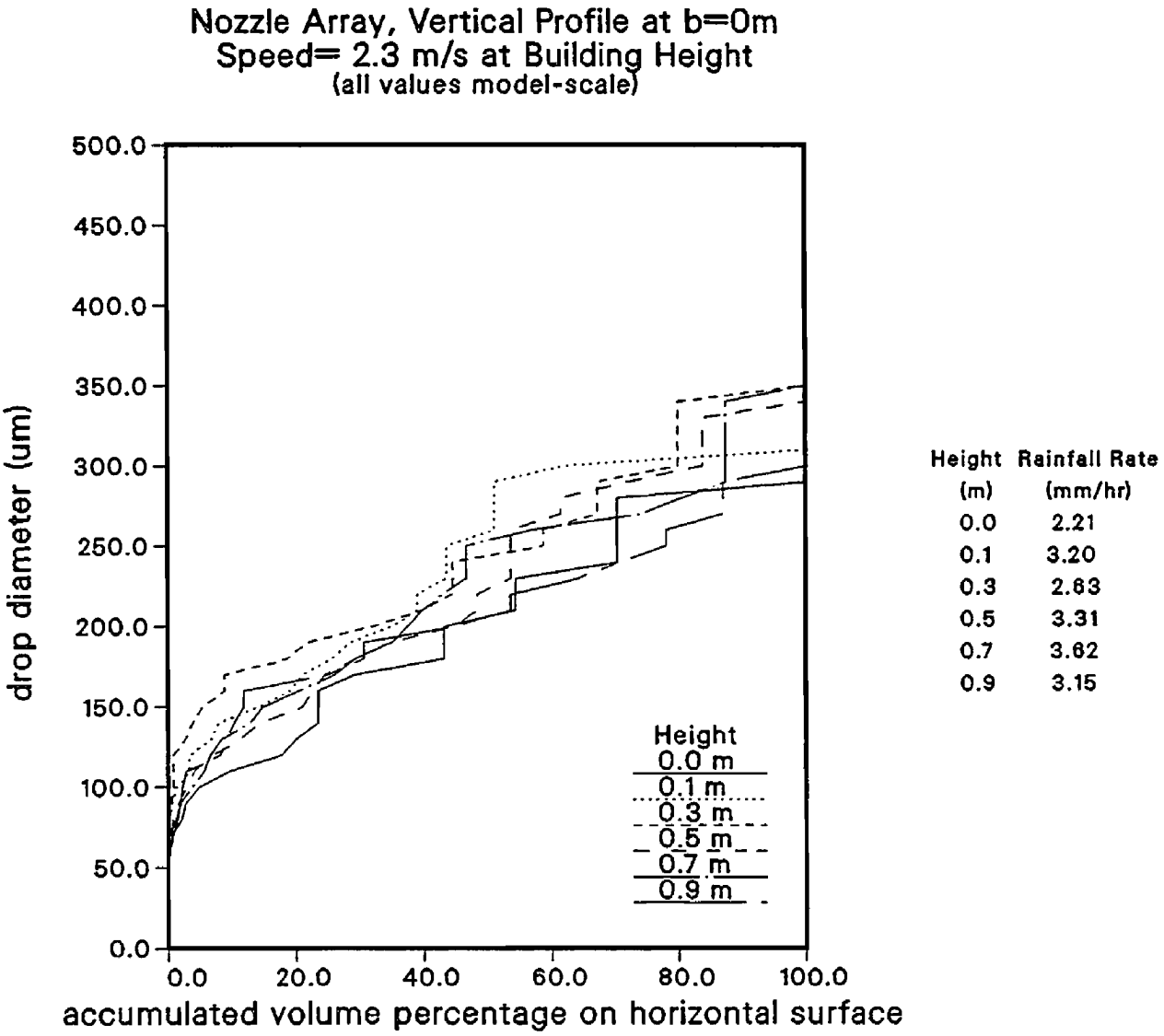

Figure B.1c. Model Scale Drop Size Distributions from Nozzle Array, Wind Tunnel Speed at Building Height= 2.3 m/s

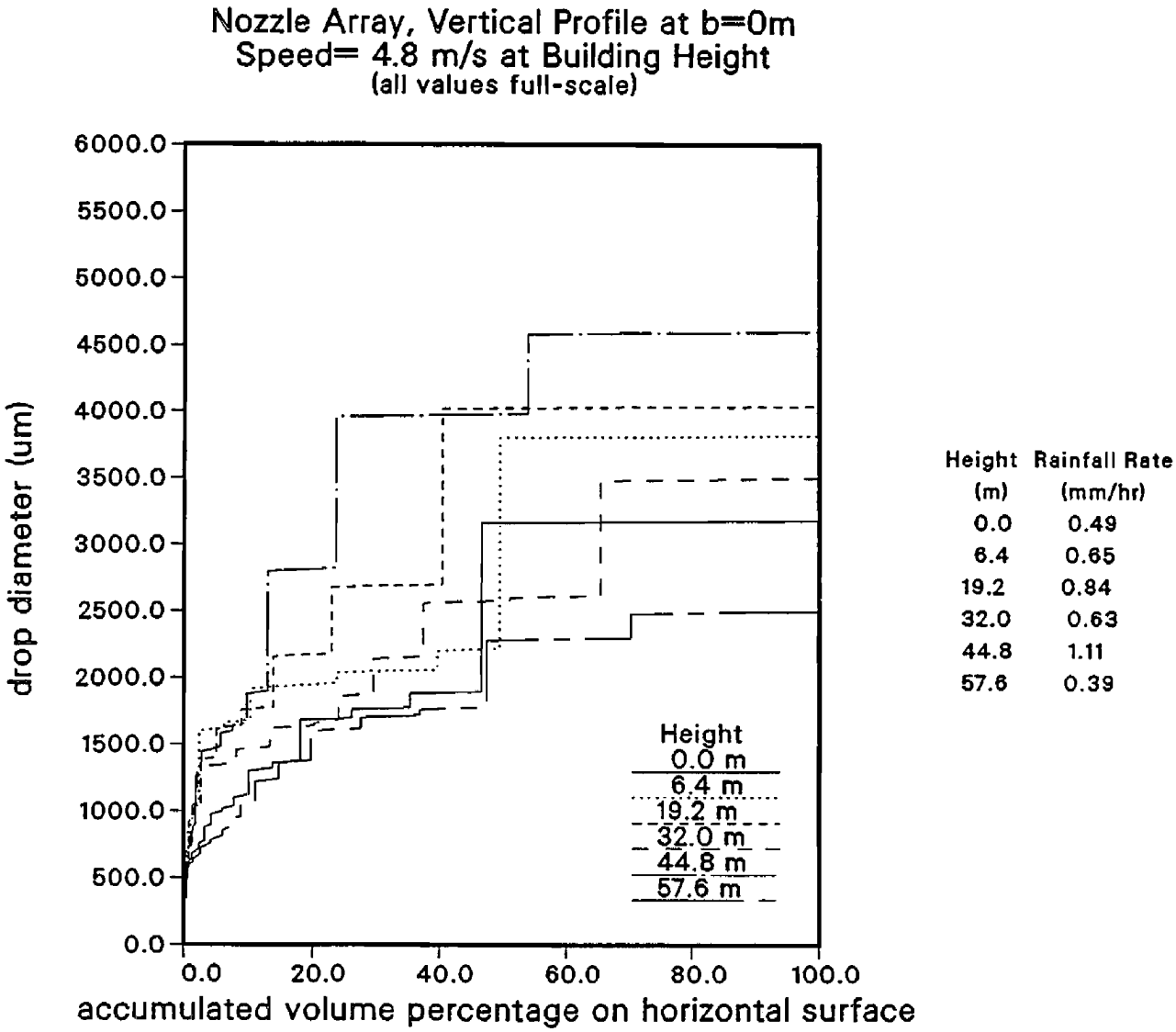

Figure B.2a. Full Scale Drop Size Distributions from Nozzle Array, Wind Speed at Building Height= 4.8 m/s

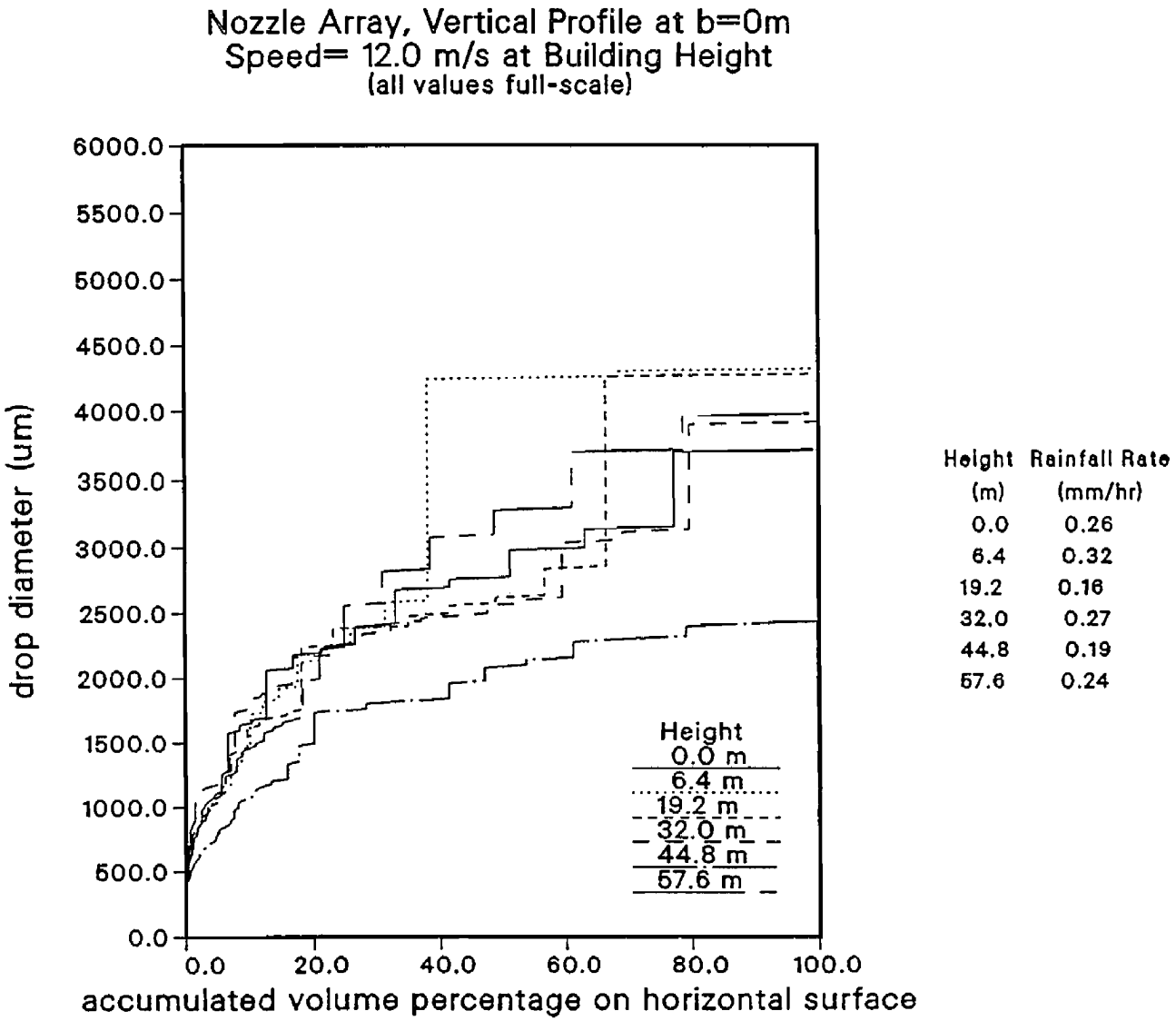

Figure B.2b. Full Scale Drop Size Distributions from Nozzle Array, Wind Speed at Building Height= 12.0 m/s

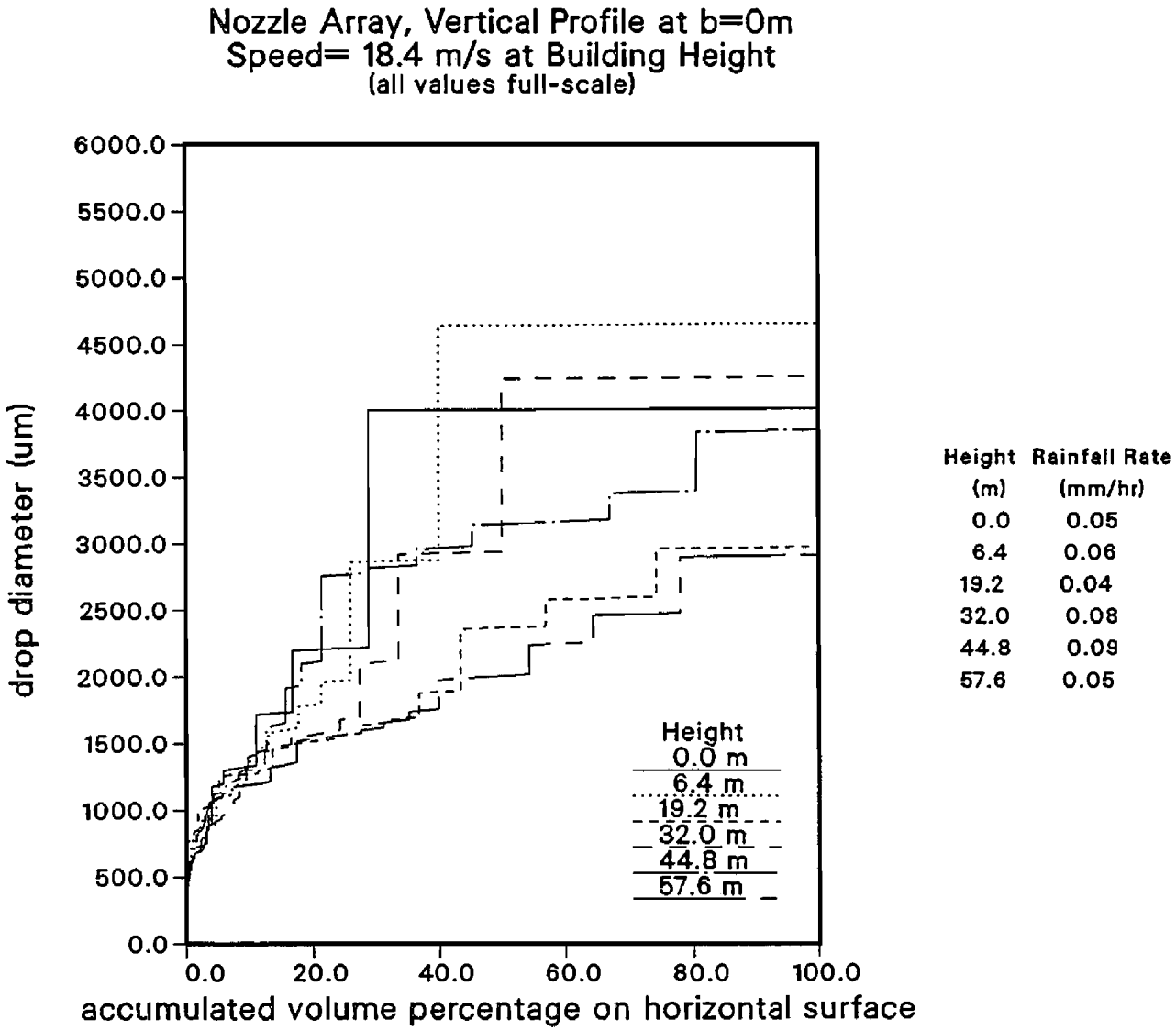

Figure B.2c. Full Scale Drop Size Distributions from Nozzle Array, Wind Speed at Building Height= 18.4 m/s

APPENDIX C

PHOTOGRAPHS OF WETTING PATTERNS FOR PHASE I

Speed at H (m/s) model scale	Building Angle (degrees)	Duration (s) model scale	Building Configuration
0.6	0	10	basic
0.6	45	10	basic
0.6	90	10	basic
1.5	0	5	basic
1.5	30	5	basic
1.5	45	5	basic
1.5	60	5	basic
1.5	90	5	basic
2.3	0	6	basic
2.3	45	6	basic
2.3	90	6	basic
1.5	0	5	basic with balconies
1.5	45	5	basic with balconies
1.5	90	5	basic with balconies
1.5	0	5	basic with cornice

Table C.1. Summary of Wetting Pattern Tests, Phase I

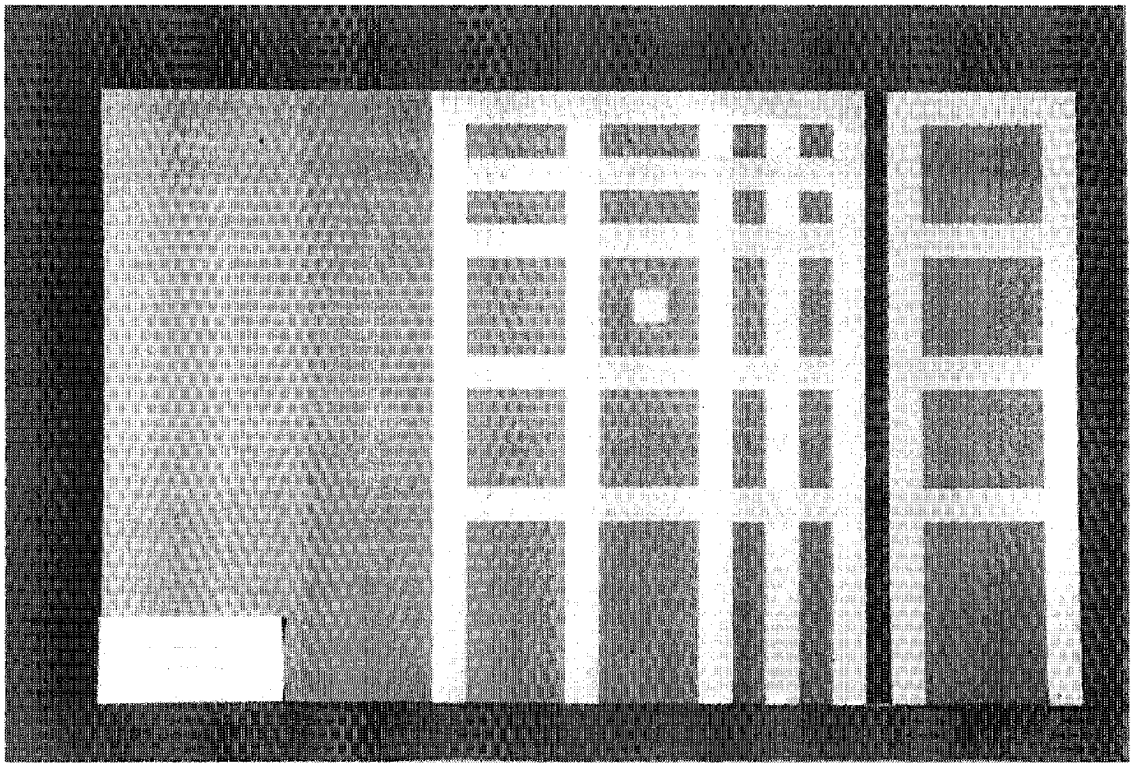

a) complete

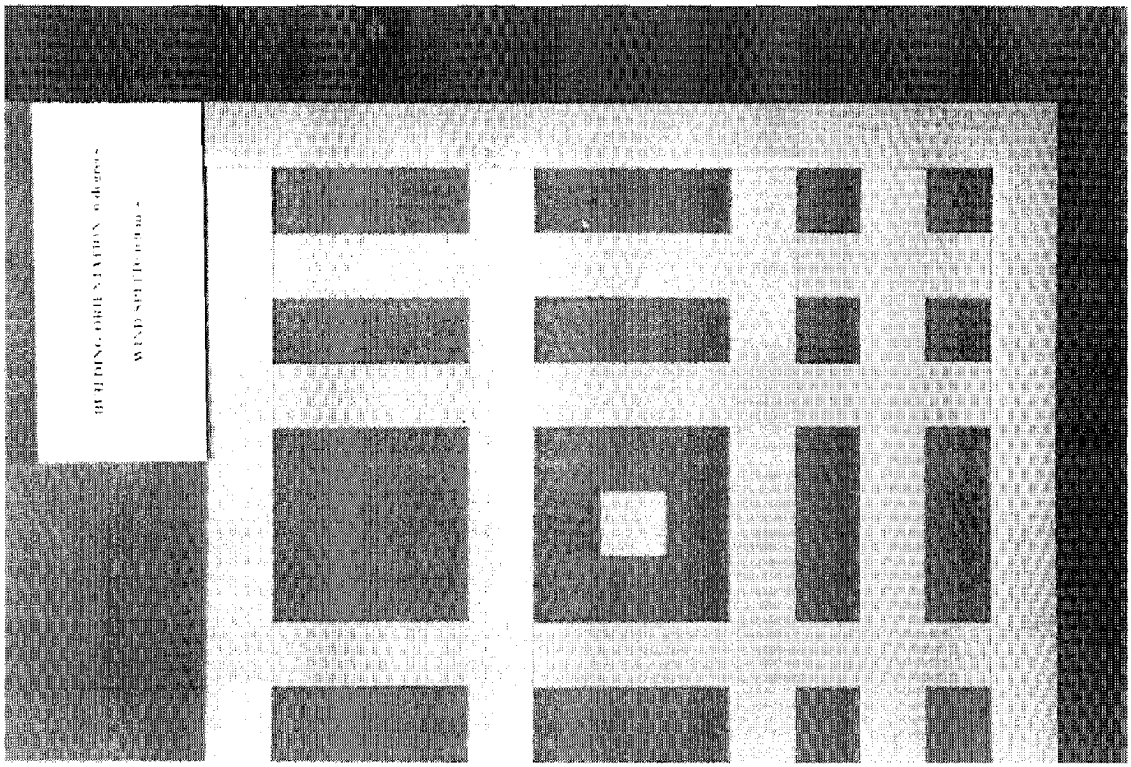

b) wide side, top quarter

Figure C.1 Wetting Patterns for Phase I, Building Angle= 0 degrees, Wind Tunnel Speed= 0.6 m/s at building height

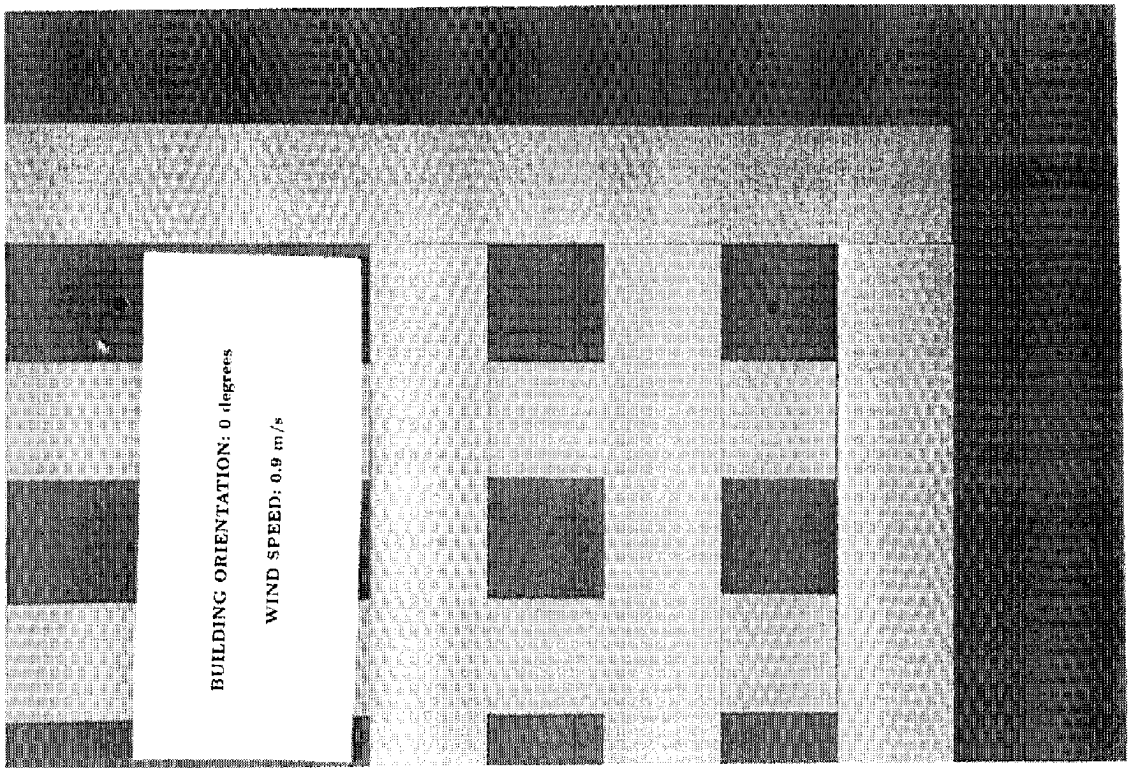

c) wide side, top corner

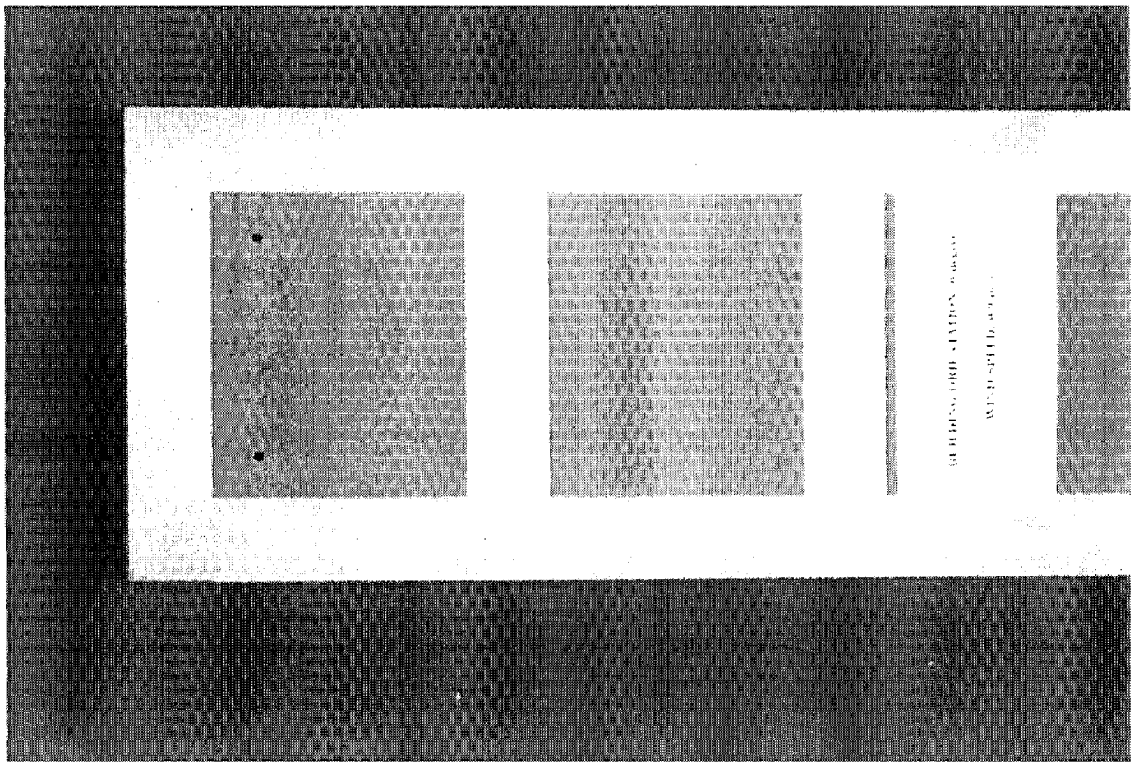

d) narrow side, top half

Figure C.1 Cont'd

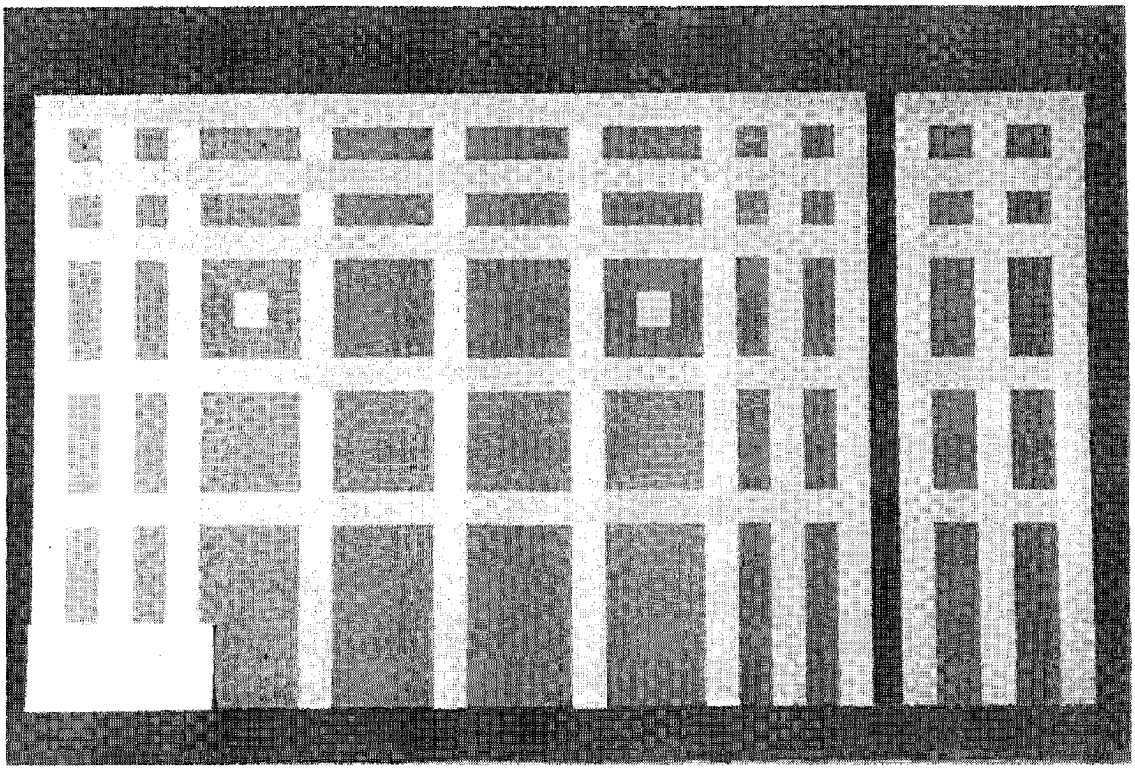

a) complete

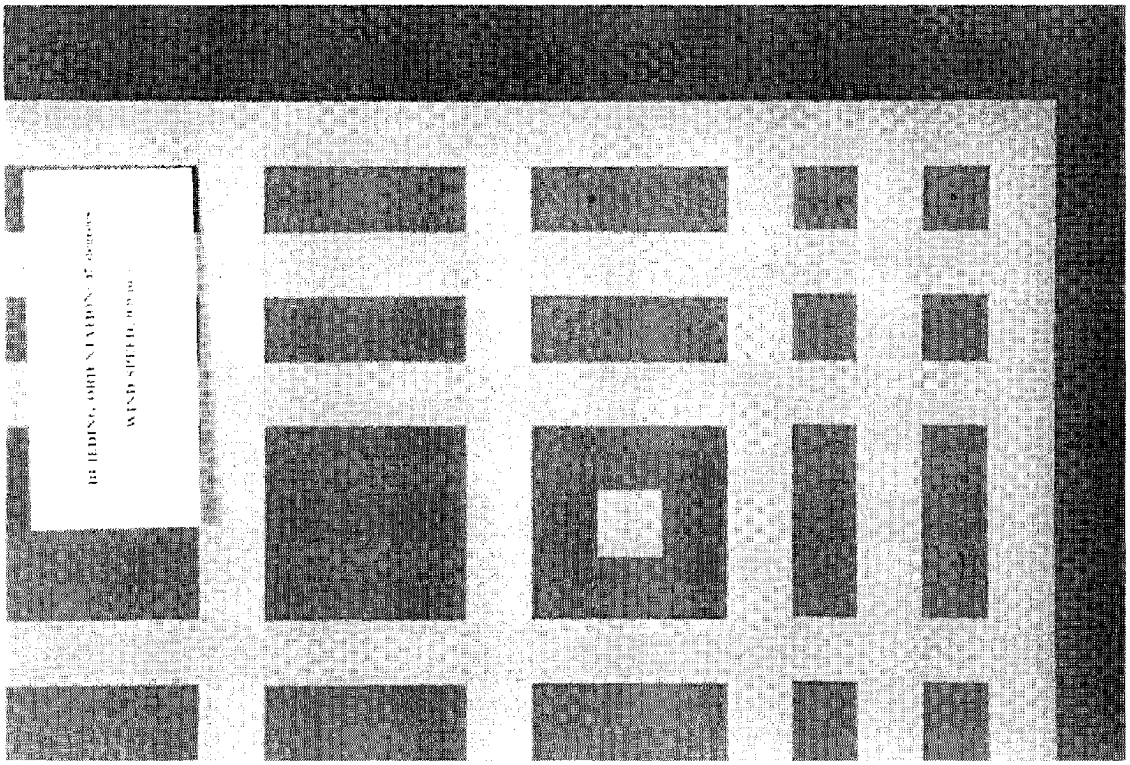

b) wide side, top quarter

Figure C.2 Wetting Patterns for Phase I, Building Angle= 45 degrees, Wind Tunnel Speed= 0.6 m/s at building height

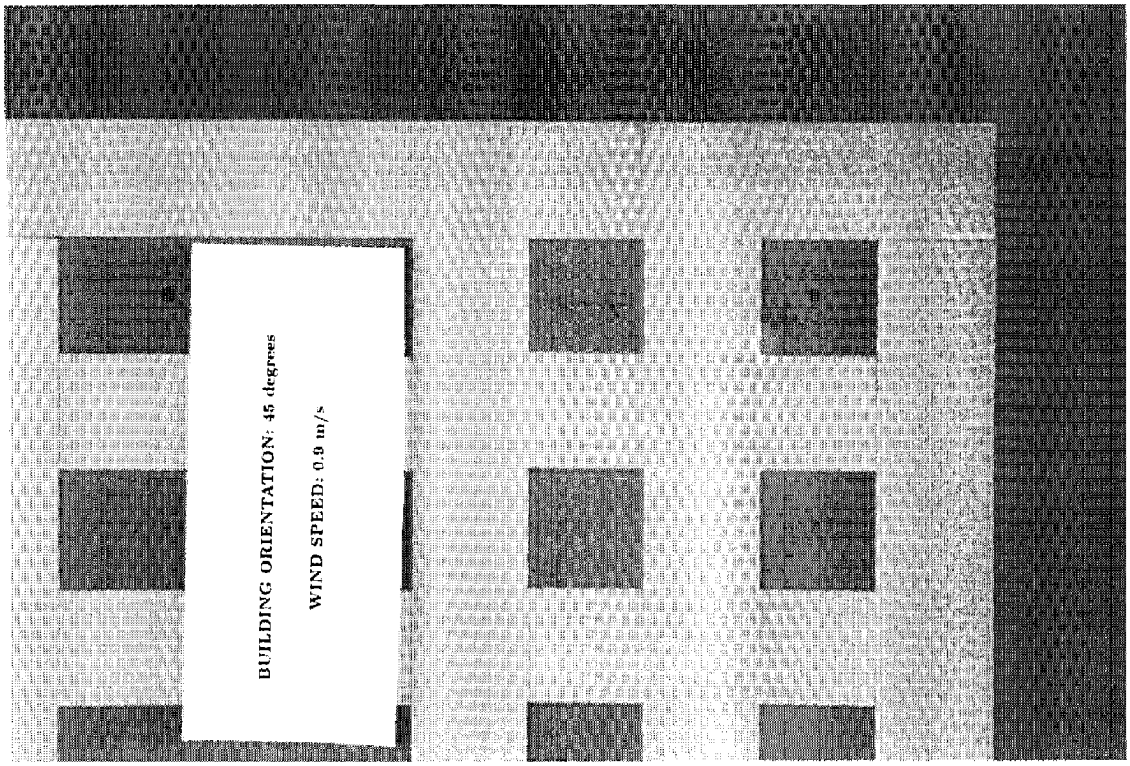

c) wide side, top corner

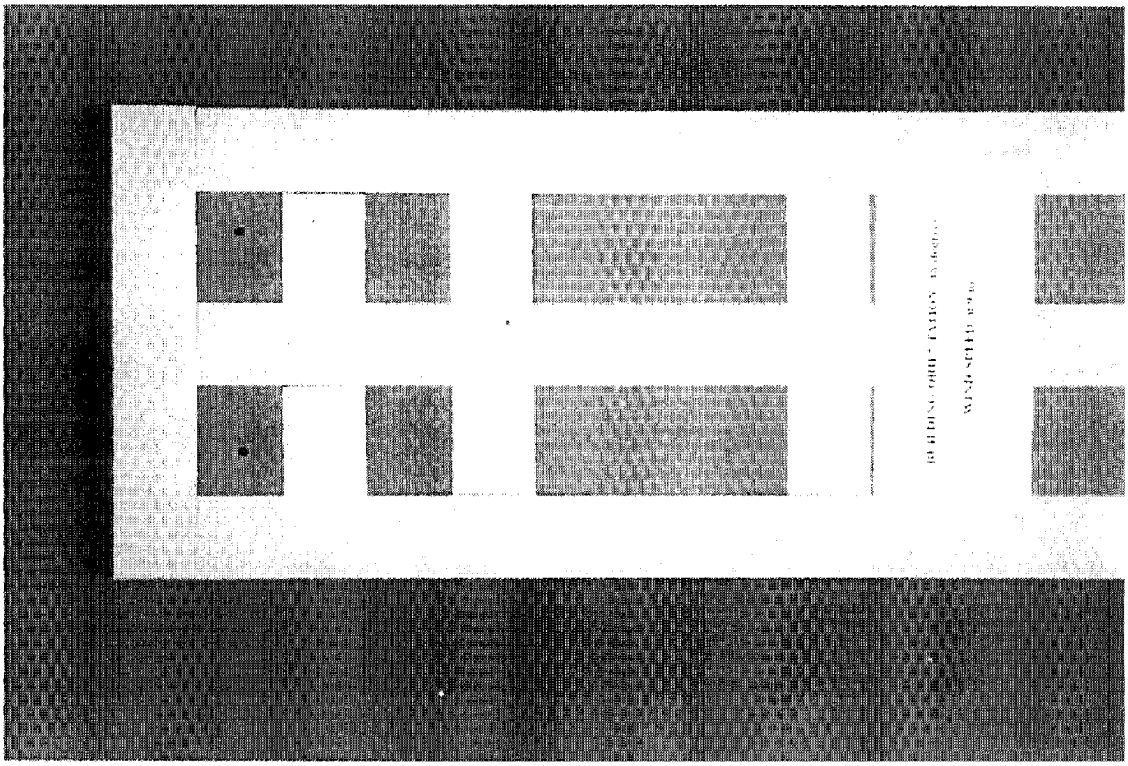

d) narrow side, top half

Figure C.2 Cont'd

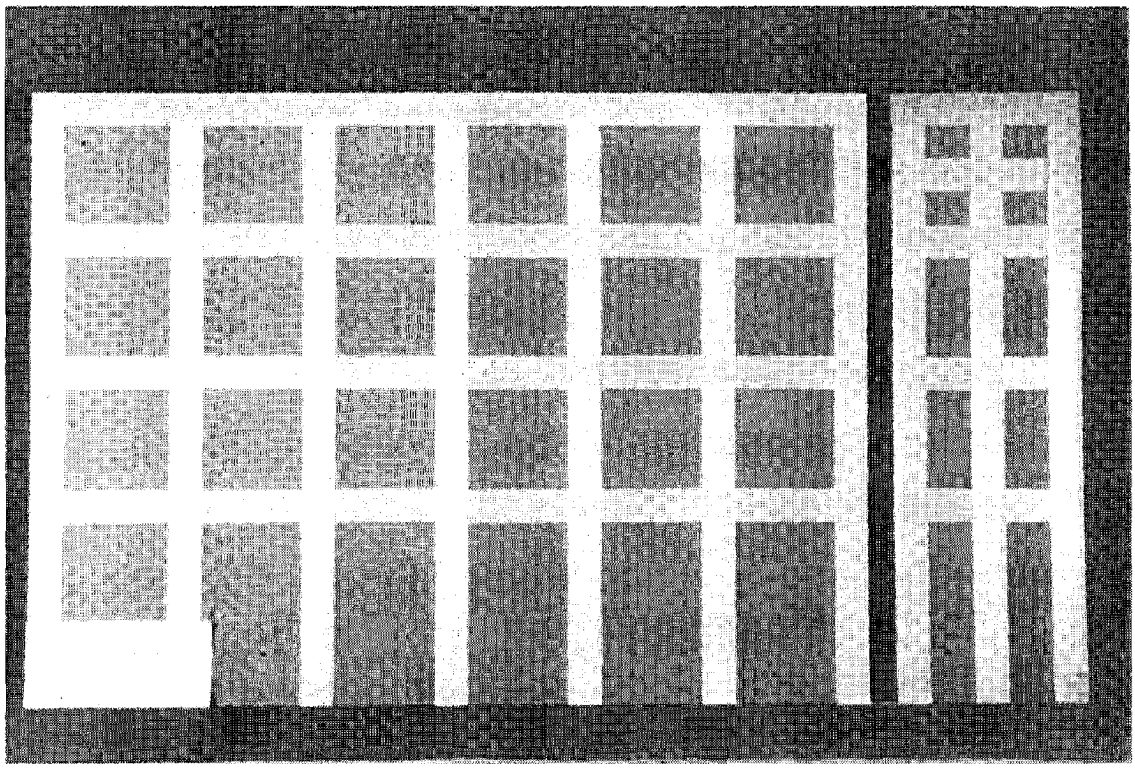

a) complete

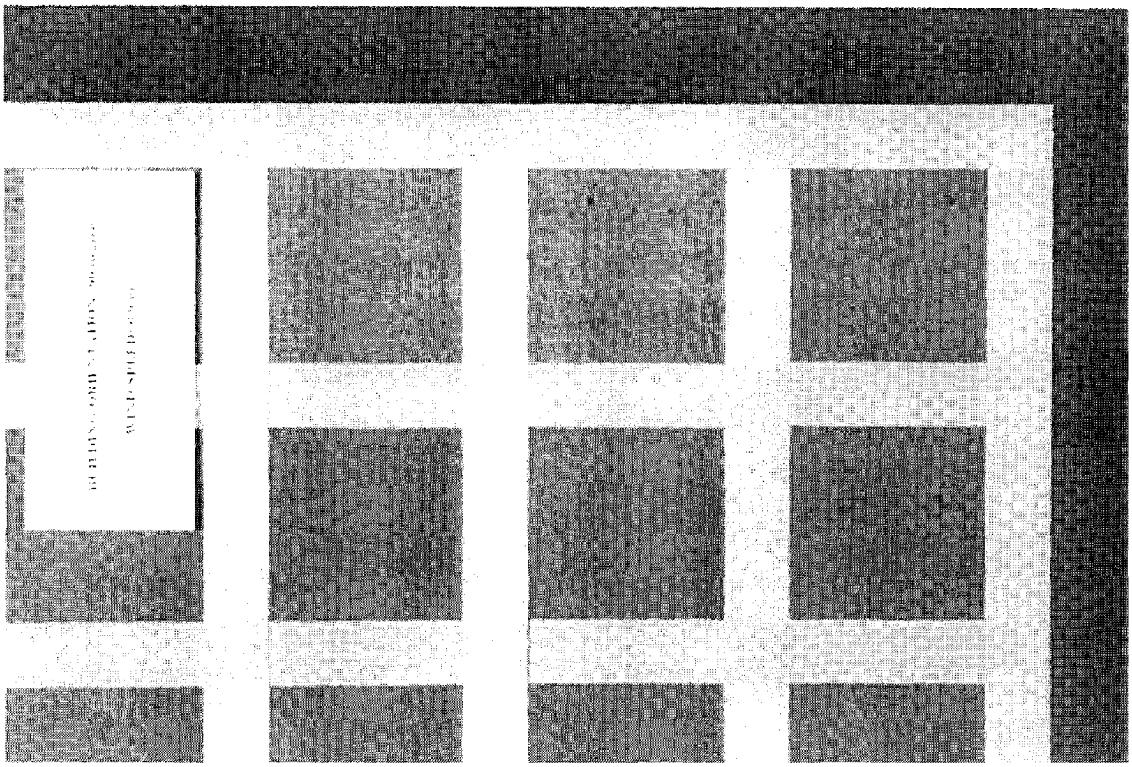

b) wide side, top quarter

Figure C.3 Wetting Patterns for Phase I, Building Angle= 90 degrees, Wind Tunnel Speed= 0.6 m/s at building height

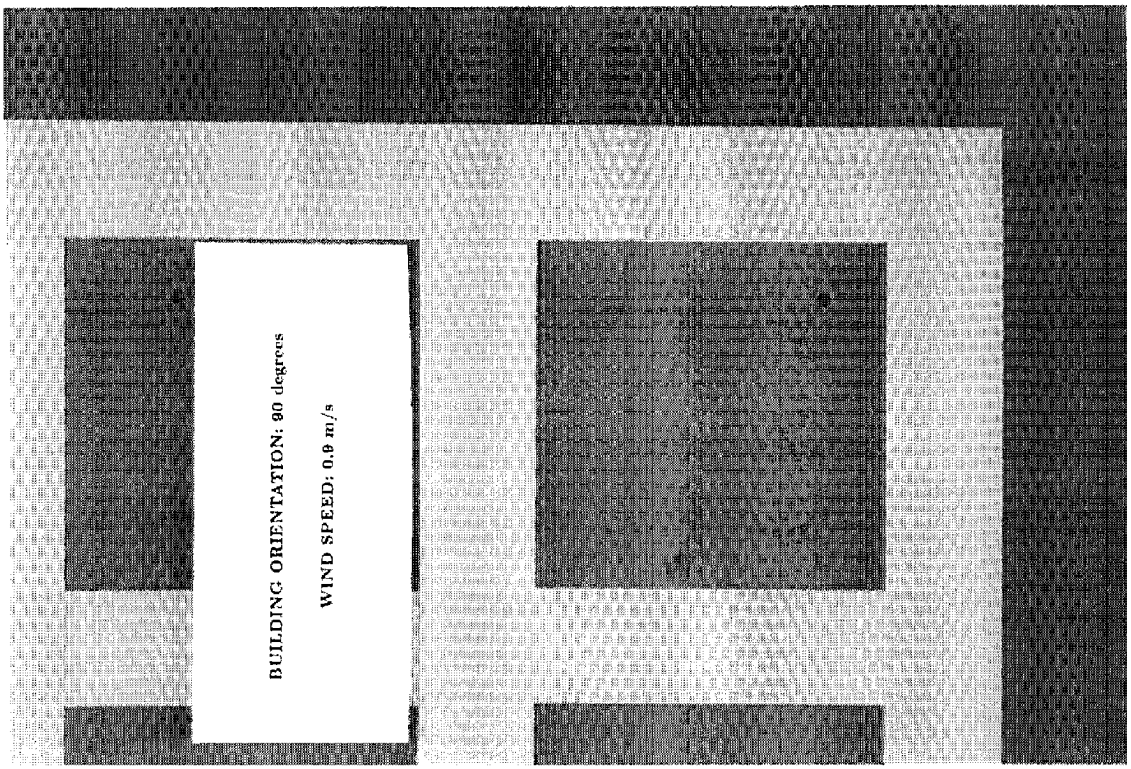

c) wide side, top corner

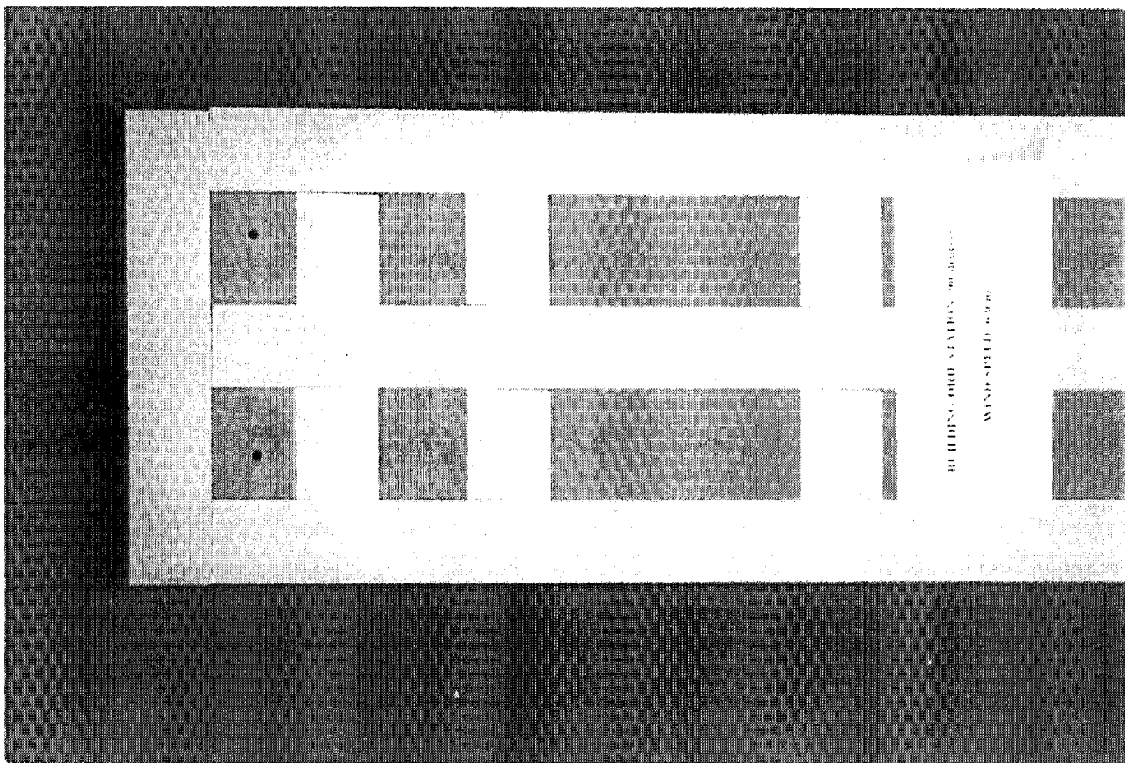

d) narrow side, top half

Figure C.3 Cont'd

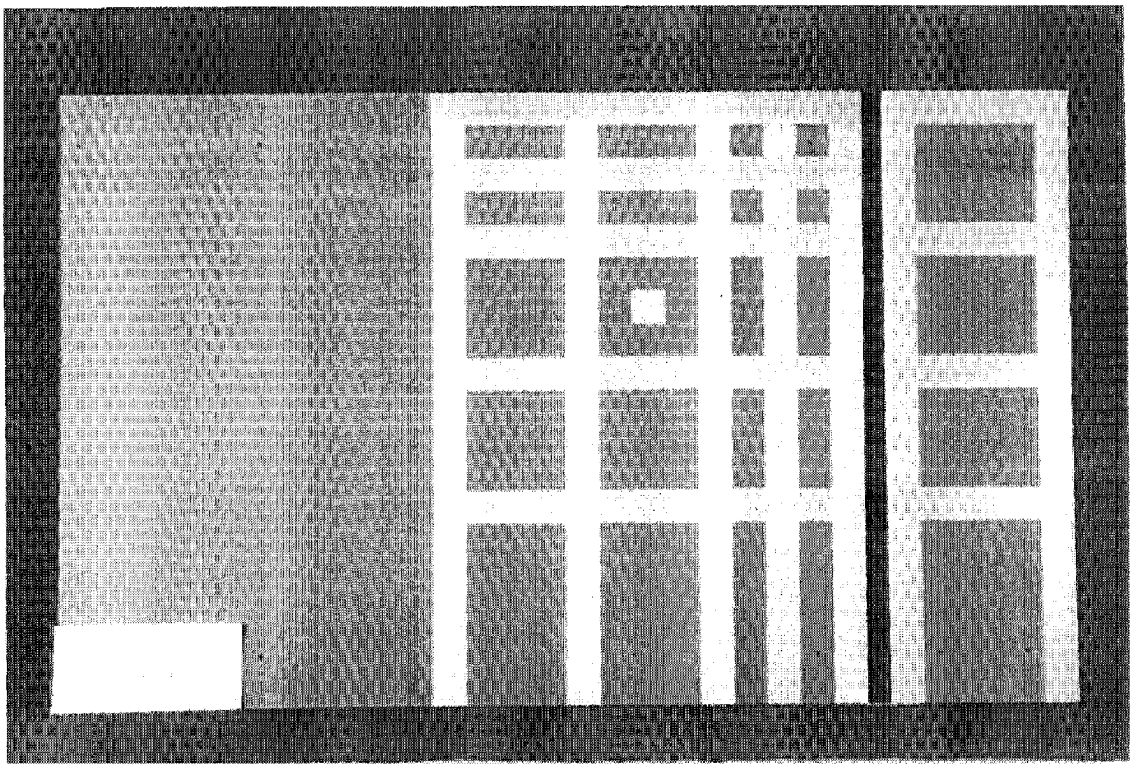

a) complete

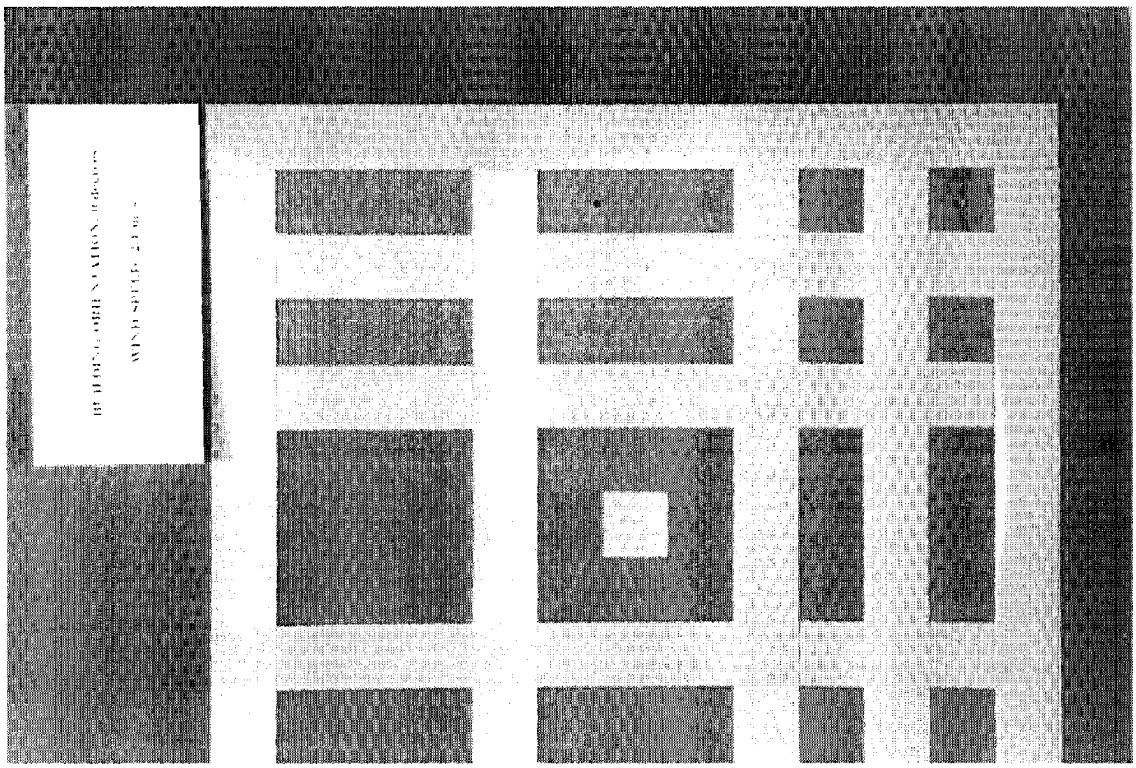

b) wide side, top quarter

Figure C.4 Wetting Patterns for Phase I, Building Angle= 0 degrees, Wind Tunnel Speed= 1.5 m/s at building height

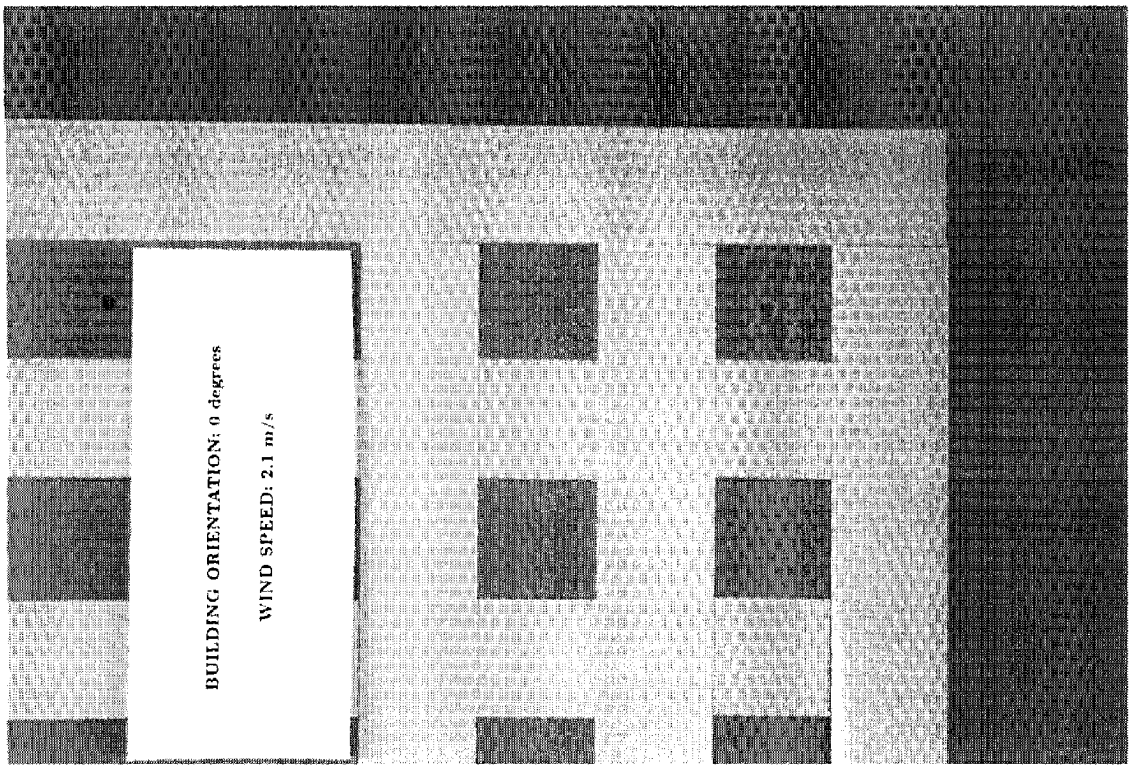

c) wide side, top corner

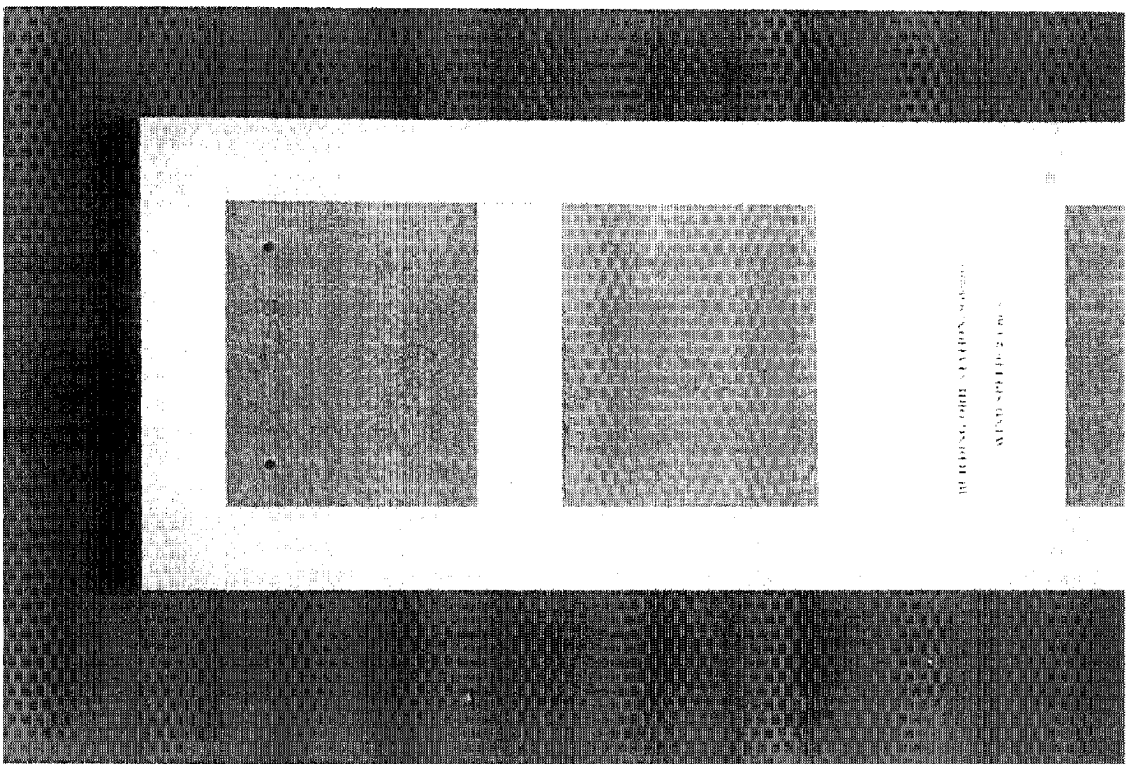

d) narrow side, top half

Figure C.4 Cont'd

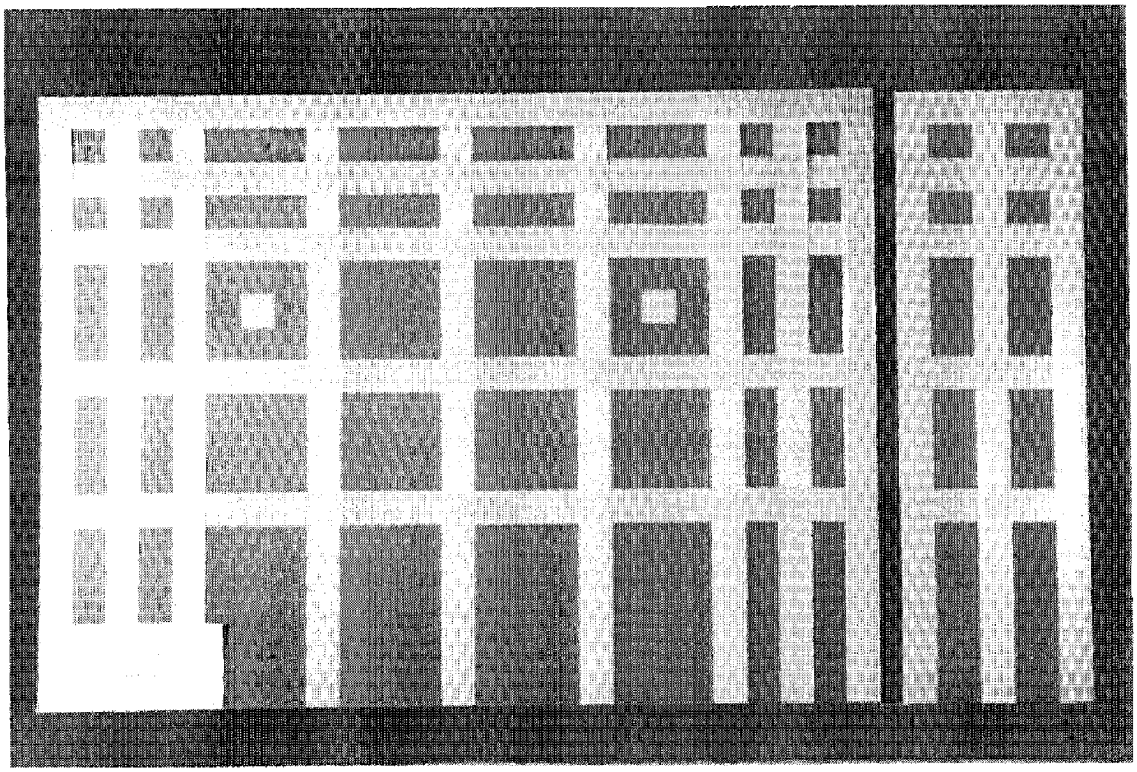

a) complete

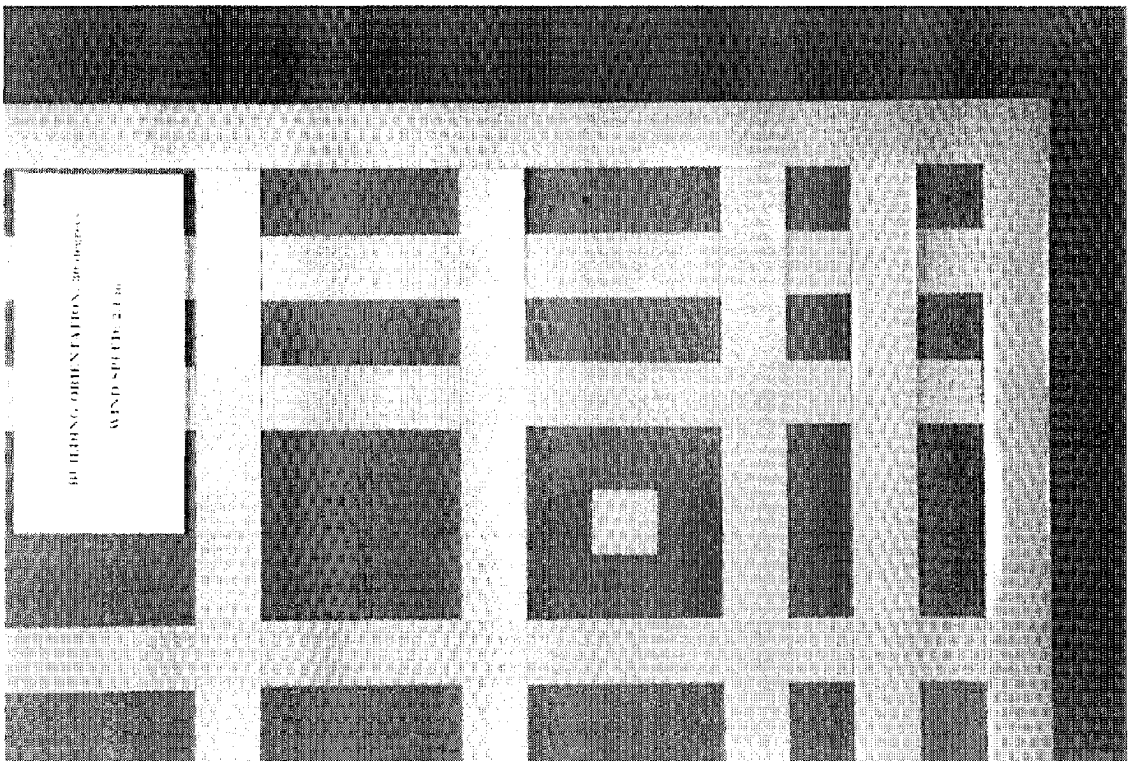

b) wide side, top quarter

Figure C.5 Wetting Patterns for Phase I, Building Angle=30 degrees, Wind Tunnel Speed= 1.5 m/s at building height

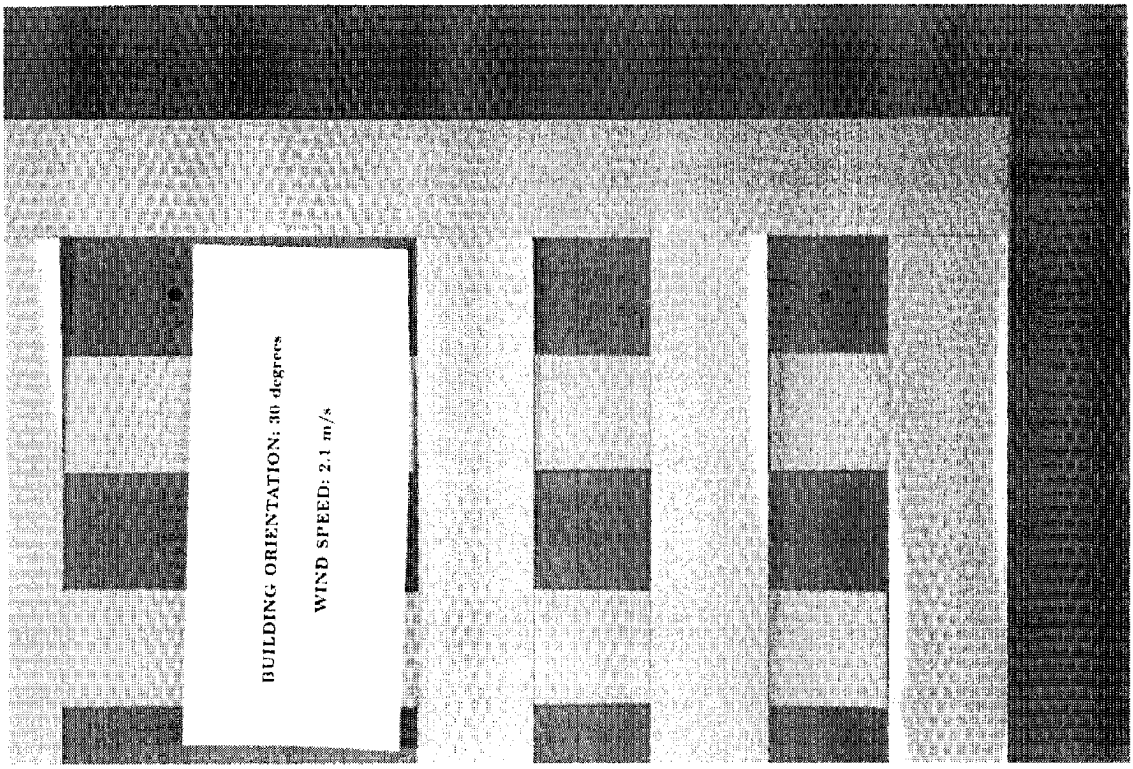

c) wide side, top corner

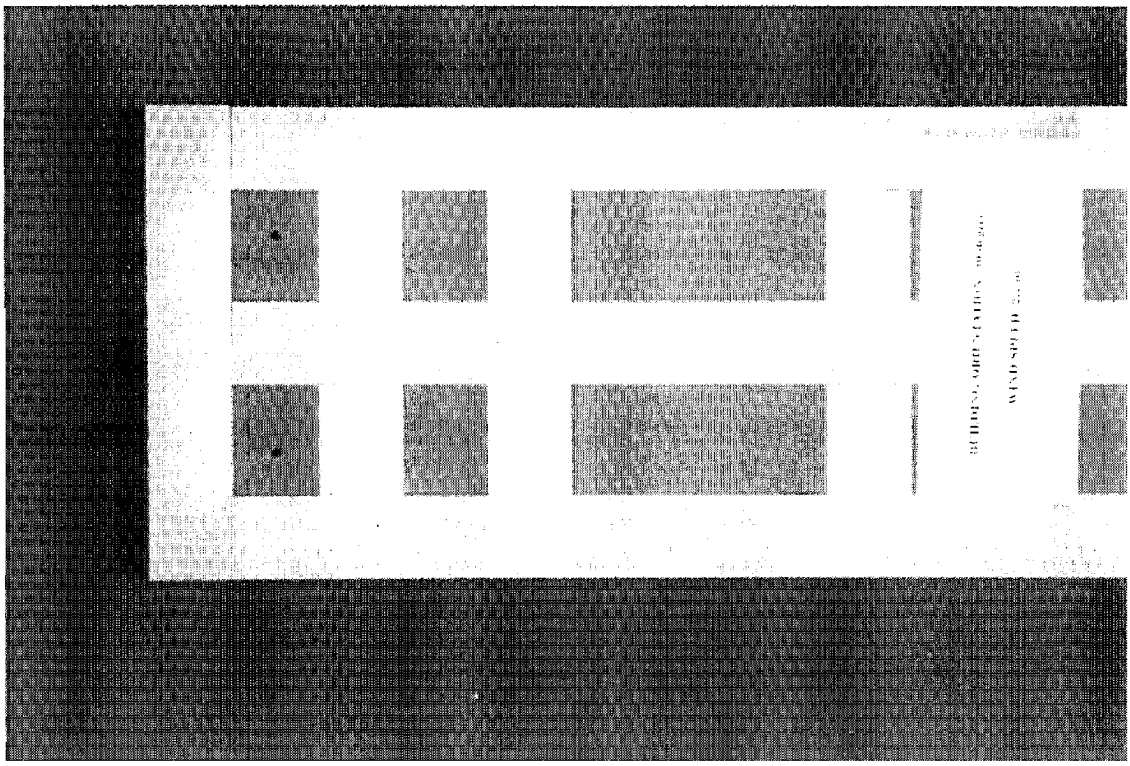

d) narrow side, top half

Figure C.5 Cont'd

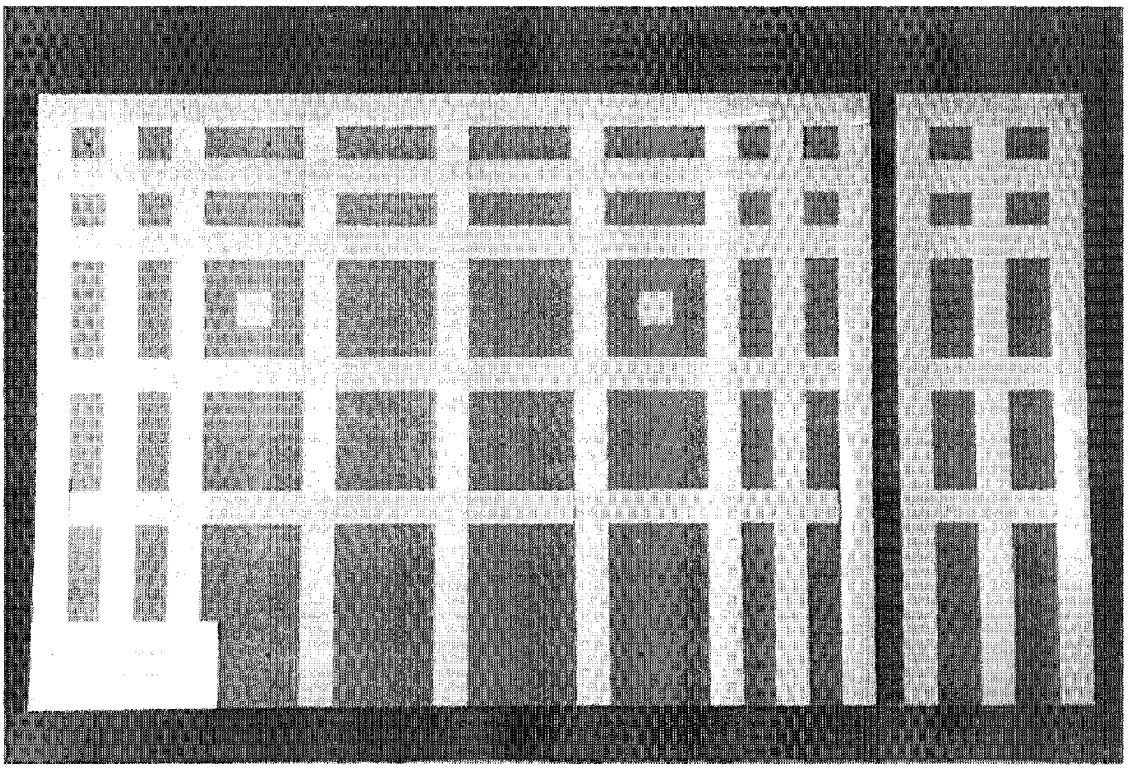

a) complete

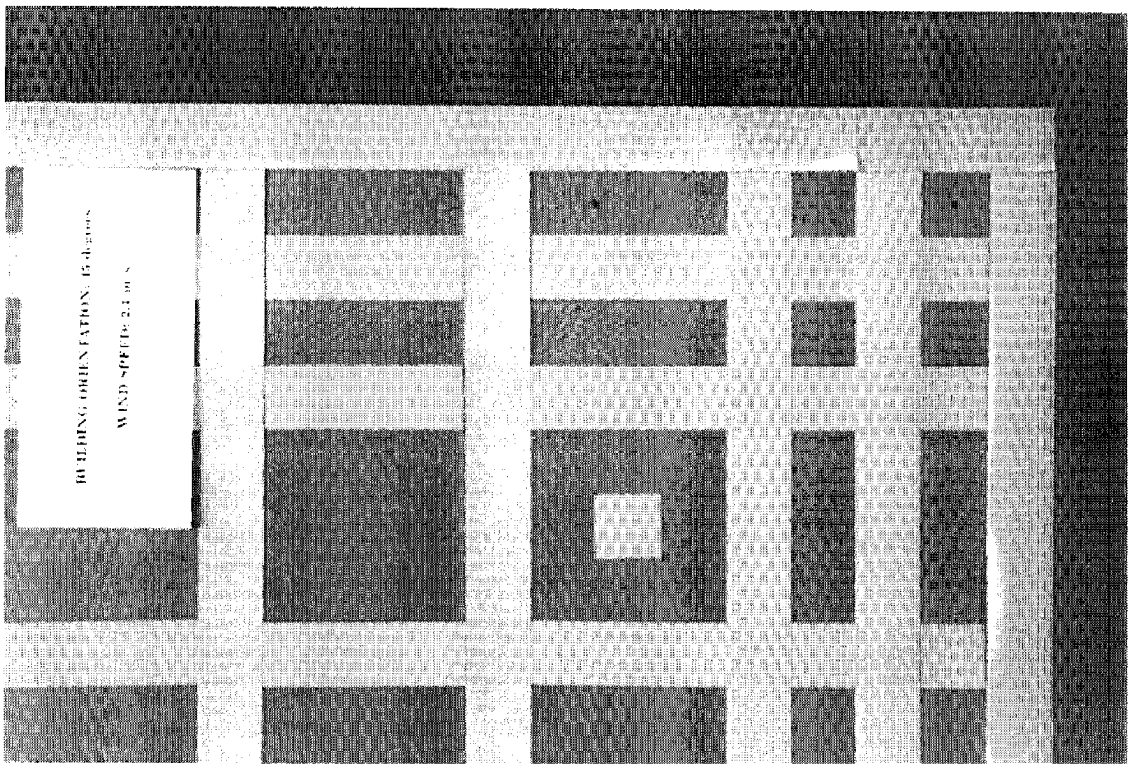

b) wide side, top quarter

Figure C.6 Wetting Patterns for Phase I, Building Angle= 45 degrees, Wind Tunnel Speed= 1.5 m/s at building height

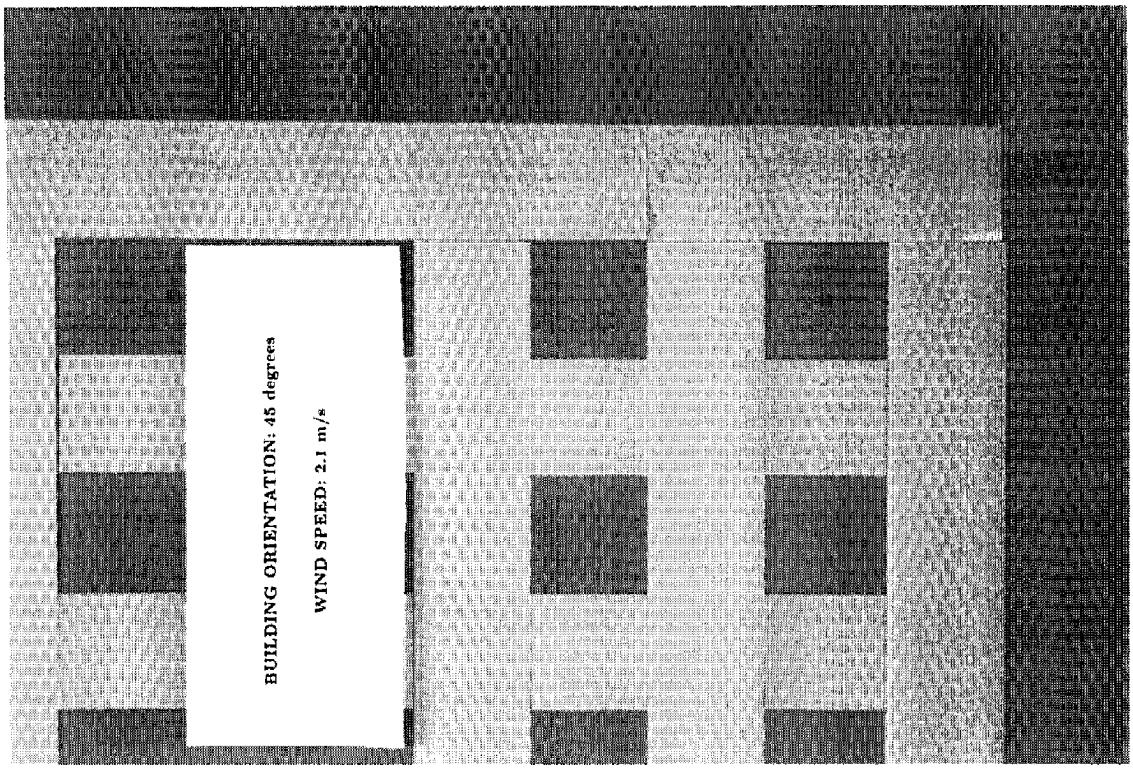

c) wide side, top corner

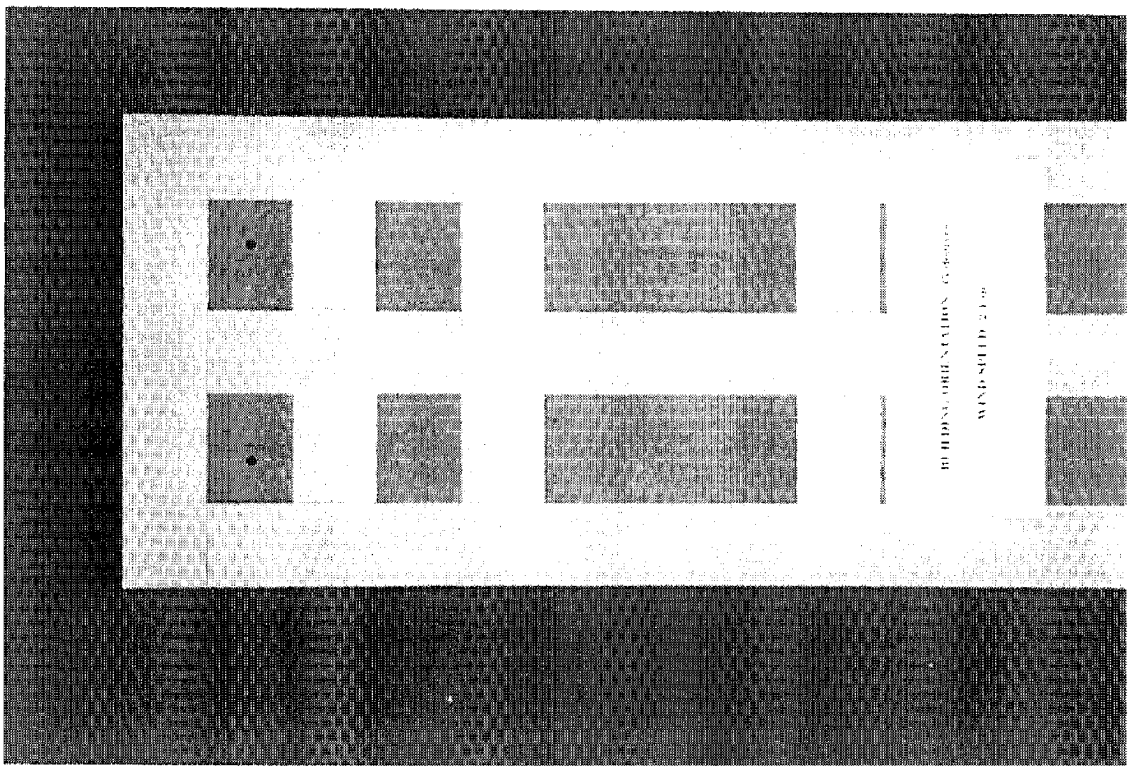

d) narrow side, top half

Figure C.6 Cont'd

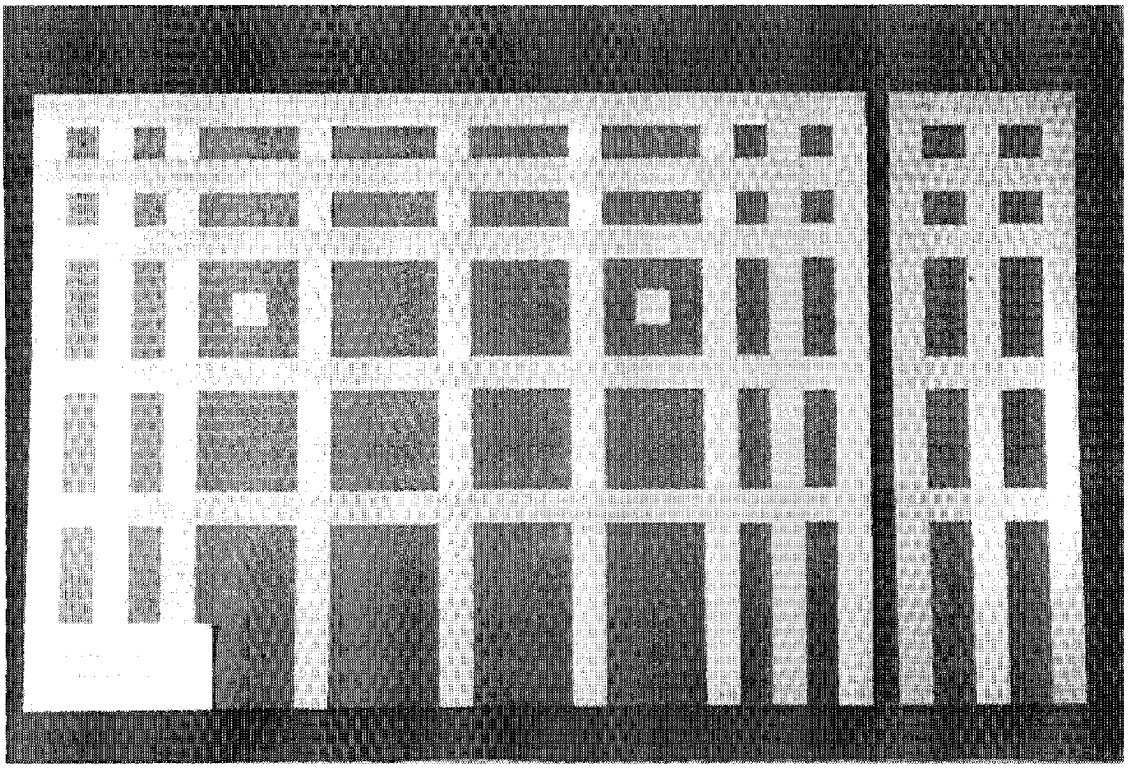

a) complete

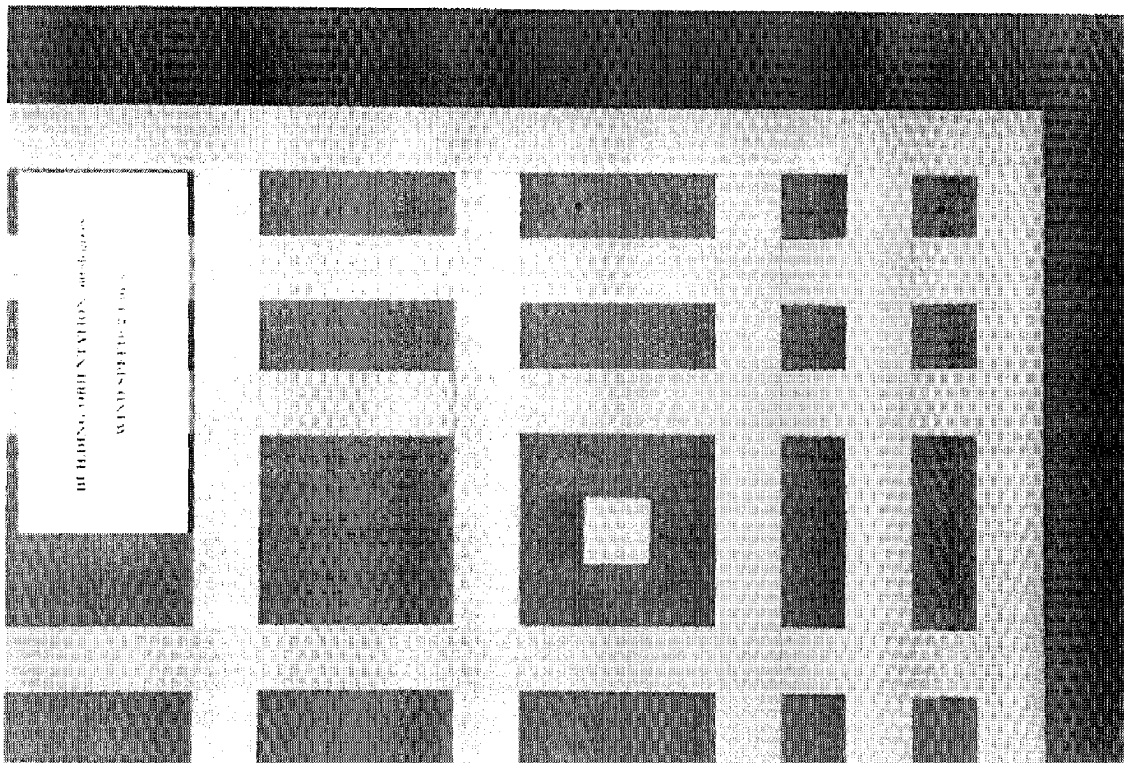

b) wide side, top quarter

Figure C.7 Wetting Patterns for Phase I, Building Angle= 60 degrees, Wind Tunnel Speed= 1.5 m/s at building height

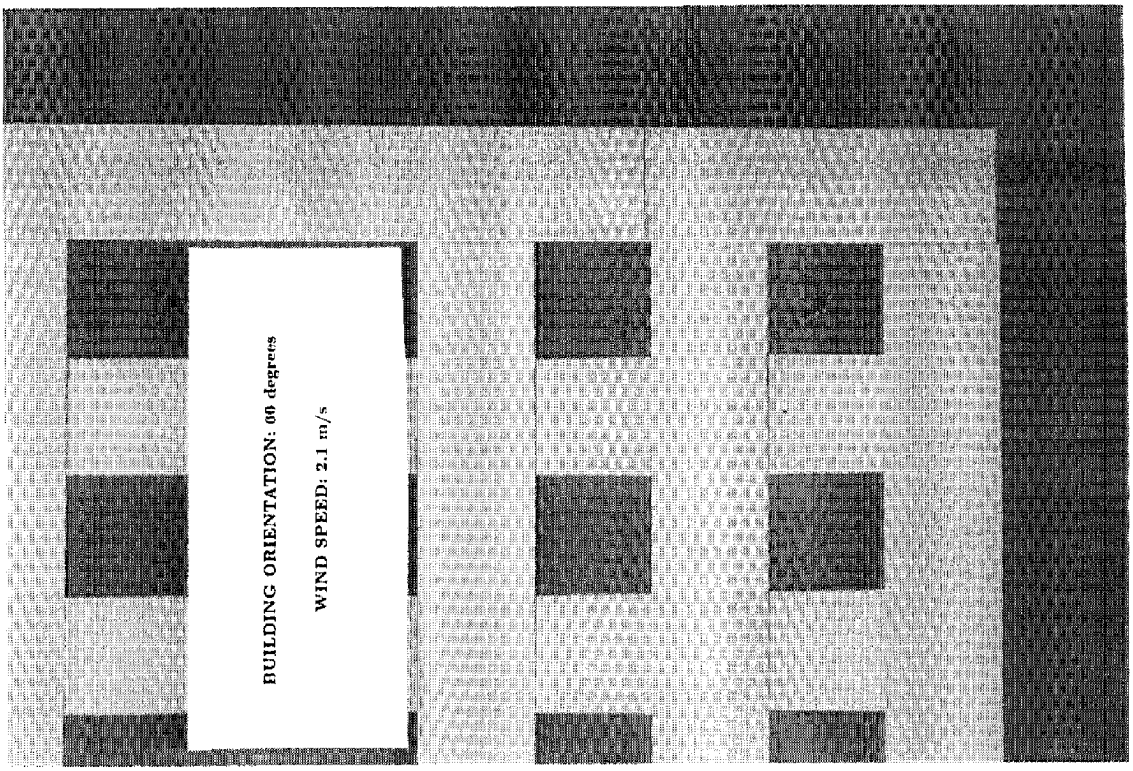

c) wide side, top corner

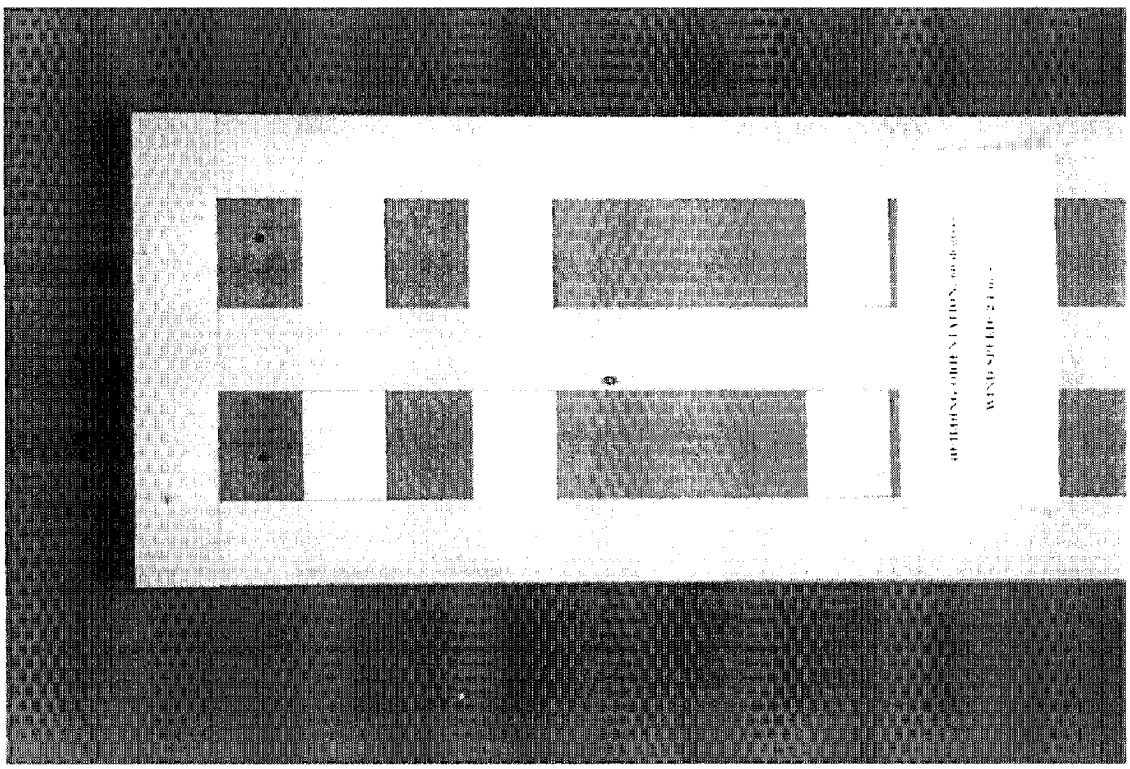

d) narrow side, top half

Figure C.7 Cont'd

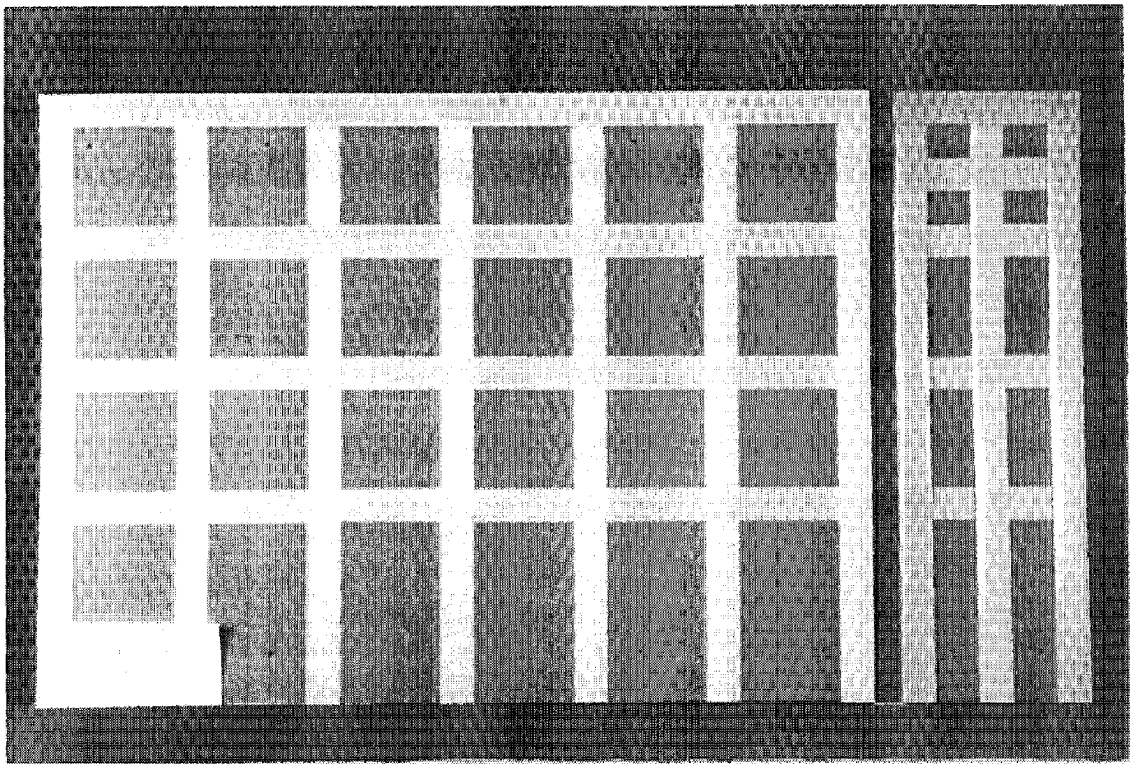

a) complete

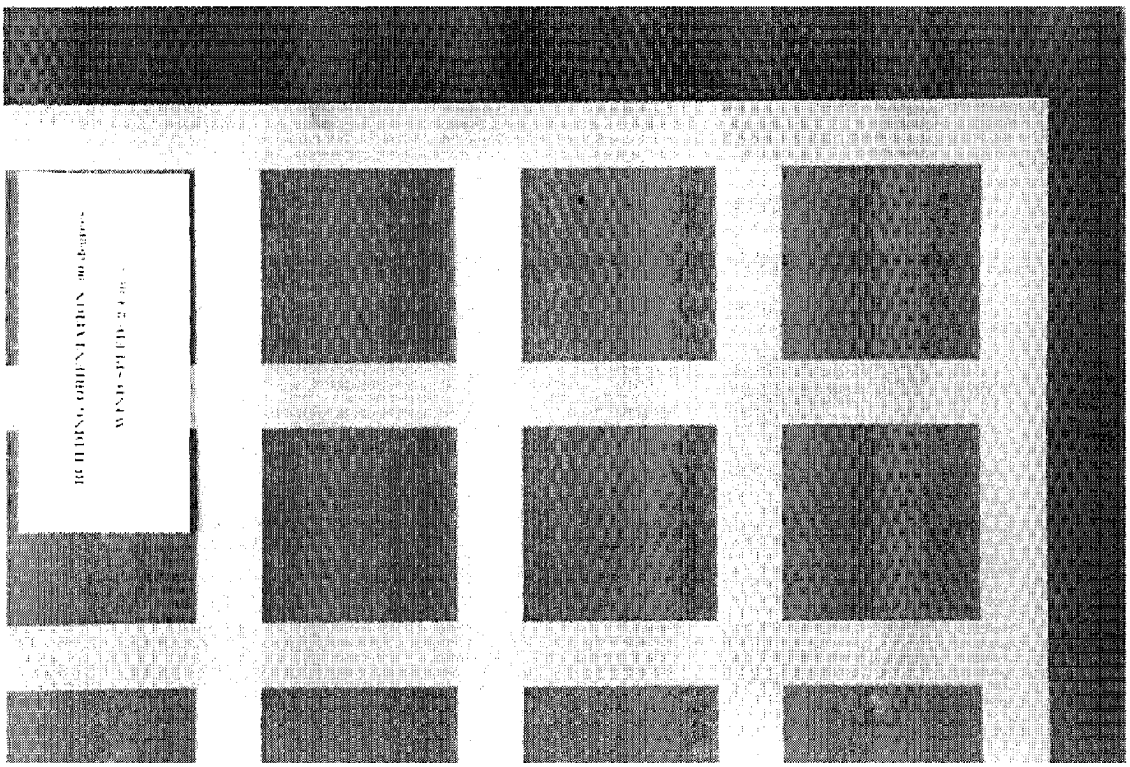

b) wide side, top quarter

Figure C.8 Wetting Patterns for Phase I, Building Angle= 90 degrees, Wind Tunnel Speed= 1.5 m/s at building height

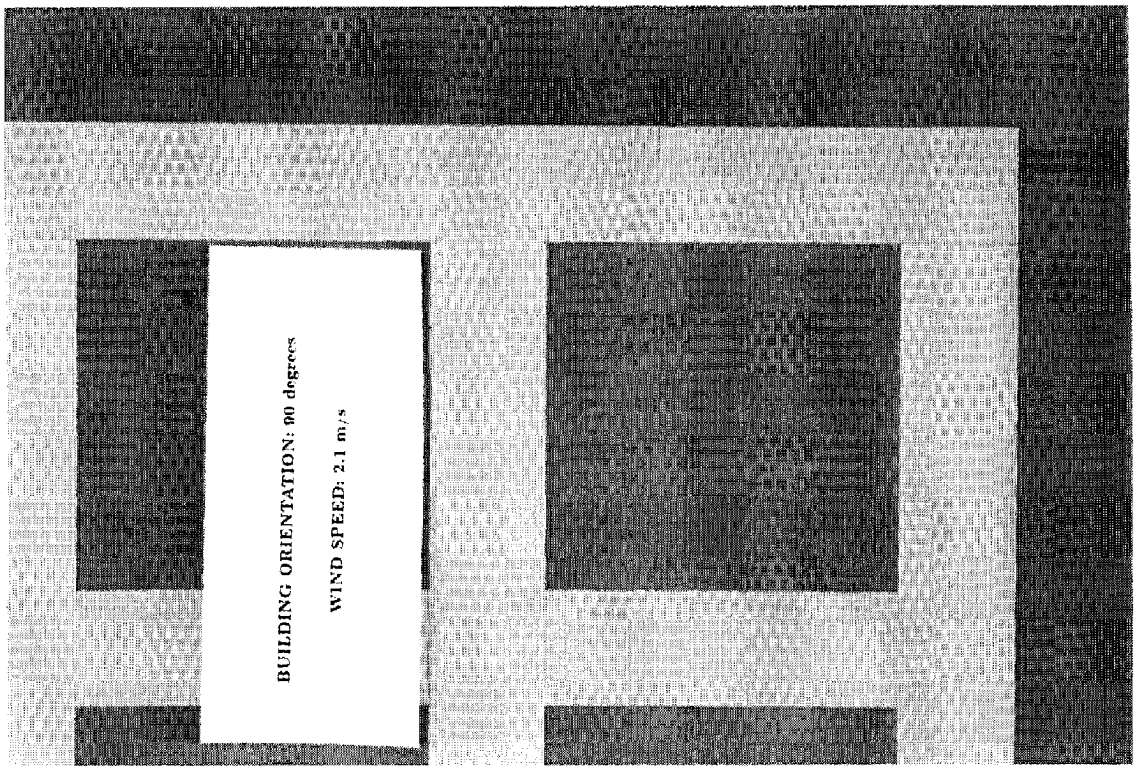

c) wide side, top corner

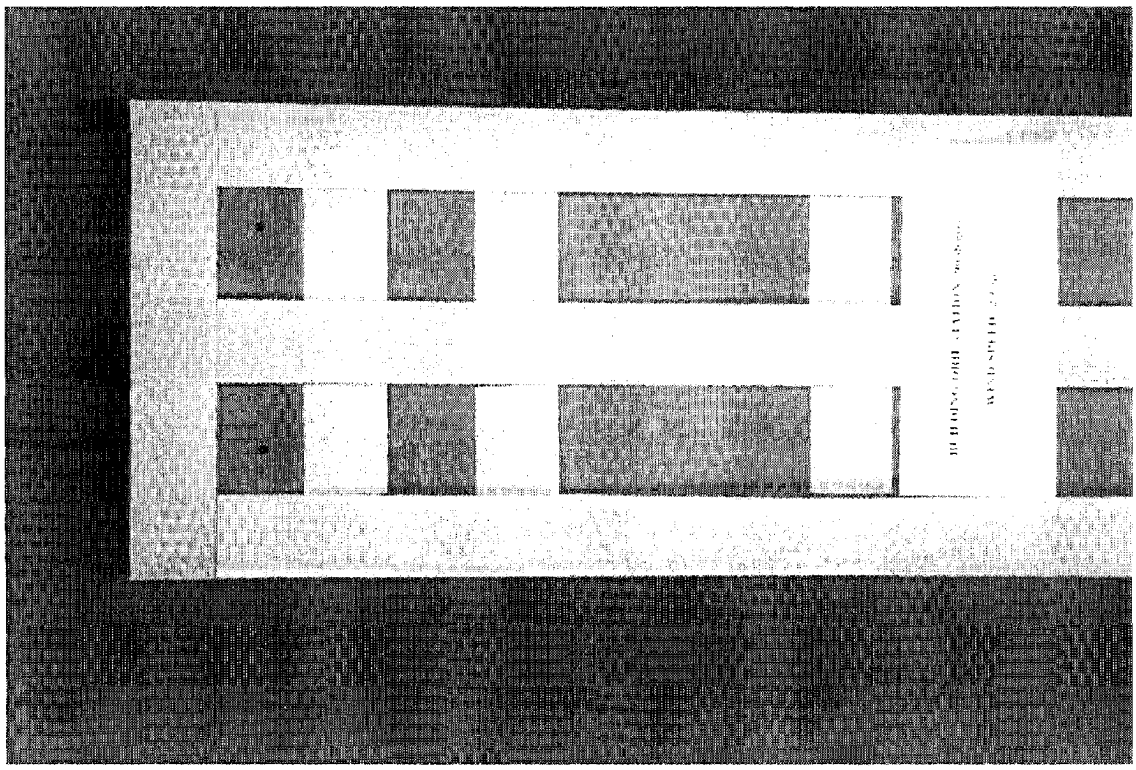

d) narrow side, top half

Figure C.8 Cont'd

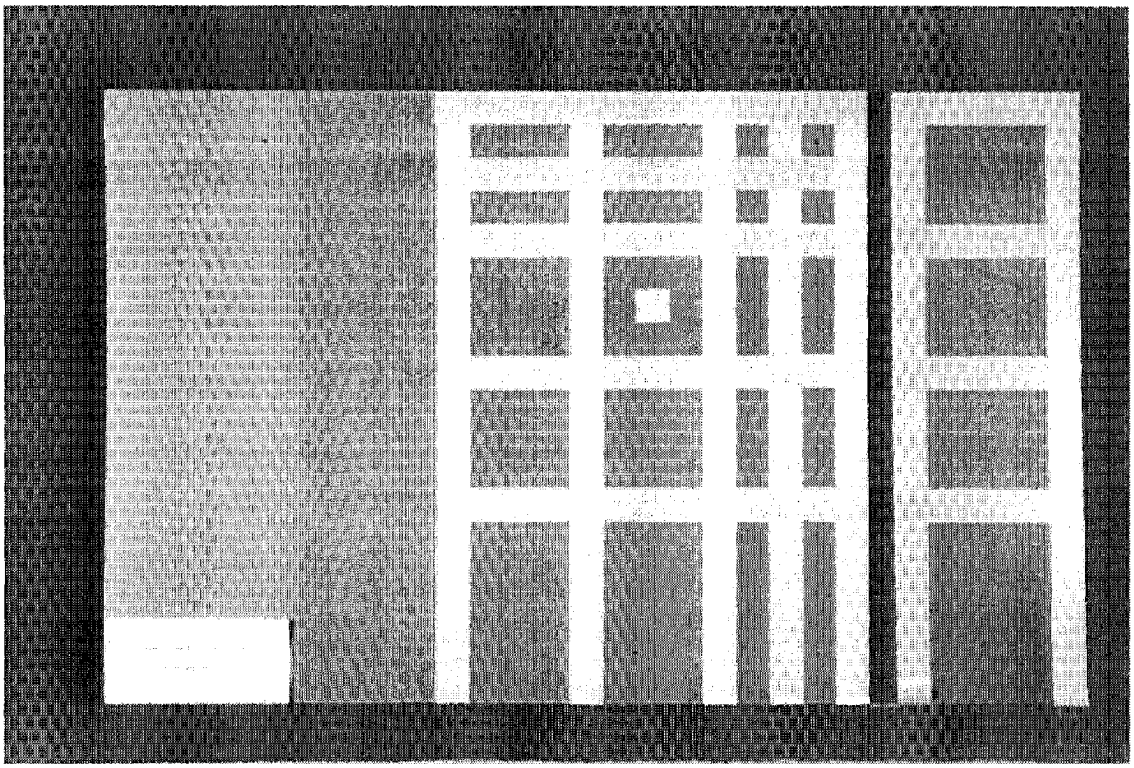

a) complete

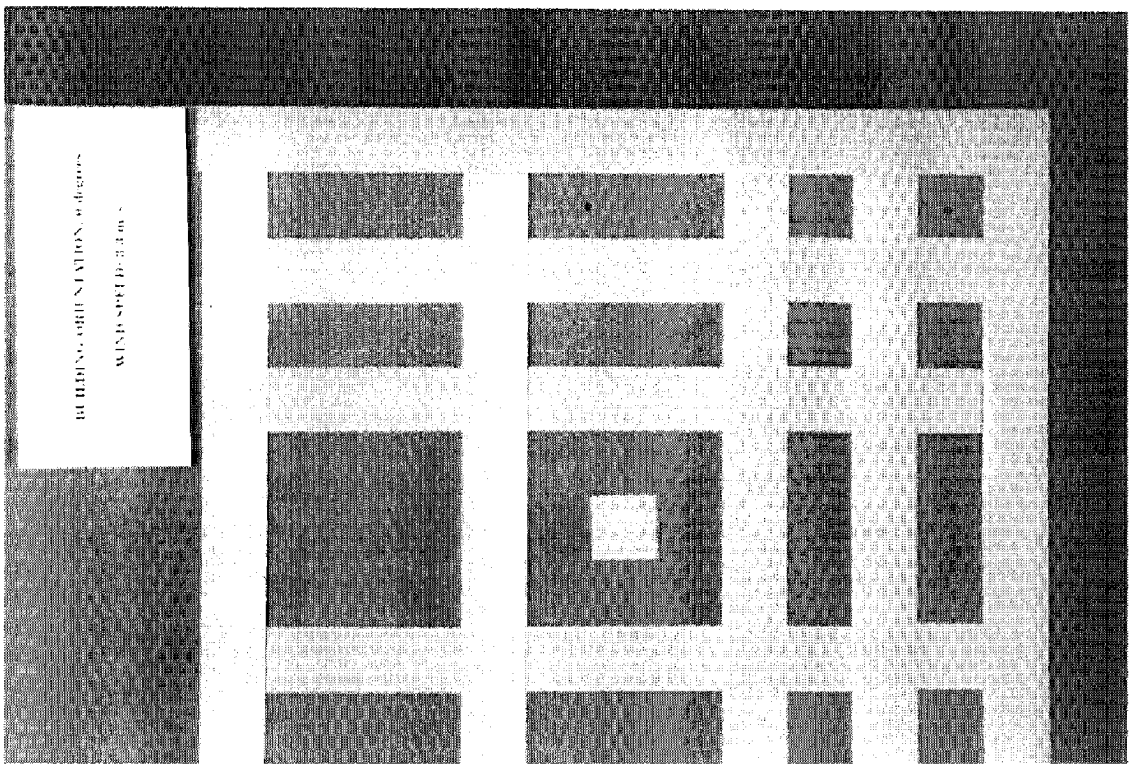

b) wide side, top quarter

Figure C.9 Wetting Patterns for Phase I, Building Angle= 0 degrees, Wind Tunnel Speed= 2.3 m/s at building height

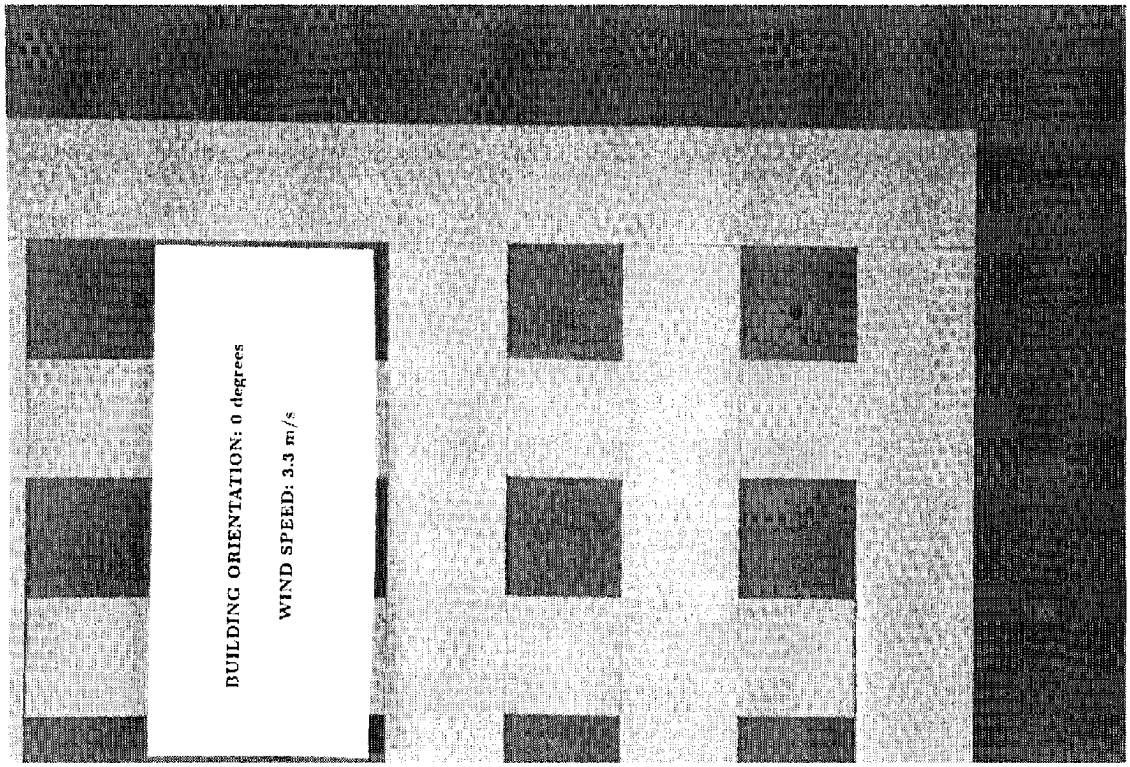

c) wide side, top corner

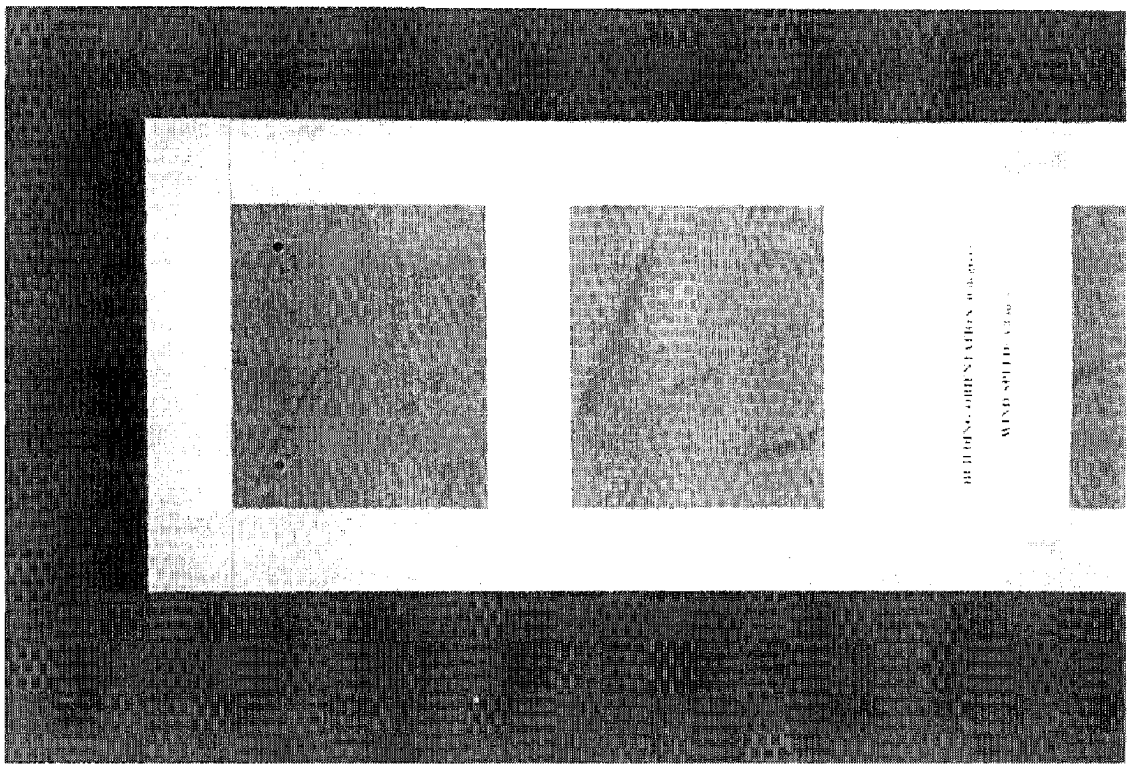

d) narrow side, top half

Figure C.9 Cont'd

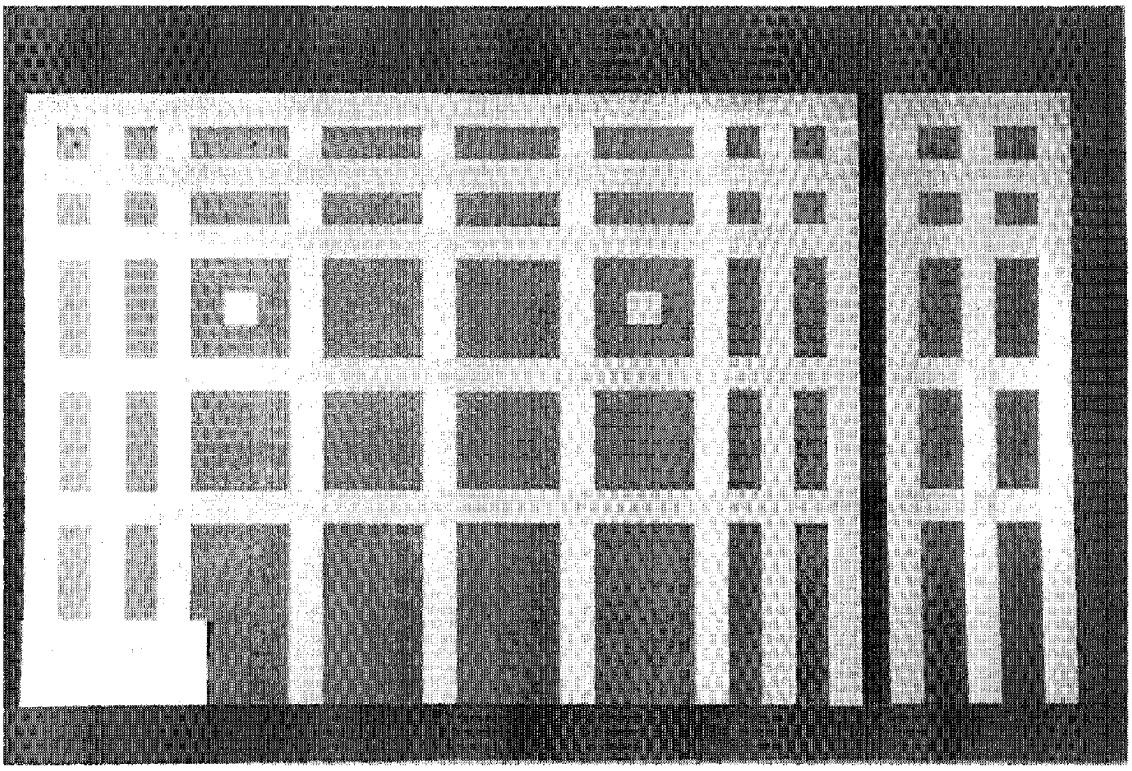

a) complete

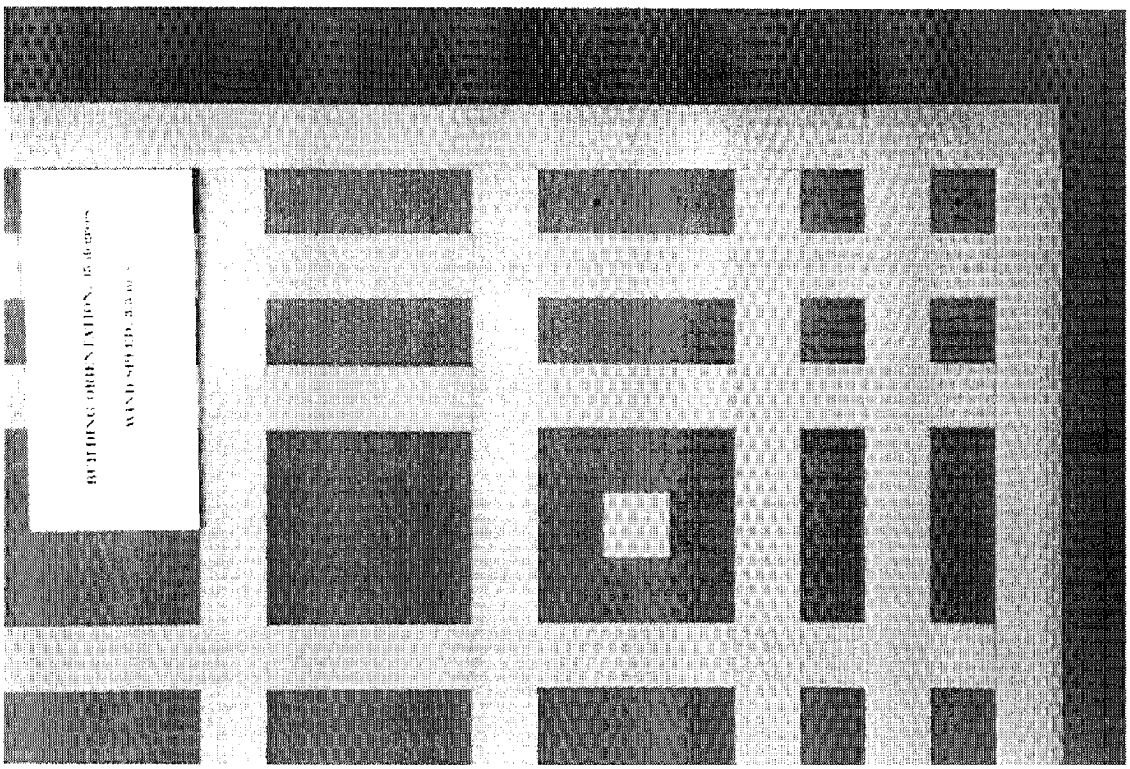

b) wide side, top quarter

Figure C.10 Wetting Patterns for Phase I, Building Angle= 45 degrees, Wind Tunnel Speed= 2.3 m/s at building height

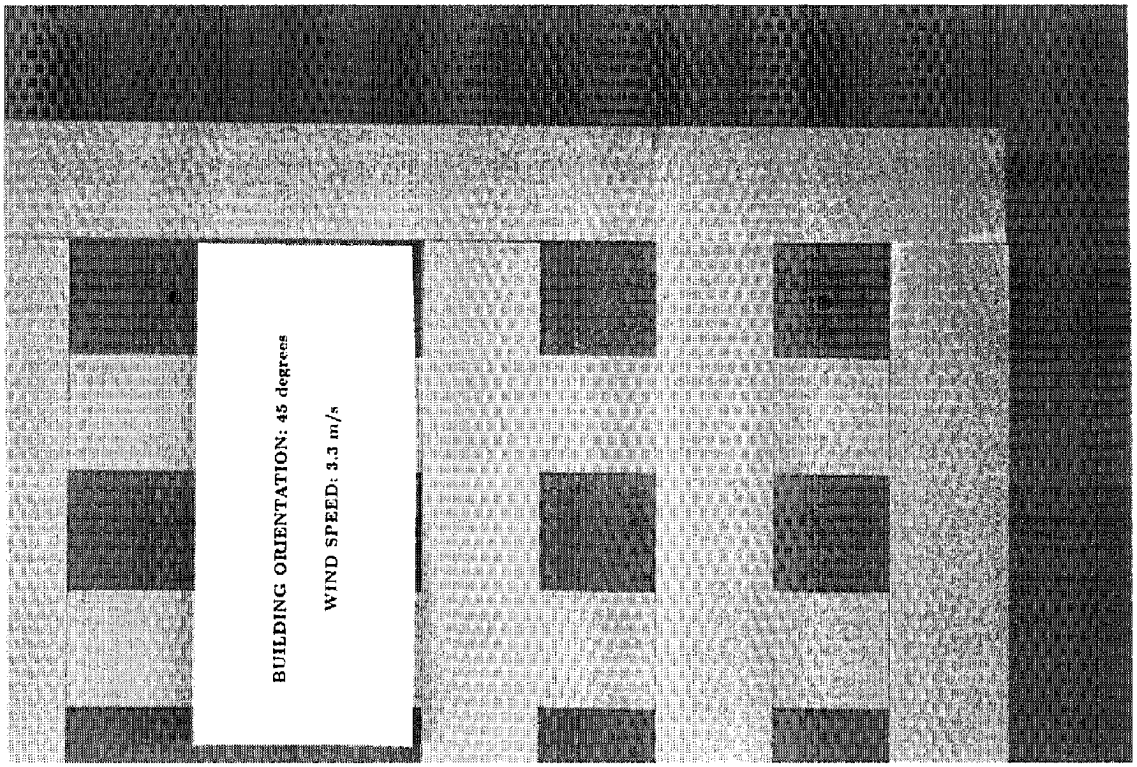

c) wide side, top corner

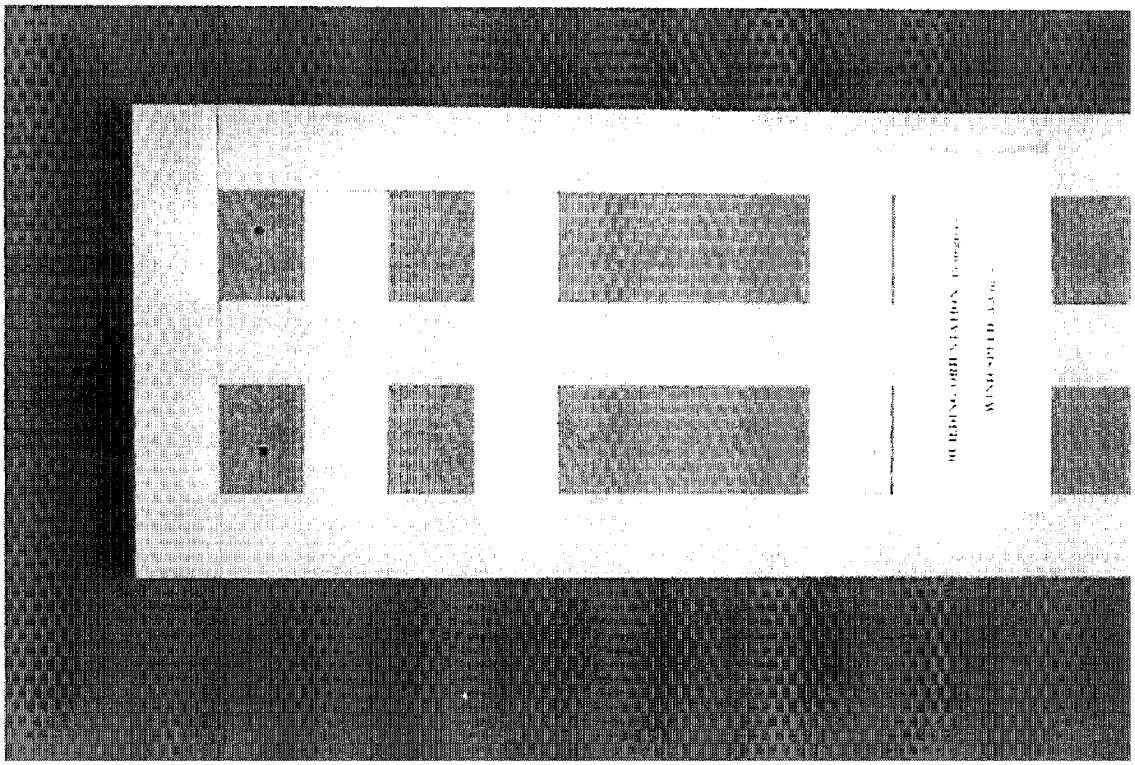

d) narrow side, top half

Figure C.10 Cont'd

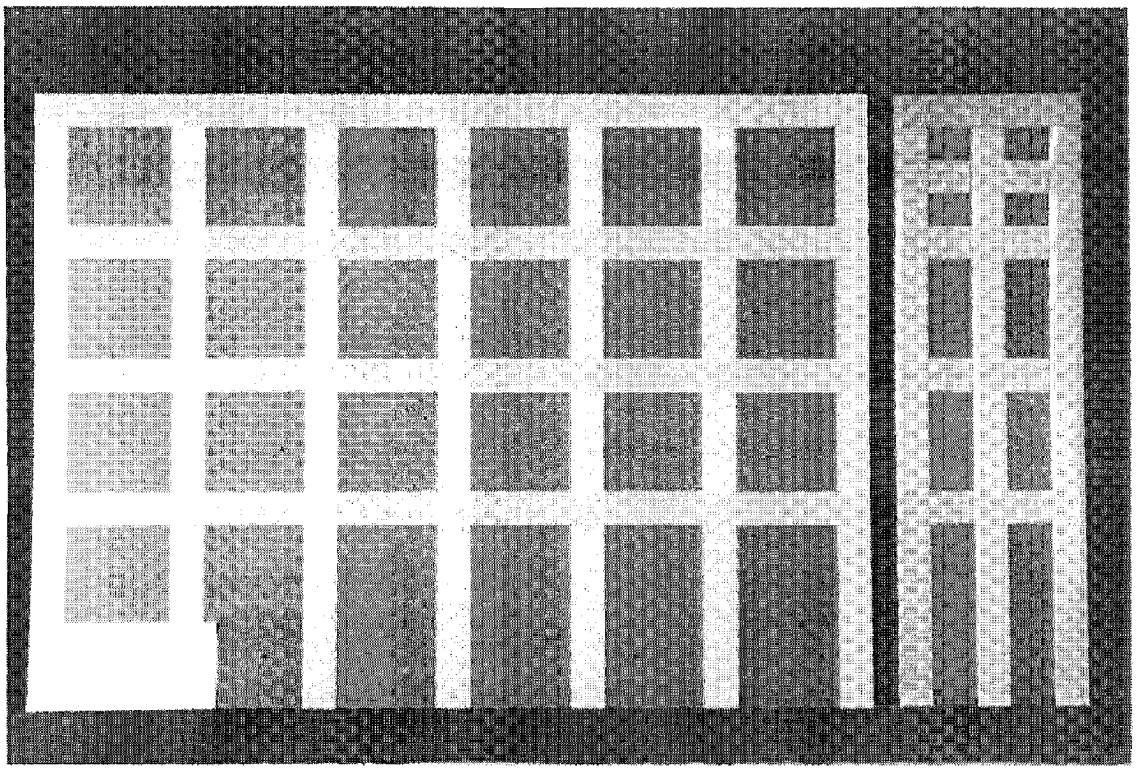

a) complete

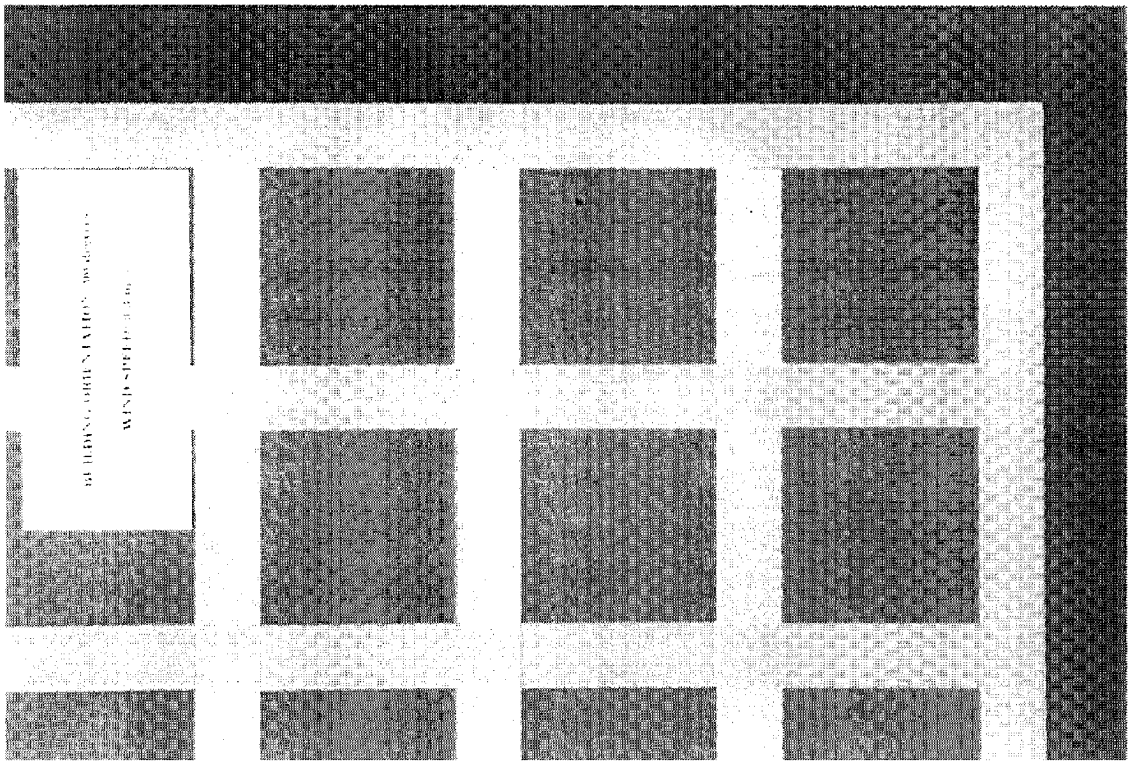

b) wide side, top quarter

Figure C.11 Wetting Patterns for Phase I, Building Angle= 90 degrees, Wind Tunnel Speed= 2.3 m/s at building height

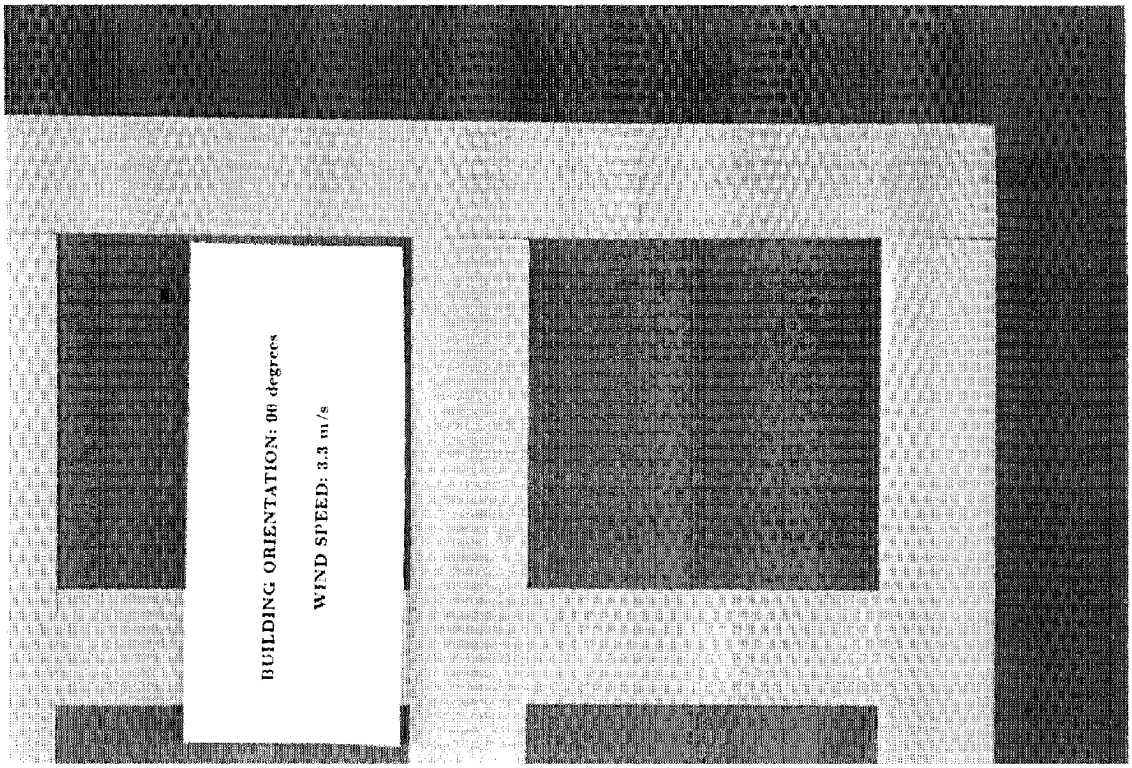

c) wide side, top corner

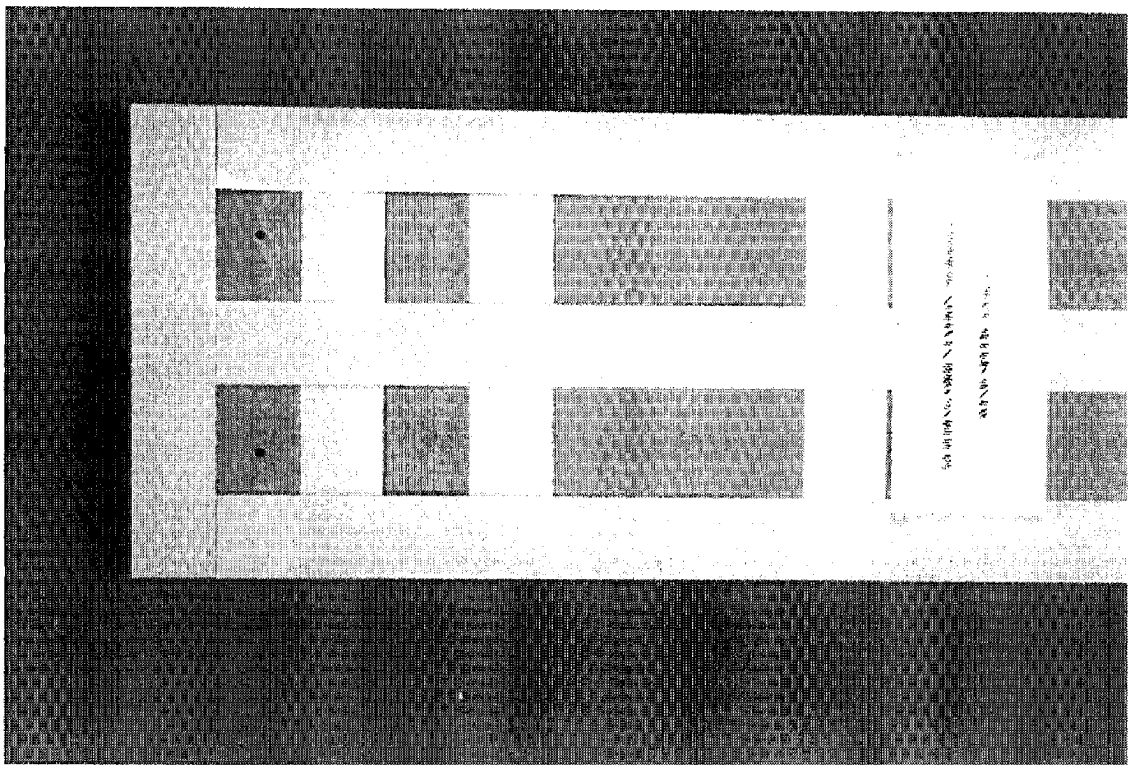

d) narrow side, top half

Figure C.11 Cont'd

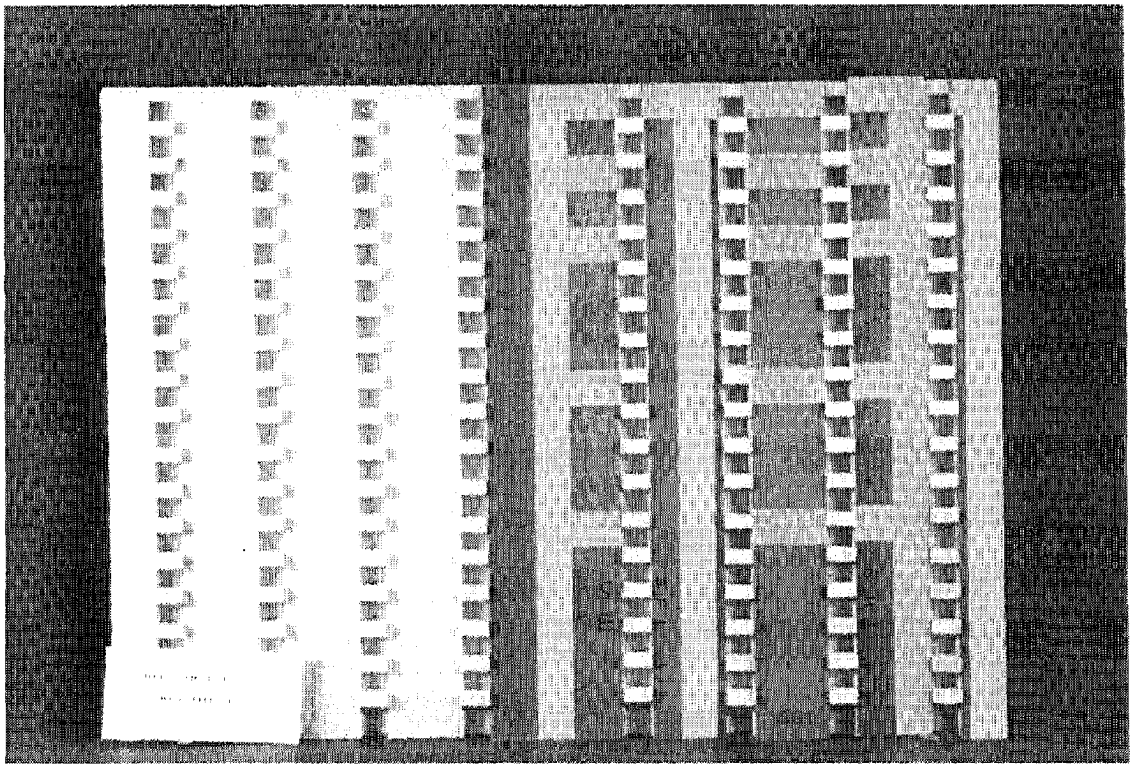

a) complete, building angle= 0

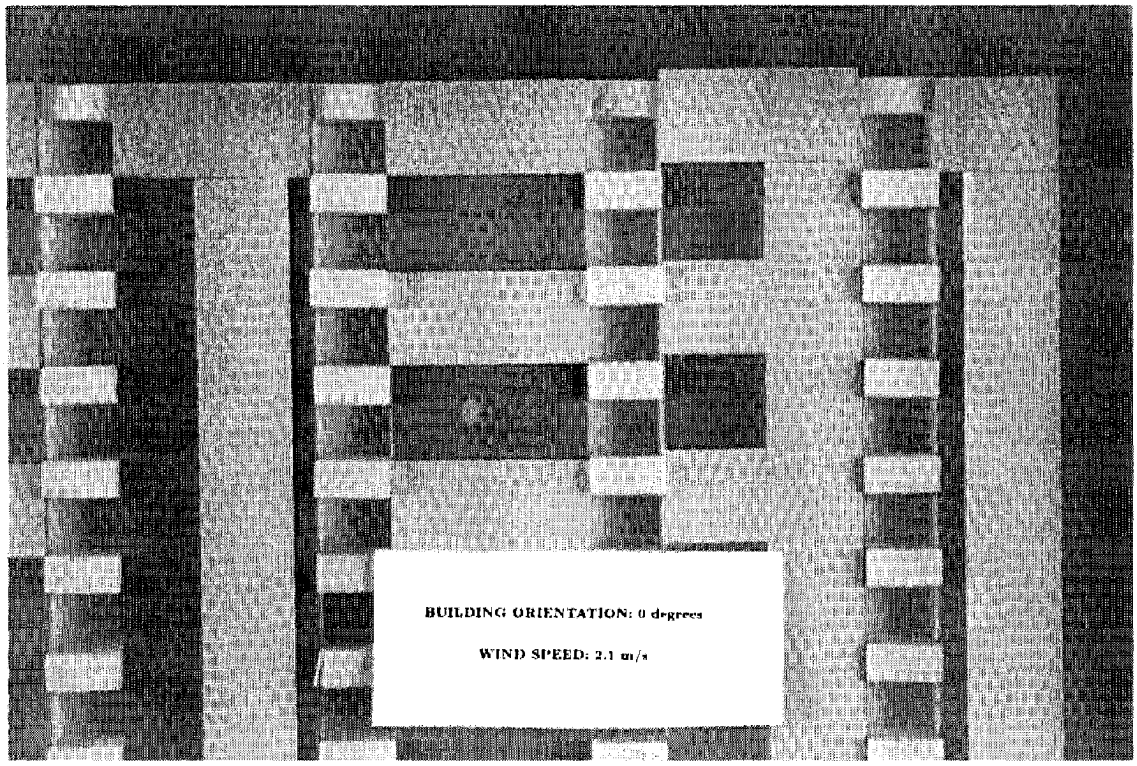

b) detail, building angle= 0

Figure C.12 Wetting Patterns for Phase I Building with Balconies, Wind Tunnel Speed= 1.5 m/s at building height

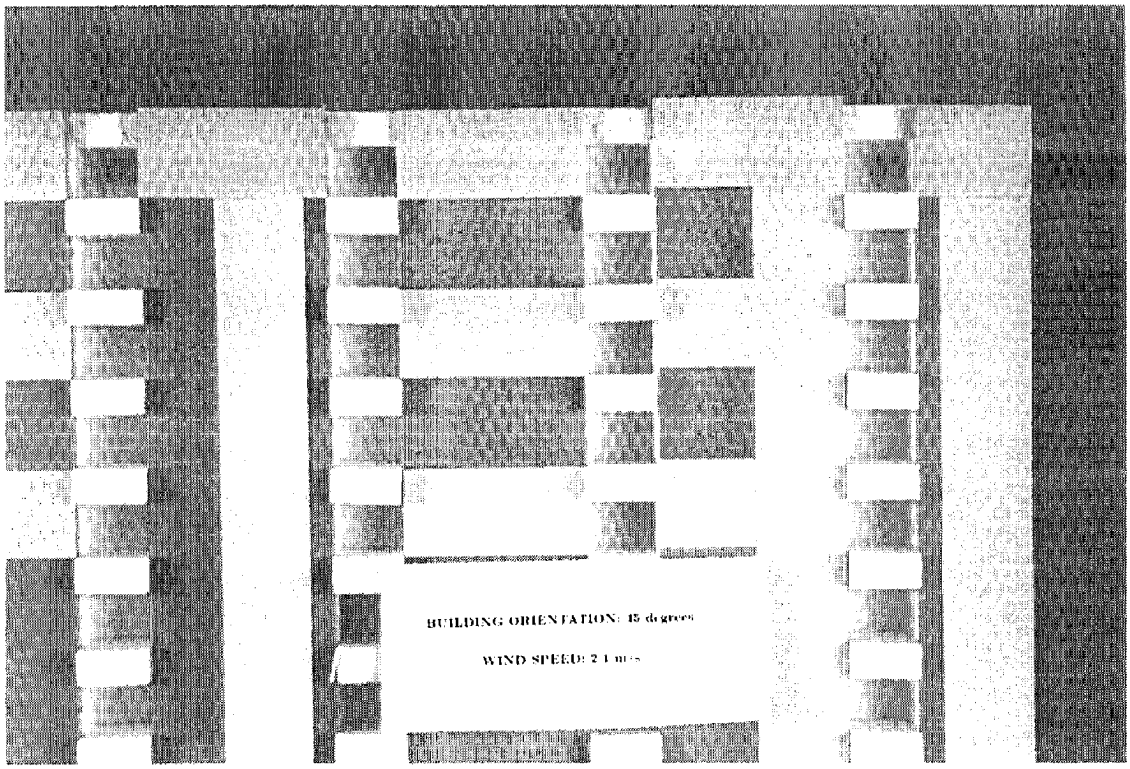

c) detail , building angle= 45

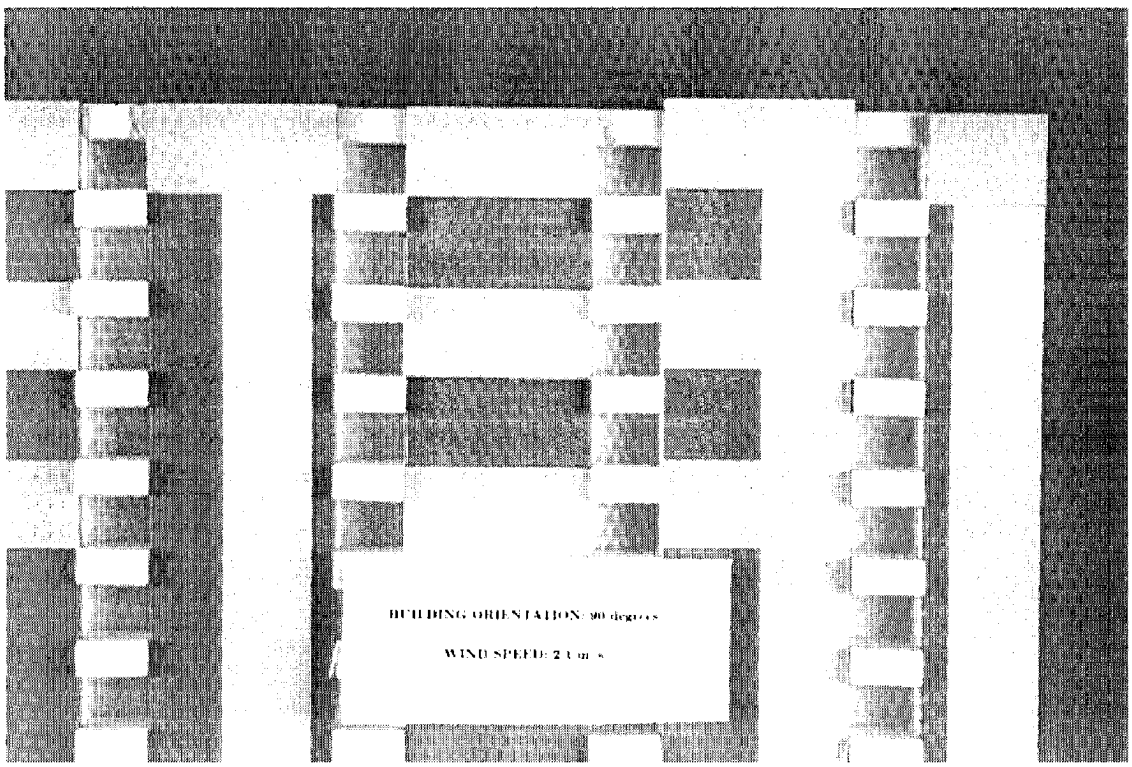

d) detail , building angle= 90

Figure C.12 Cont'd

APPENDIX D

PHOTOGRAPHS OF WETTING PATTERNS FOR PHASE II

Test #	Building	Building Angle	Building Configuration
2, 20	A	0	basic
1, 18	B	0	basic
3, 19	C	0	basic
7	A	45	basic
6	B	45	basic
5	C	45	basic
10	A	90	basic
8	B	90	basic
9	C	90	basic
15	A	0	2m cornice
11	B	0	2m cornice
14	C	0	2m cornice
12	B	45	2m cornice
13	B	90	2m cornice
24	A	0	1m cornice
22	B	0	1m cornice
23	C	0	1m cornice
16	B	0	peaked roof
17	B	0	inset corners
4	cylinder	-	-
21	B	0	2m cornice duration 27 sec

Table D.1. Summary of Wetting Pattern Tests, Phase II

Notes:

1] All tests except Test #21 had a duration of 6 seconds. Test #21 was stopped when water started dripping from the cornice.

2] The wind speed for all tests was 1.5 m/s at a height of 0.94 m (Phase I building height).

3] The relative humidity for Tests # 1-13 varied between 63% and 68%. For Tests # 14-21, it varied between 77% and 80%.

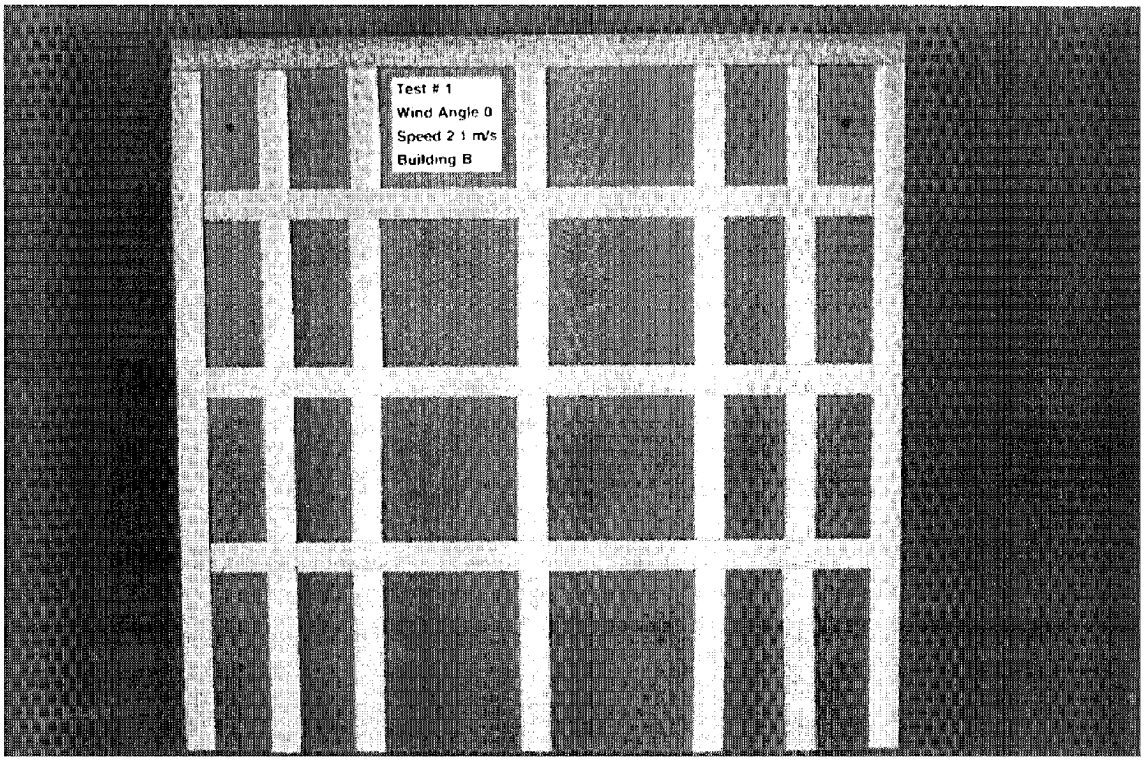

Figure D.1a. Complete Wetting Pattern for Phase II Building B, Building Angle= 0 degrees, Wide Face only

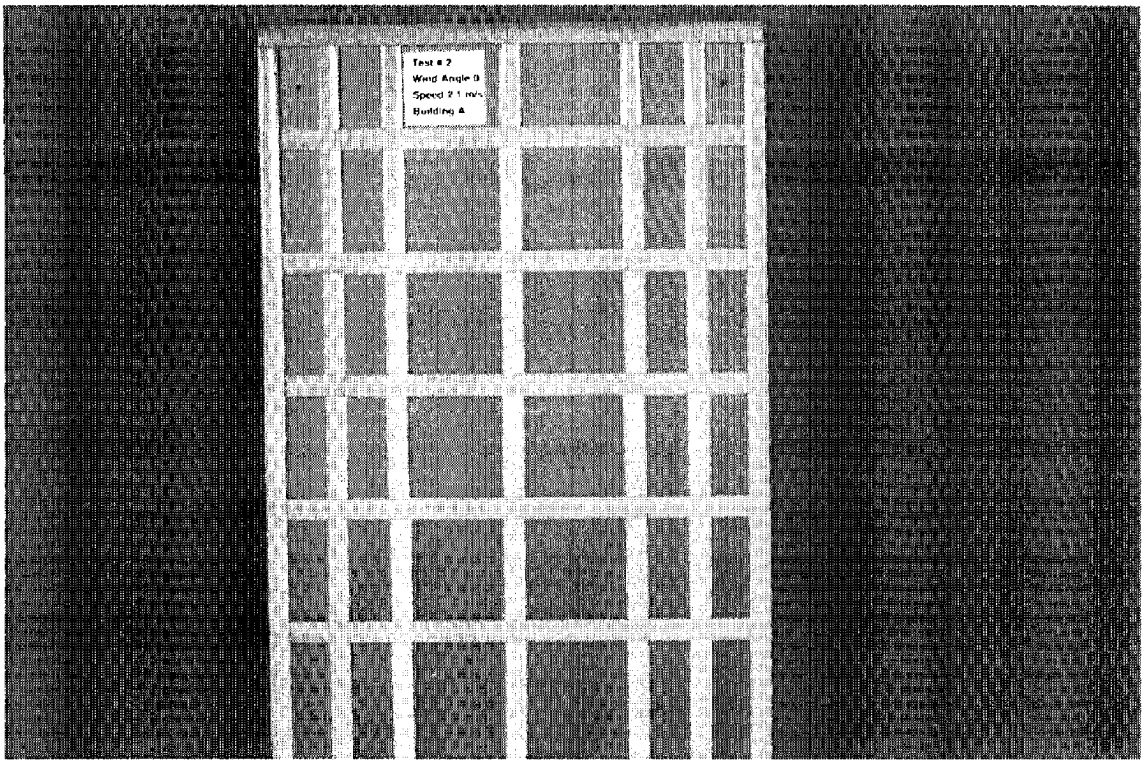

Figure D.1b. Complete Wetting Pattern for Phase II Building A, Building Angle= 0 degrees, Wide Face only

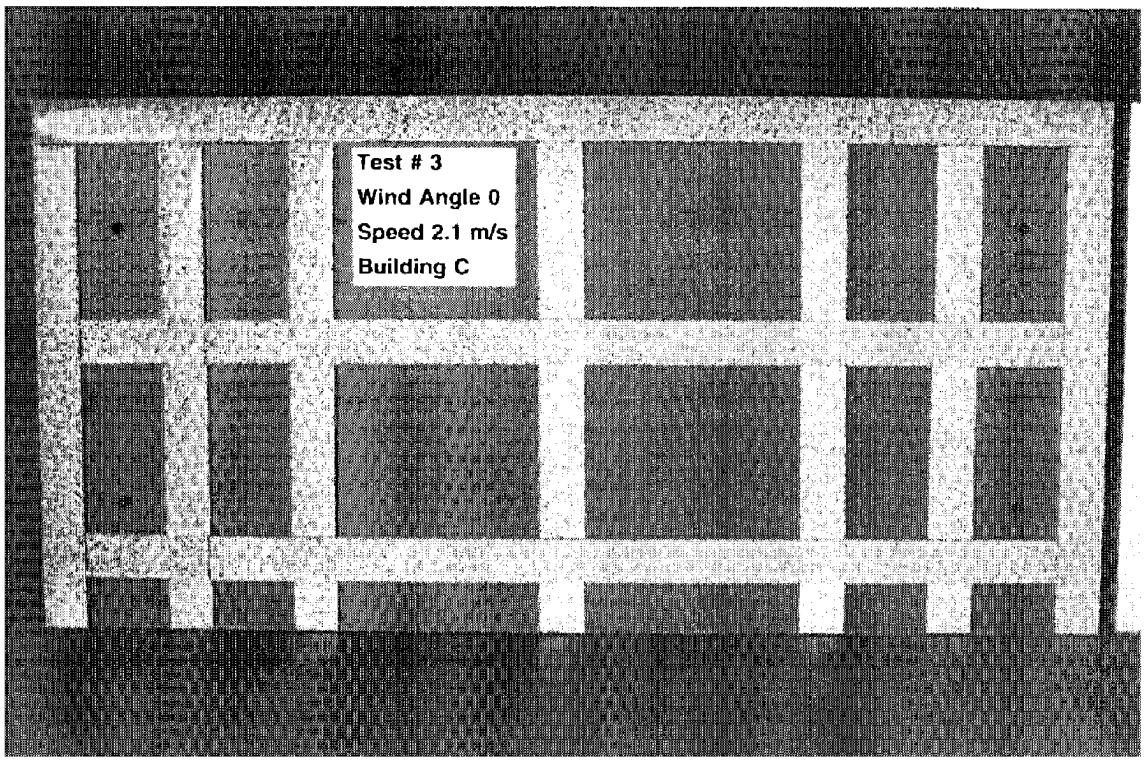

Figure D.1c. Complete Wetting Pattern for Phase II Building C, Building Angle= 0 degrees, Wide Face only

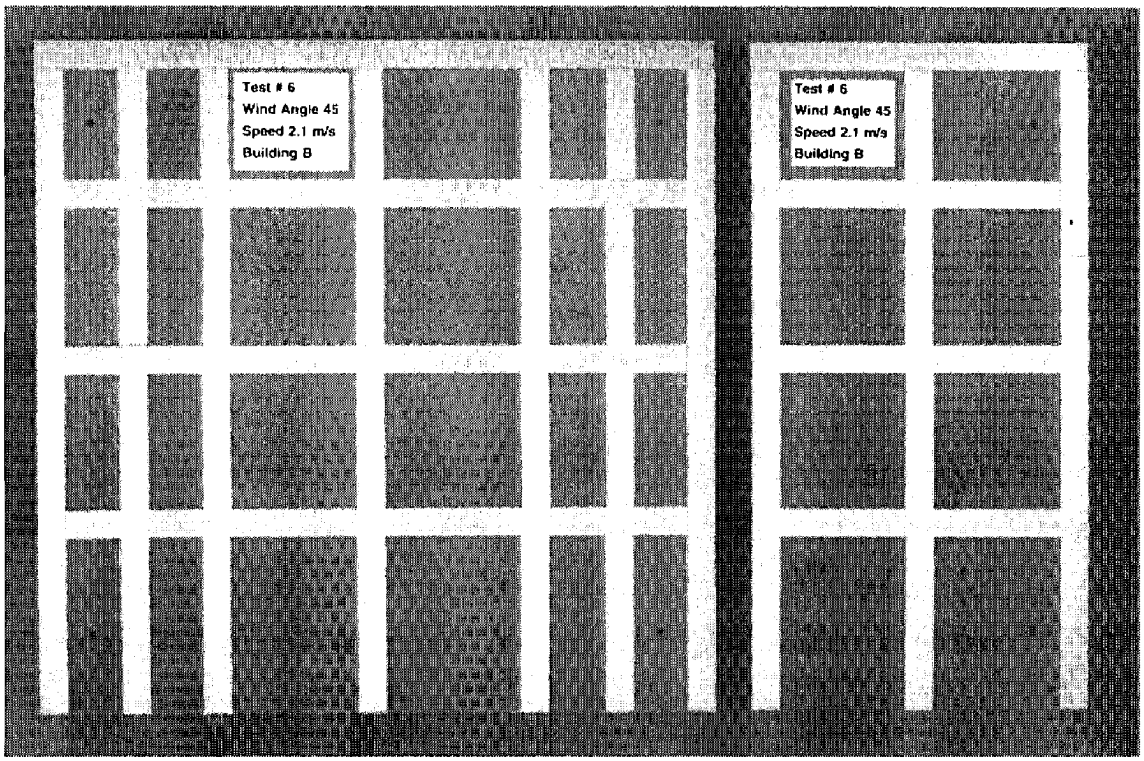

Figure D.2a. Complete Wetting Patterns for Phase II Building B, Building Angle= 45 degrees

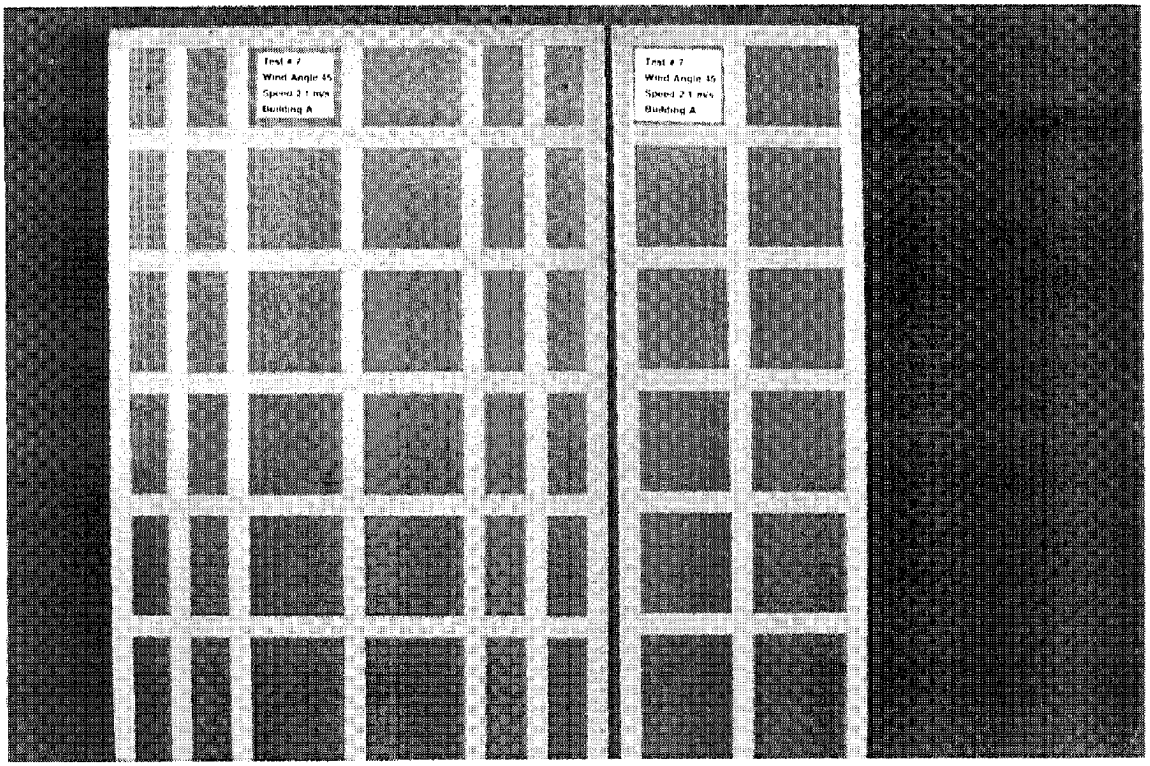

Figure D.2b. Complete Wetting Patterns for Phase II Building A, Building Angle= 45 degrees

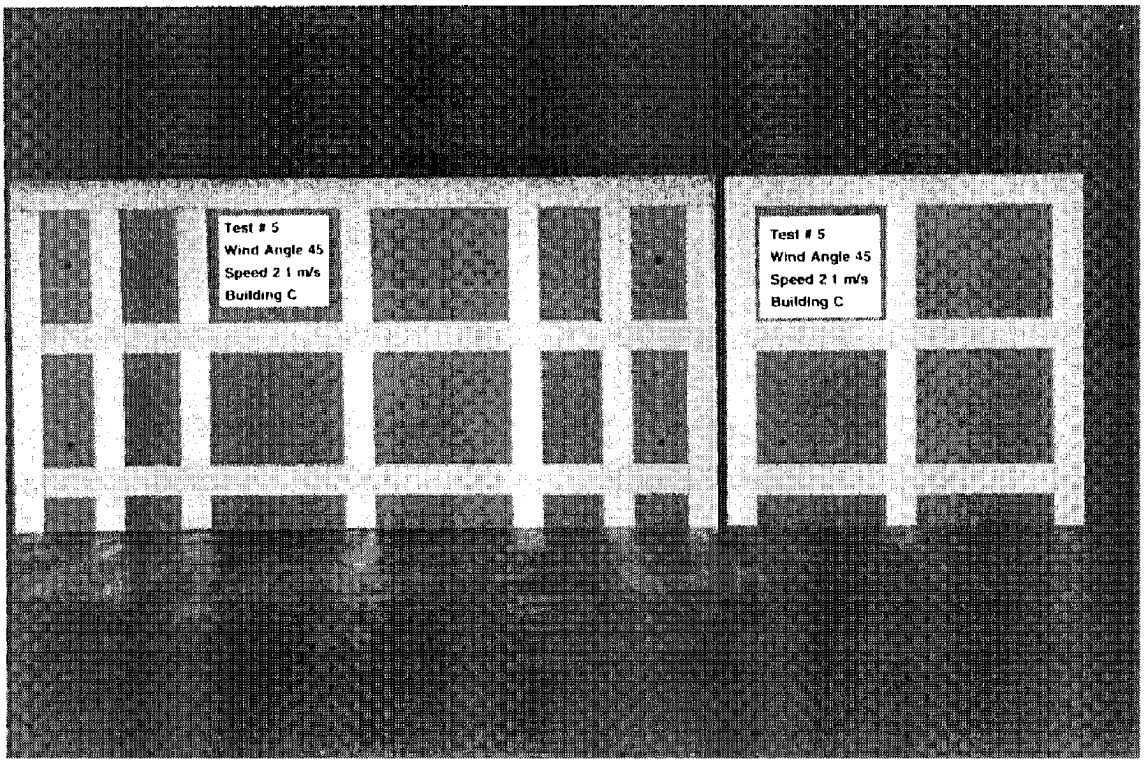

Figure D.2c. Complete Wetting Patterns for Phase II Building C, Building Angle= 45 degrees

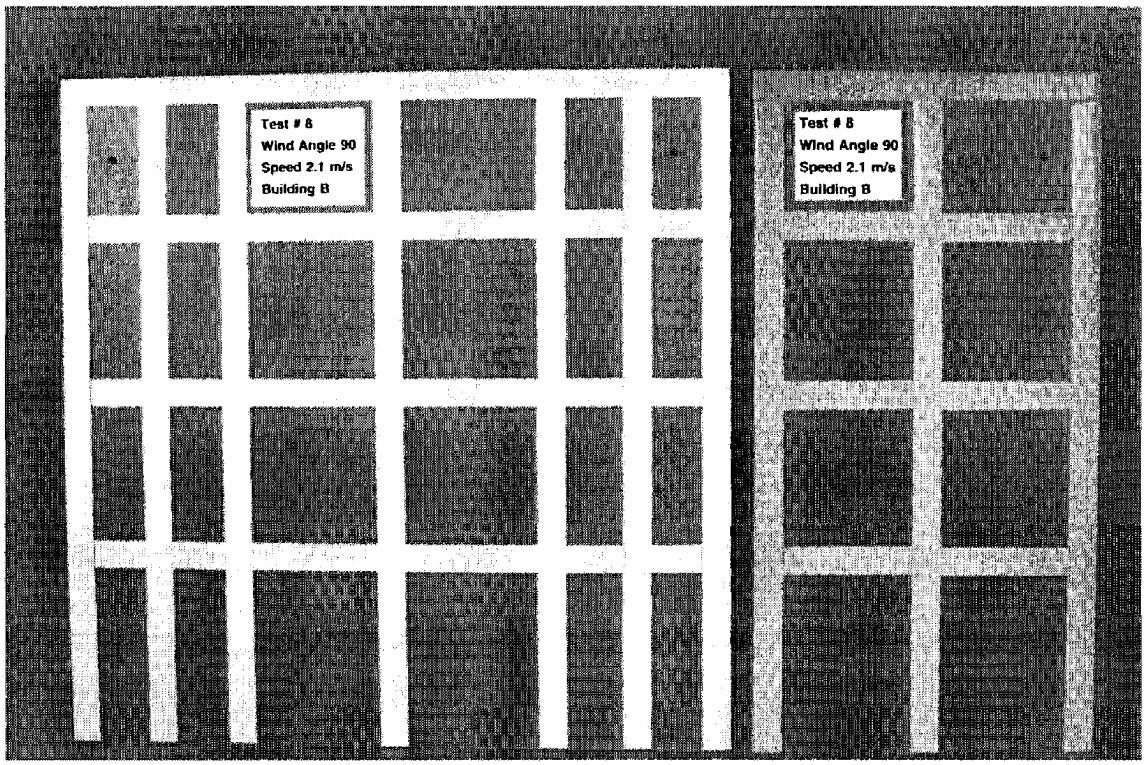

Figure D.3a. Complete Wetting Patterns for Phase II Building B, Building Angle= 90 degrees

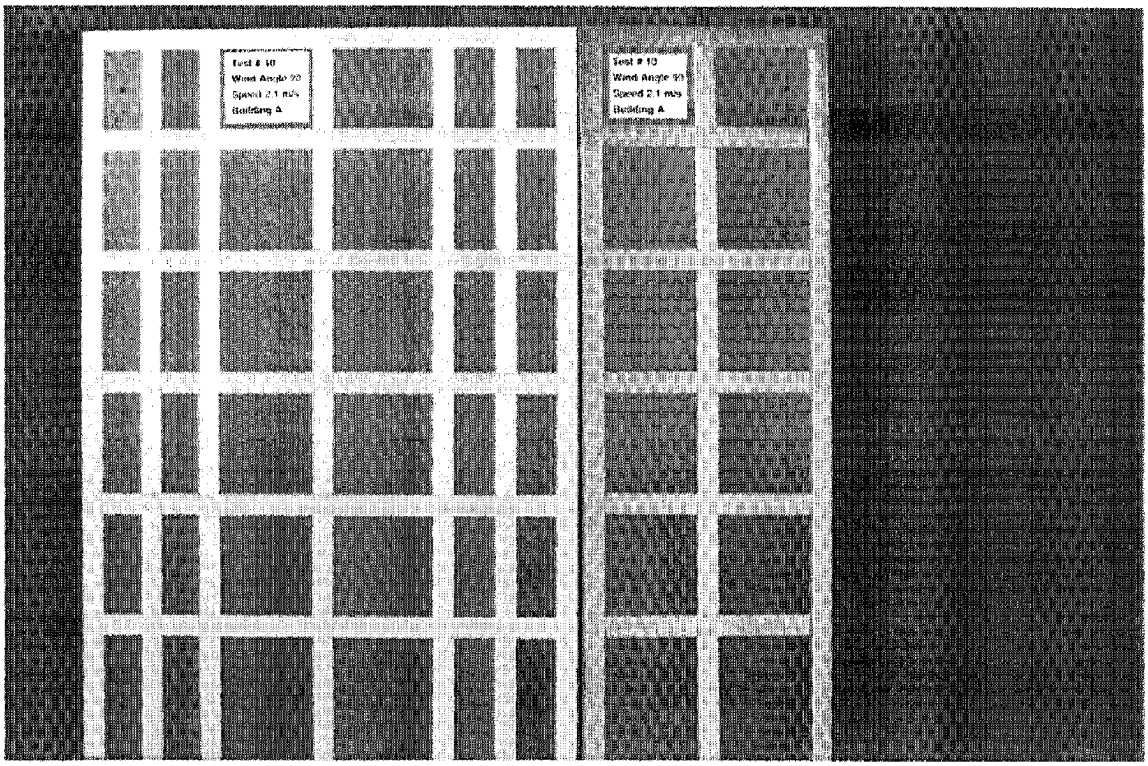

Figure D.3b. Complete Wetting Patterns for Phase II Building A, Building Angle= 90 degrees

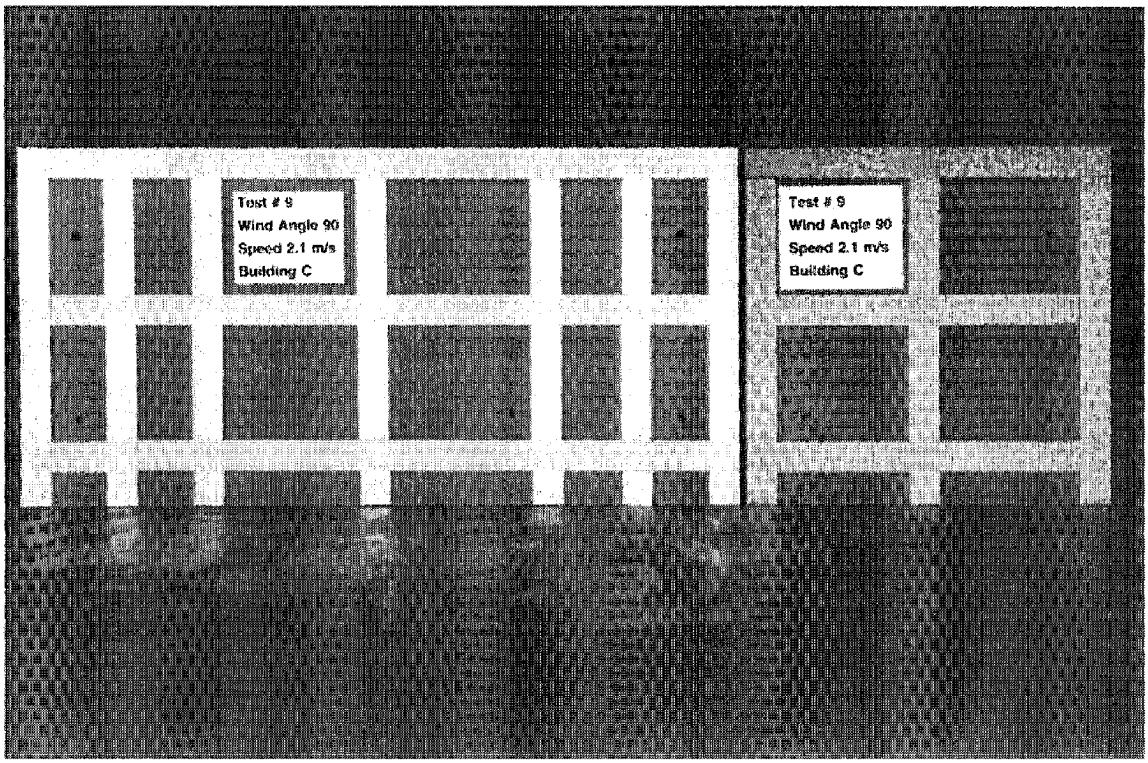

Figure D.3c. Complete Wetting Patterns for Phase II Building C, Building Angle= 90 degrees

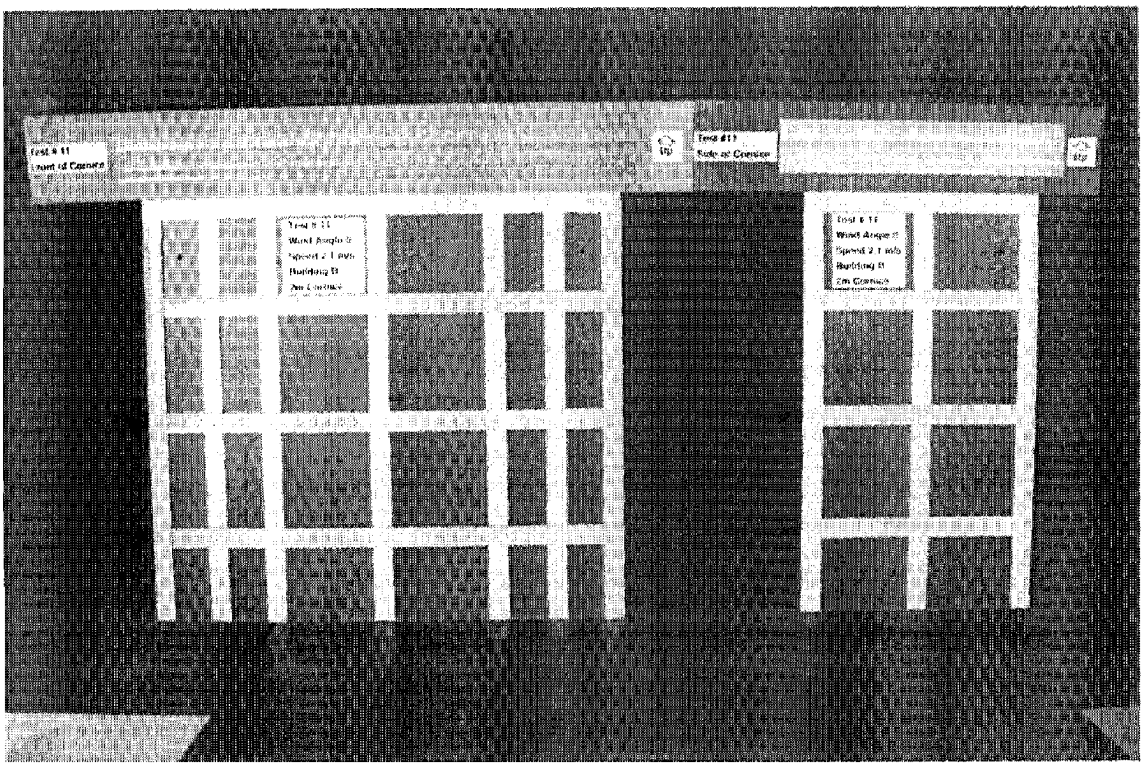

note: cornice is mounted upside down in photograph

Figure D.4a. Complete Wetting Patterns for Phase II Building B with 2m Cornice, Building Angle= 0 degrees

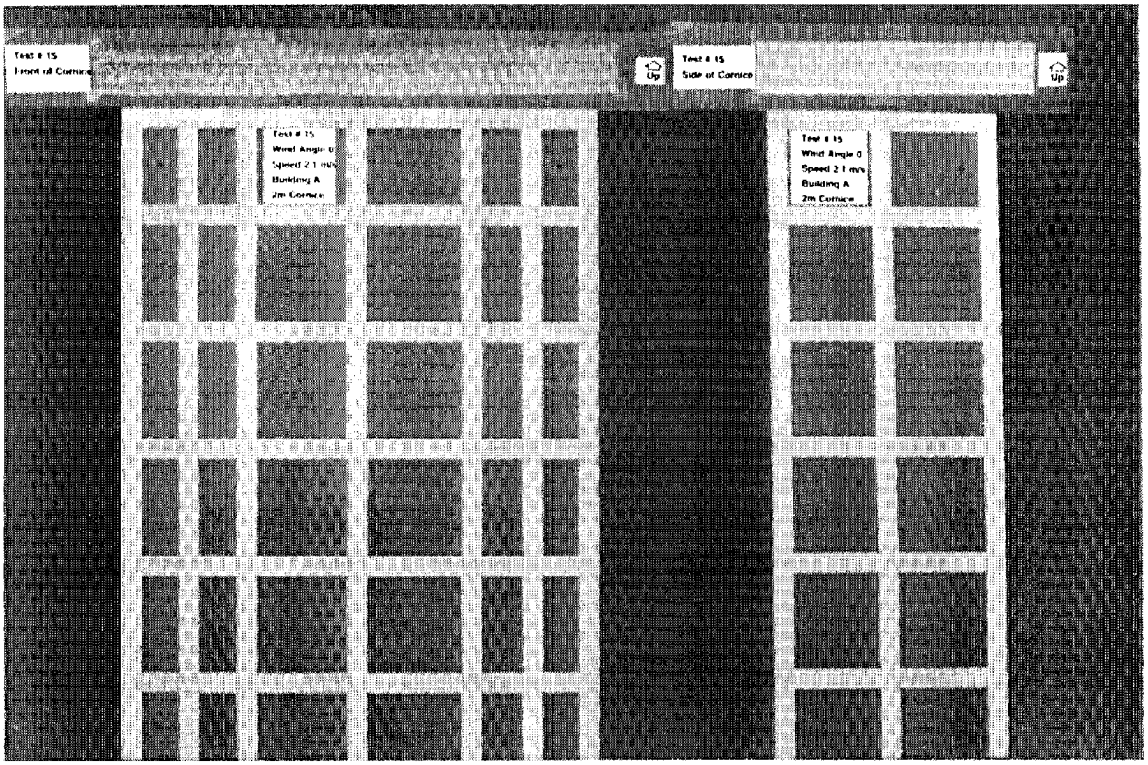

Figure D.4b. Complete Wetting Patterns for Phase II Building A with 2m Cornice, Building Angle= 0 degrees

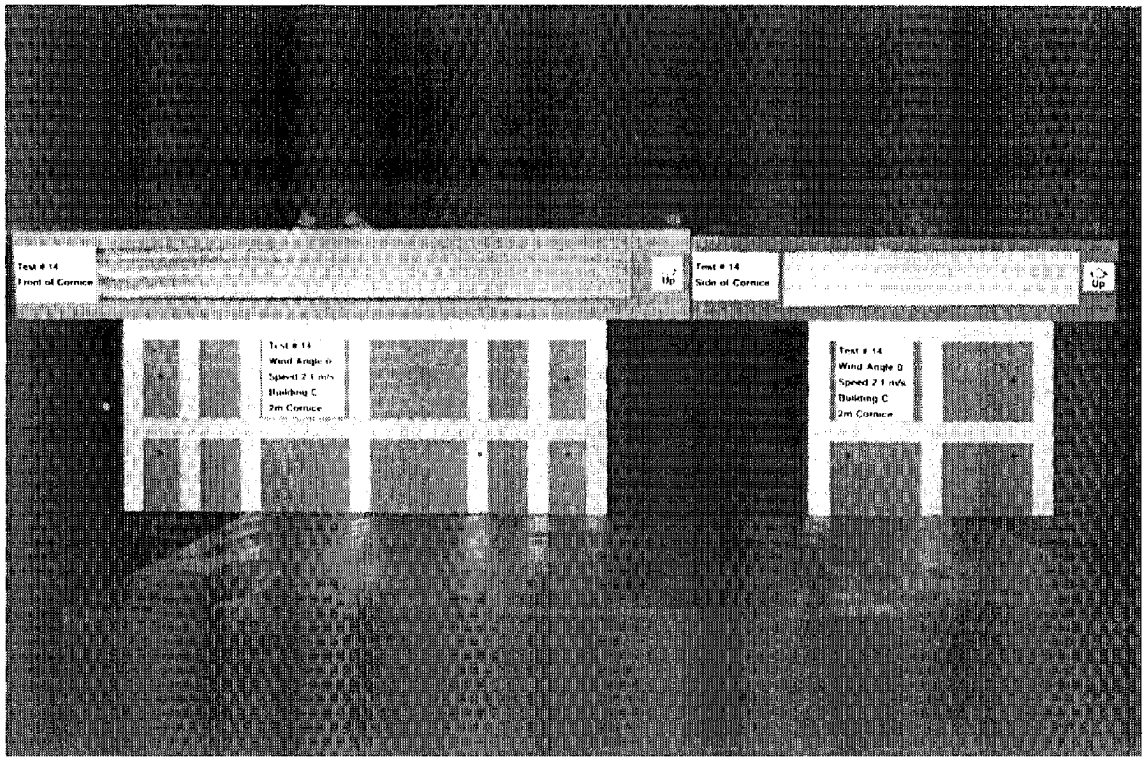

Figure D.4c. Complete Wetting Patterns for Phase II Building C with 2m Cornice, Building Angle= 0 degrees

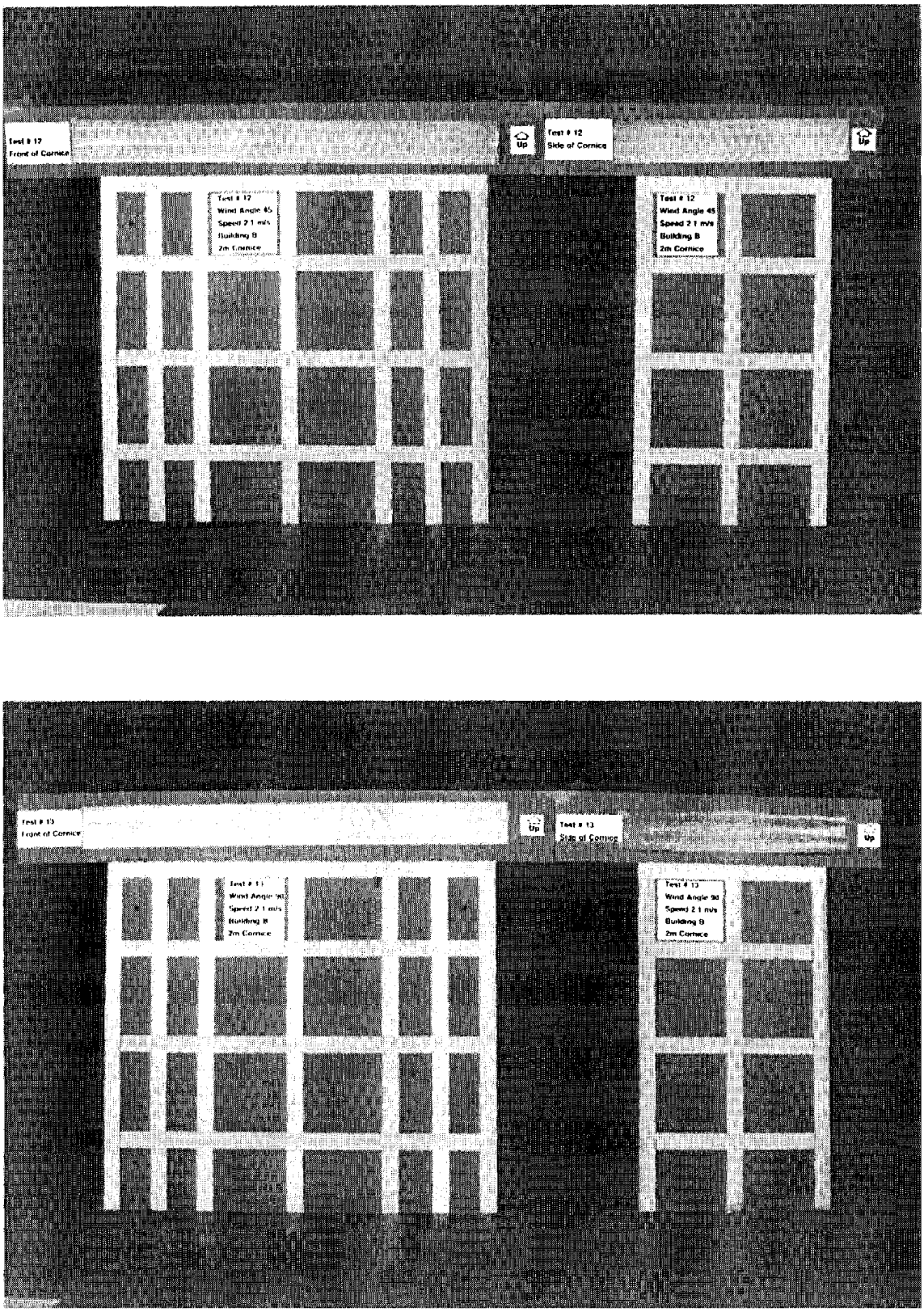

Figure D.5. Complete Wetting Patterns for Phase II Building B with 2m Cornice, Building Angles= 45 and 90 degrees

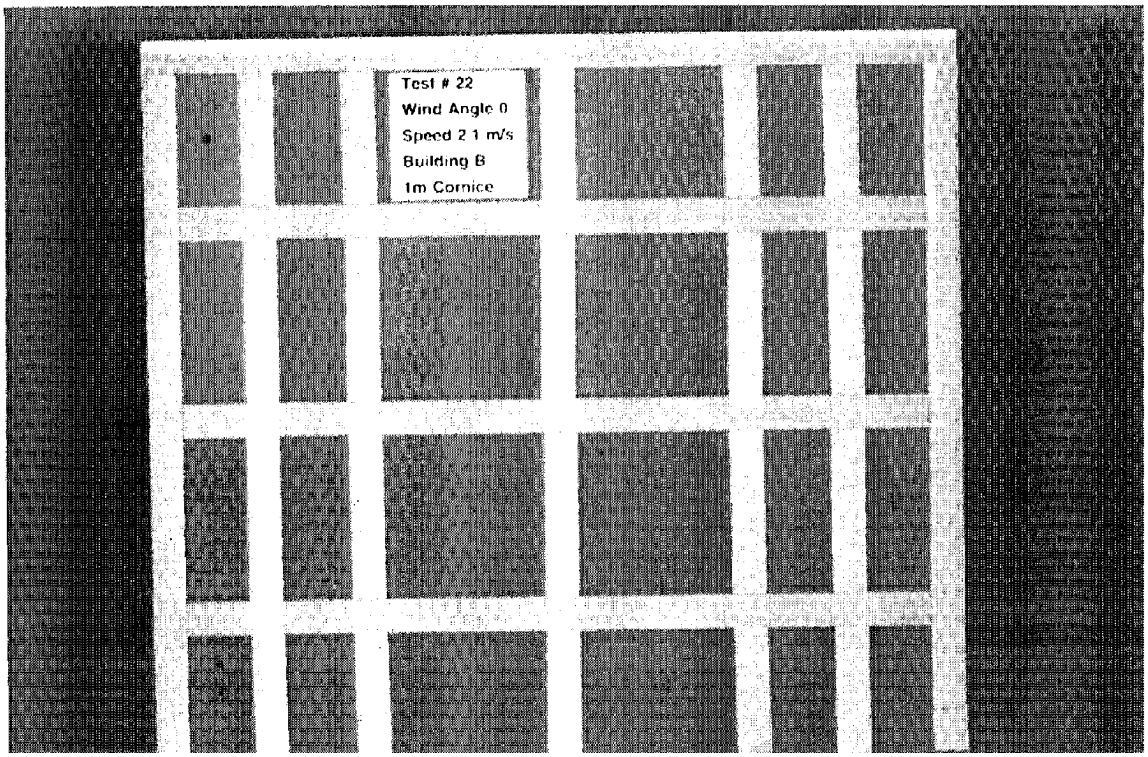

Figure D.6a. Complete Wetting Pattern for Phase II Building B with 1m Cornice, Building Angle= 0 degrees, Wide Face only

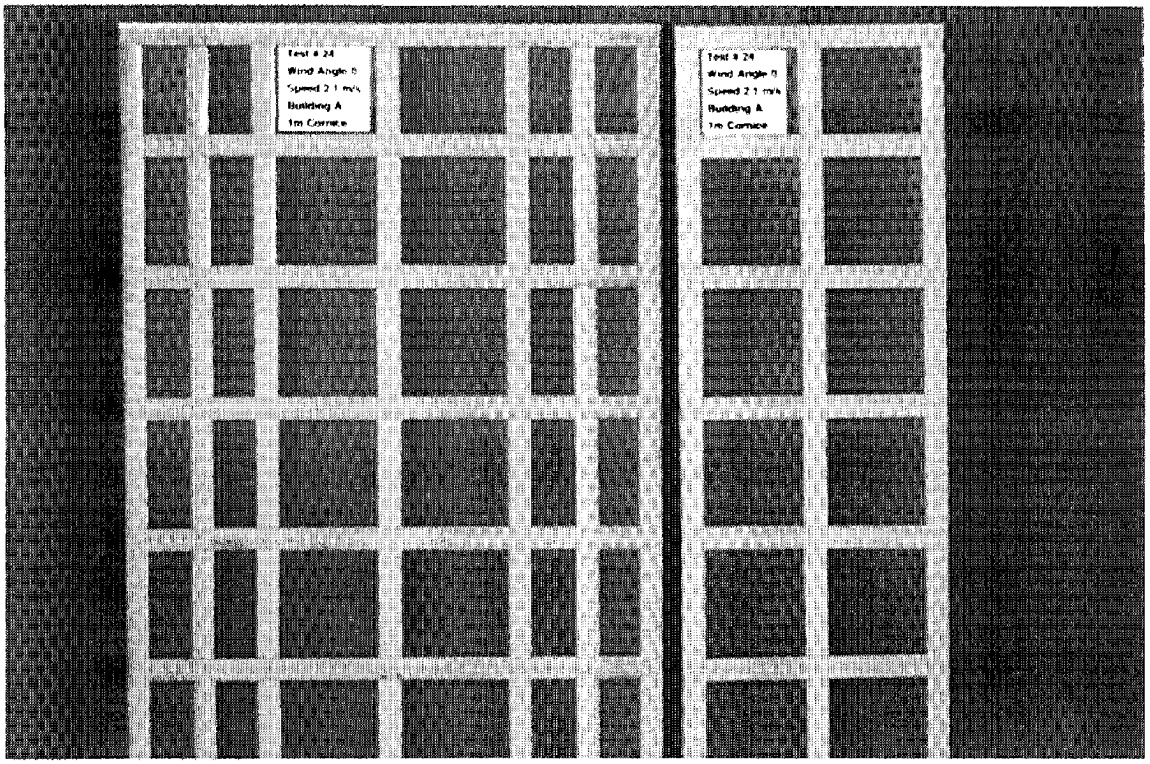

Figure D.6b. Complete Wetting Patterns for Phase II Building A with 1m Cornice, Building Angle= 0 degrees

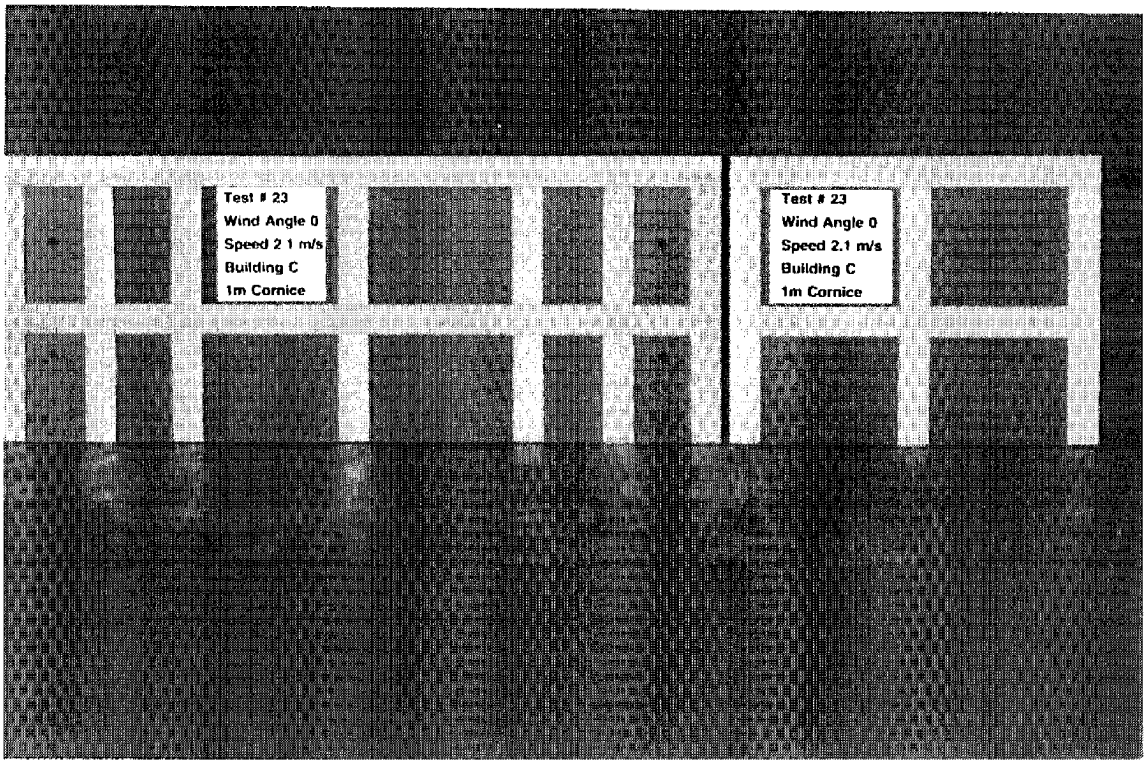

Figure D.6c. Complete Wetting Patterns for Phase II Building C with 1m Cornice, Building Angle= 0 degrees

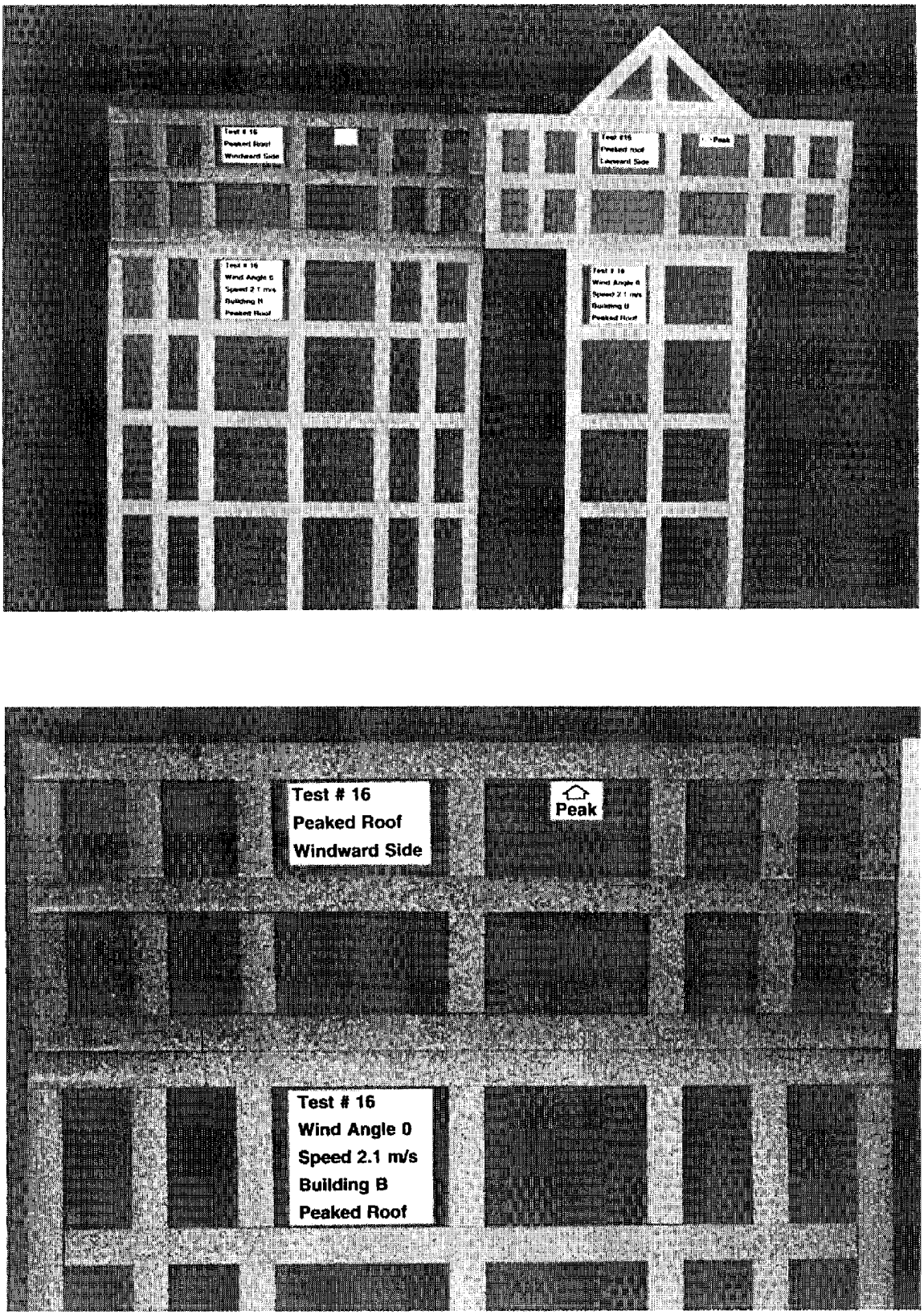

Figure D.7. Complete Wetting Patterns and Detail for Phase II Building B with Peaked Roof, Building Angle= 0 degrees

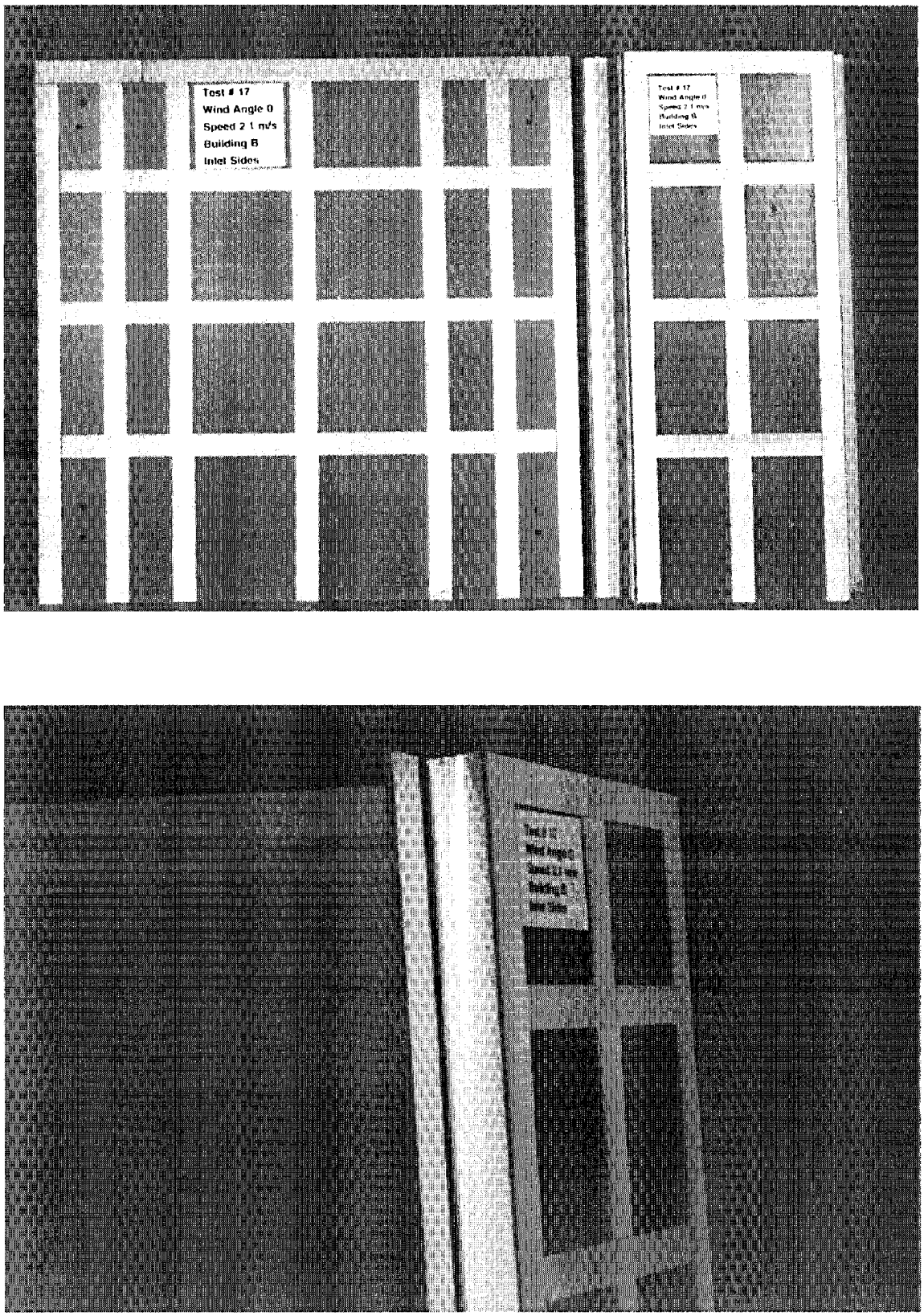

Figure D.8. Complete Wetting Patterns and Detail for Phase II Building B with Inset Corners, Building Angle= 0 degrees

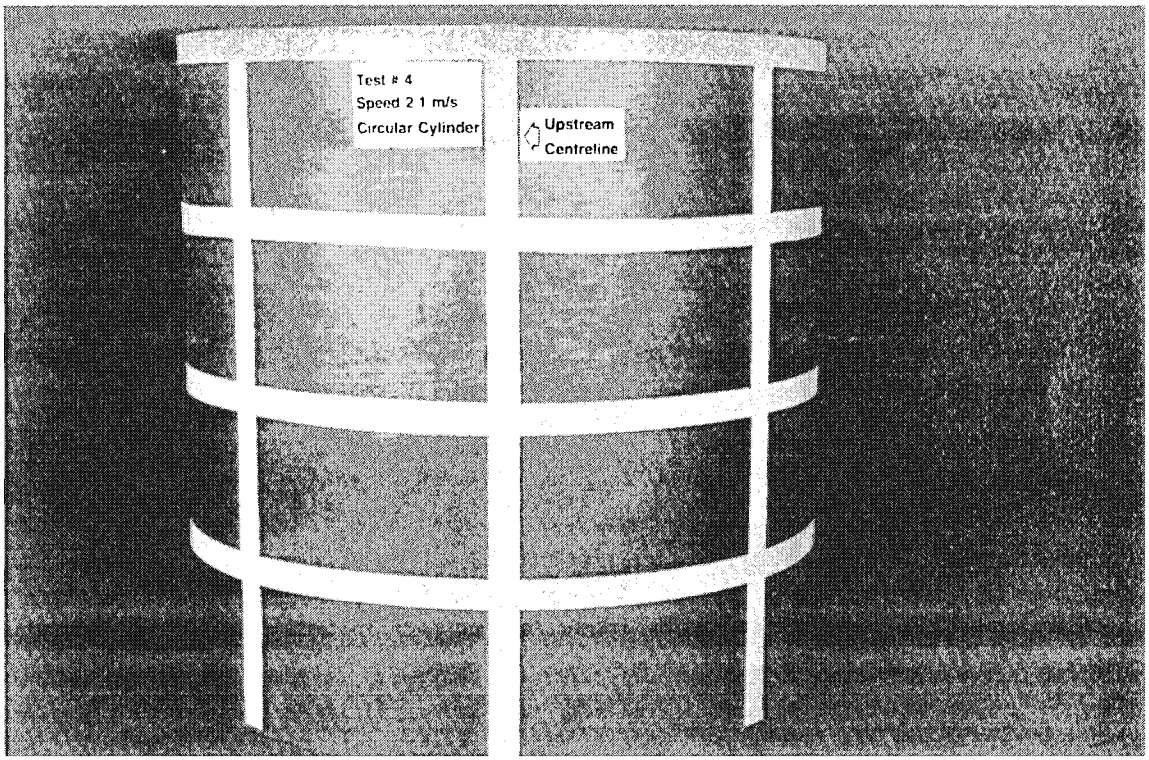

Figure D.9a. Wetting Pattern for Circular Cylinder

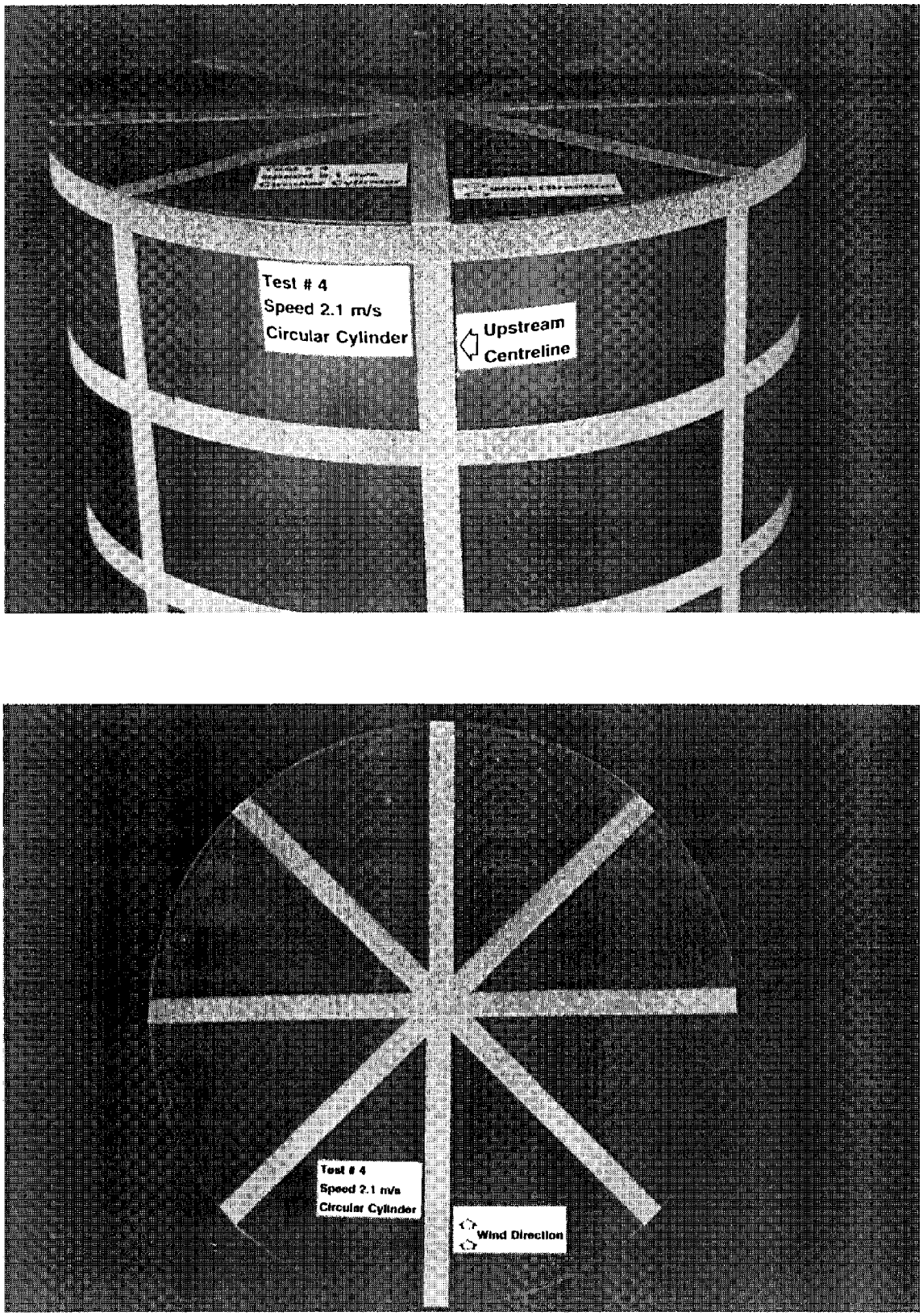

Figure D.9b. Detail of Wetting Pattern for Circular Cylinder

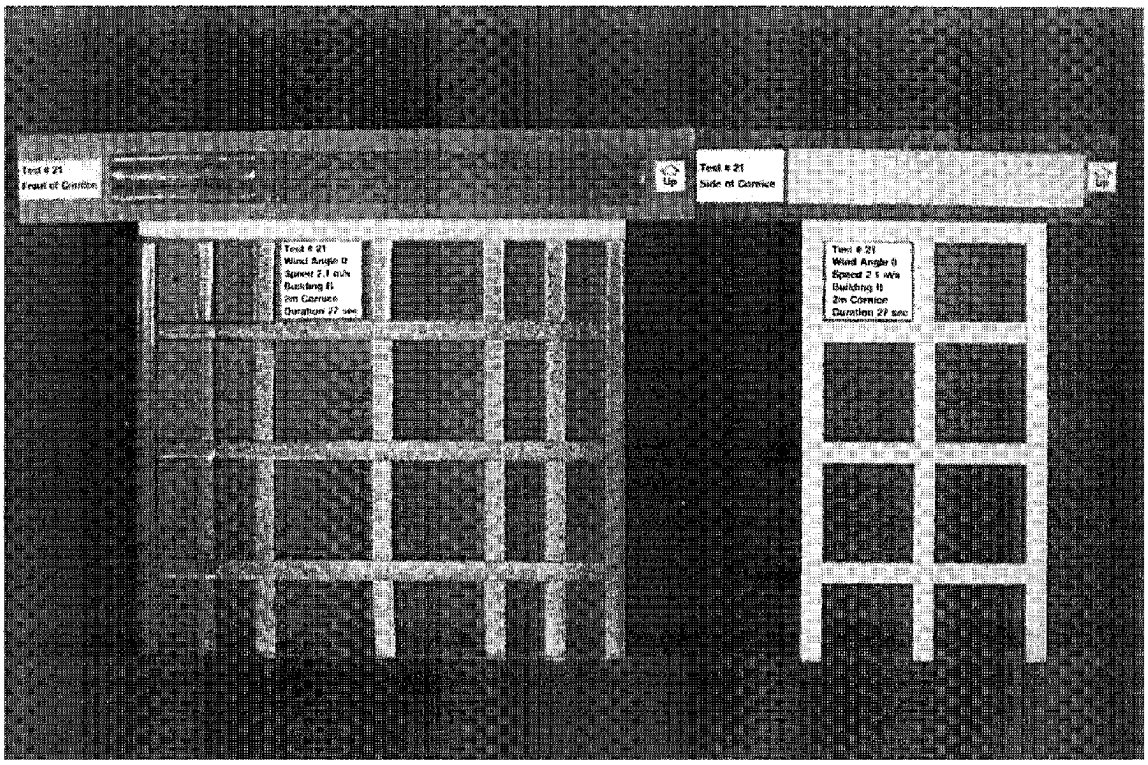

Figure D.10a. Complete Wetting Patterns for Phase II Building B with 2m Cornice, Building Angle= 0°, Test duration= 27 sec

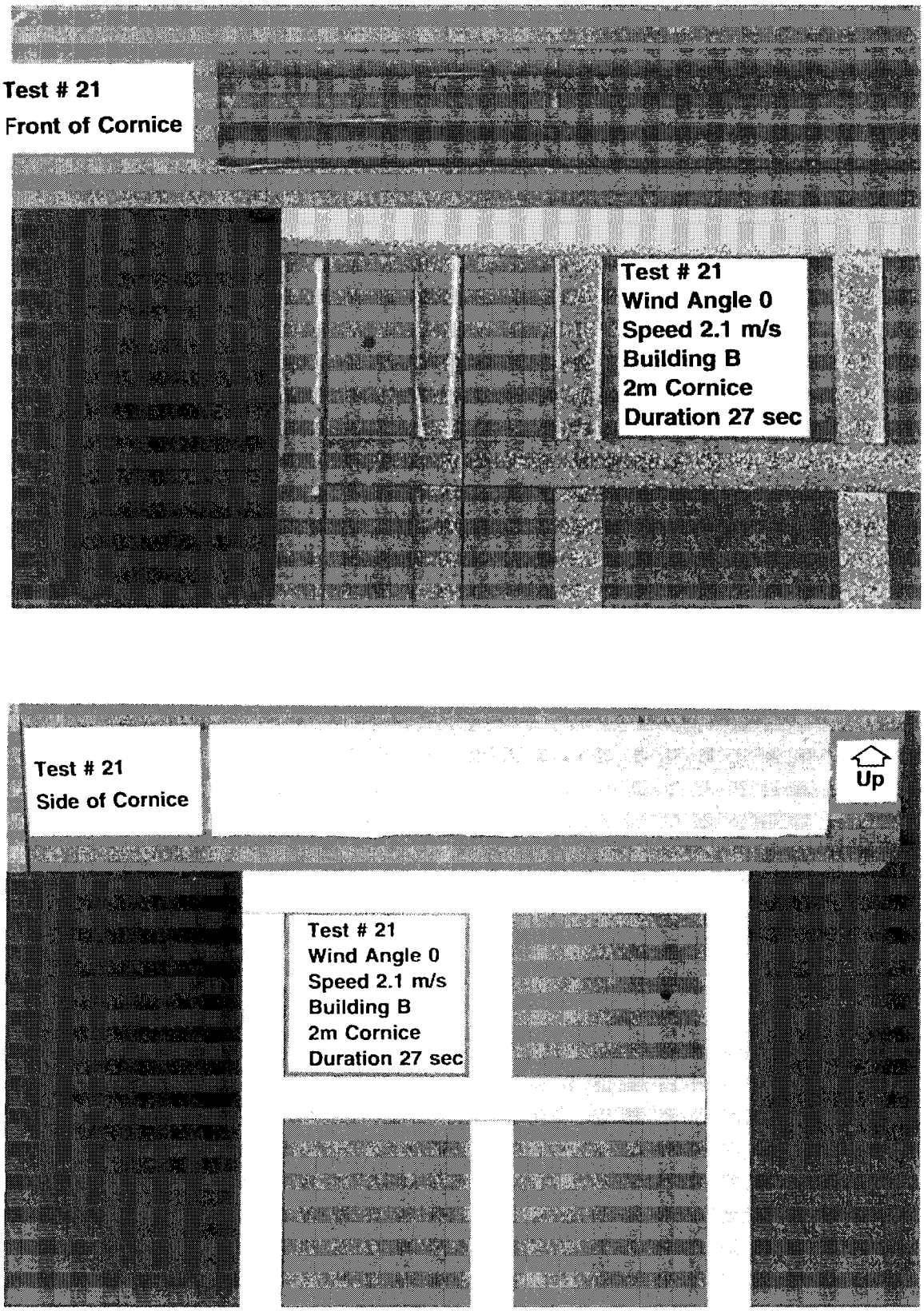

Figure D.10b. Detail of Wetting Patterns for Phase II Building B with 2m Cornice, Building Angle= 0°, Test duration= 27 sec

APPENDIX E

TERMINAL VELOCITIES OF WATER DROPS

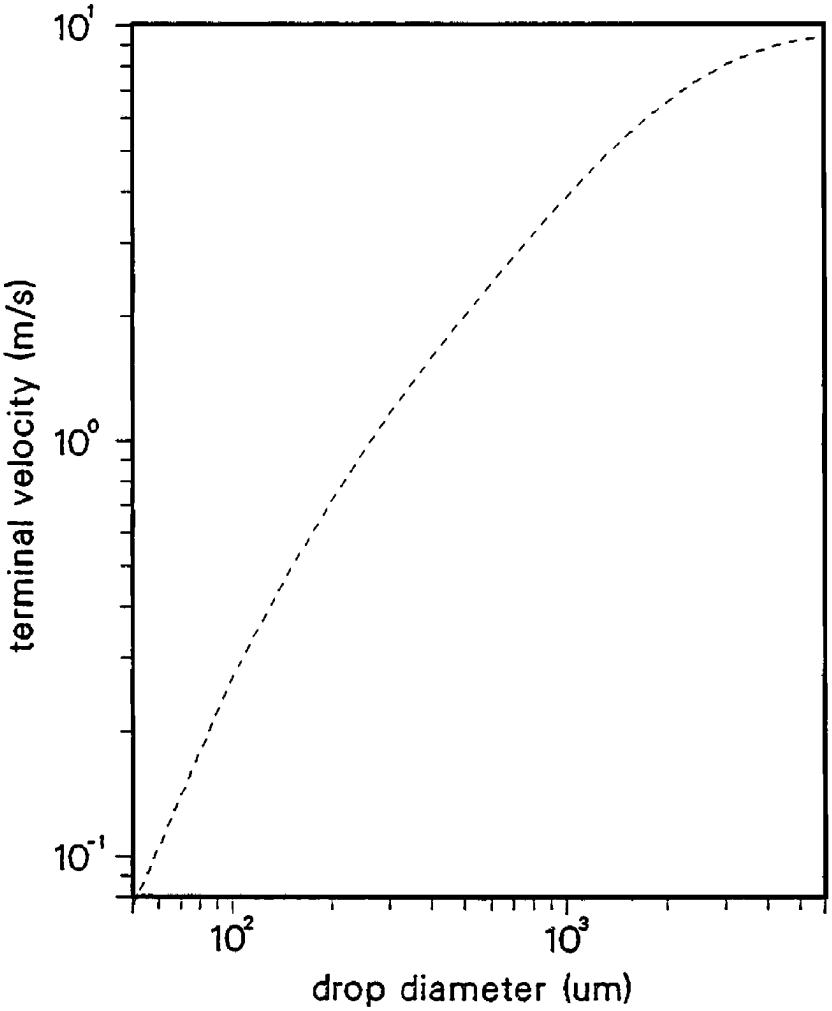

Figure E.1. Terminal Velocities versus Water Drop Diameter (from Stokes law, [7], [10])

APPENDIX F

THE EFFECTS OF RAIN ON WIND

As raindrops fall through a steady uniform wind, they follow a straight line path at the driving rain angle as defined by their vertical terminal speed and the horizontal wind speed with which they are being convected. That is, there is no relative horizontal speed between the wind and the raindrops under equilibrium conditions in steady uniform wind.

In a real wind, the mean wind speed reduces as the raindrops near the ground, and turbulence levels increase. This implies that the raindrops will no longer be in equilibrium. The local mean speed and turbulent deviations will lead to forces on the drops. Equal and opposite forces will be applied to the wind and turbulence. The question then arises as to whether this interaction causes significant changes to the wind characteristics. If it does, then subsequent questions arise as to whether the interaction is similar in model and full scale.

The order of magnitude of the potential effect on the mean speed profile can be considered through an example as follows: consider a rainfall rate of 10 mm/hr in a mean wind speed of 5 m/s at 10m in open country. At the top of the boundary layer, at say 300m altitude, the corresponding mean speed would be expected to be about 8 m/s. If we assume that this is the horizontal speed of the rain entering the boundary layer region and that, regardless of drop size, it loses half of this speed before it hits the ground - i.e. it hits at 4 m/s horizontally (equivalent to the mean speed at 2m height), then we can determine the momentum lost to the mean wind. The mass of water traversing the boundary layer per hour is 10 kg per square metre of surface area. Thus, the total force transferred, (which will be applied to accelerate the lower part of the boundary layer) per square metre of plan area, is $\frac{10}{3600} \times 4 = 0.011$ N. This is an equivalent shear stress acting in opposition to the normal surface drag. For comparison, the typical shear stress for this boundary layer flow at 10m is about 0.15 N/m^2.

The contribution of the rain is less than 8%. In comparison, the change from open country to a suburban area increases the shear stress by a factor of 3. Thus, at most, the rain acts to make the mean boundary layer flow behave as if it were over a marginally smoother terrain than it really is.

The effect of the rain on the turbulence is more difficult to assess analytically because the rain drops will continually be in non-equilibrium; however, the turbulent fluctuations are closely related to the shear stresses mentioned above, so there is some suggestion that a similar result might emerge. As an alternative, a simple experiment was carried out to investigate the potential effects using the wind tunnel model and set-up described in reference F.1. A pressure tap, located at the mid-width and 3/4 height point on the front face of the building, was monitored in simulated atmospheric flow with and without the rain simulation described in the main text. Since the model rain has considerably more mass per unit volume than simple geometric scaling would call for (due to the requirements on matching terminal speeds) this should be a conservative test. On the front face, there is a relatively simple linear transfer function relationship between the fluctuations in speed and the resulting fluctuations in pressure; hence the latter should indicate the former. The potential difficulty of water entering the pressure tube and distorting the results was dealt with by using hooded pressure taps. Two different hood designs were used, one shaped as a quarter sphere and the other as a half cylinder. These may have introduced a little additional high frequency pressure energy, but it was the same for both wet and dry cases. The results are shown in Figures F.1 and F.2. No significant differences in the measured spectra can be seen, suggesting that the rain does not significantly affect the turbulence properties, at least at these rainfall rates. In terms of the mass of water in the flow, the simulated rain rate can be deduced using linear scaling relations; that is, for the 1:64 model scale, the simple geometric scaling of the rainfall rate is a factor of 8. Thus, the measured rates, on this simple mass scaling basis, correspond to full scale values of the order of 25 to 100 mm/hr - very intense. (The true scaling, which removes the distorted mass required for maintaining appropriate terminal speeds, are of the order of a factor of 100 less than these values).

In summary, there appears to be little concern that rain materially affects the wind's mean or turbulence properties, for the typical model rates used, and probably for quite intense full scale rates. Other affects, such as strong convection that may accompany heavy rains and other variabilities, are likely to be dominant.

REFERENCE

F.1 P.F. Skerlj, and D. Surry, "A Study of Mean Pressure Gradients, Mean Cavity Pressures, and Resulting Residual Mean Pressures Across a Rainscreen for a Representative Building", The University of Western Ontario Research Report, BLWT-SS23-1994.

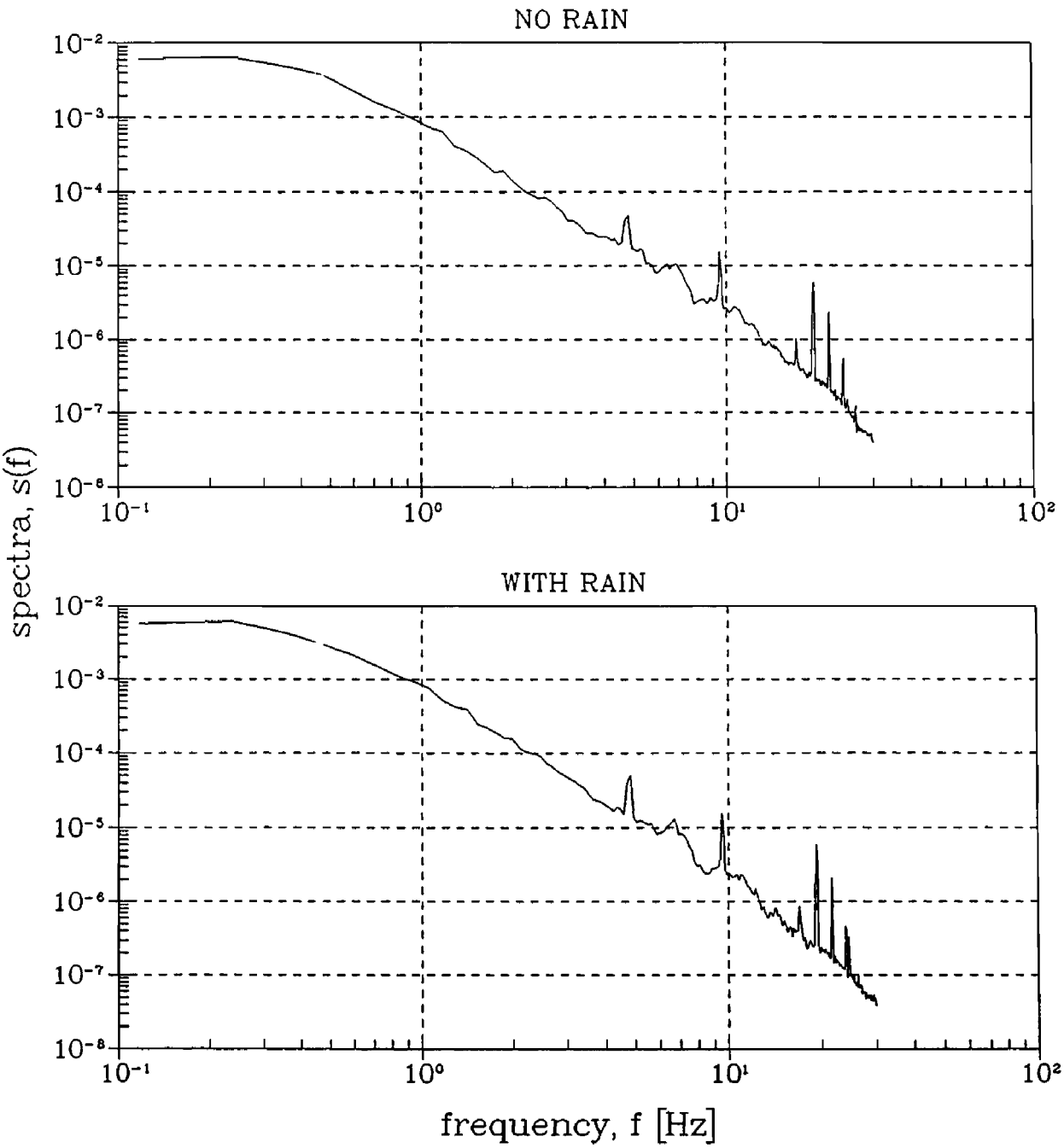

Figure F1. Power Spectra of measured pressure

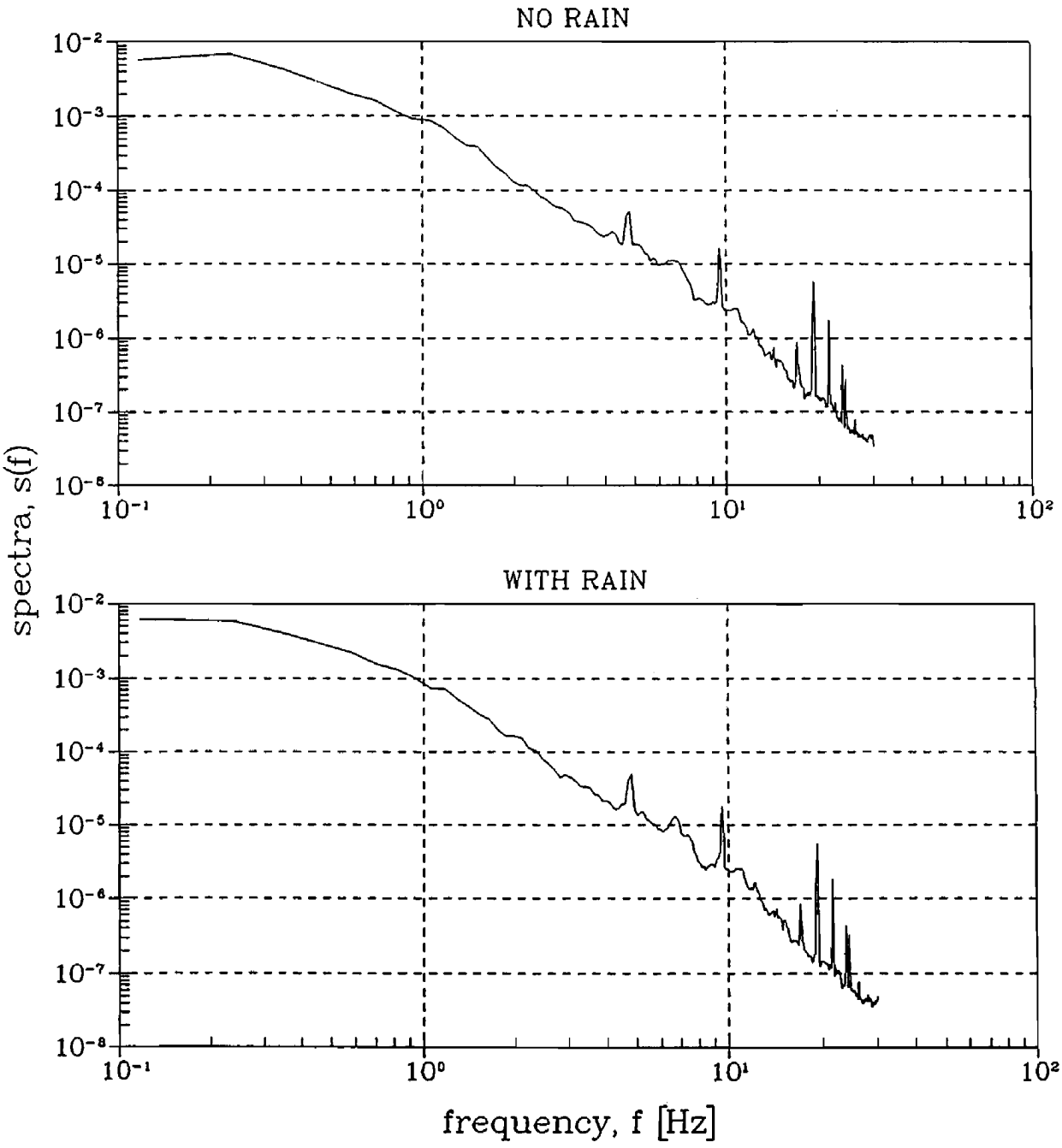

Figure F2. Power Spectra of measured pressure